بسم الله الرحمن الرحيم

THE UNIVERSITY OF KHARTOUM

FACULTY OF ENGINEERING AND ARCHITECTURE

THE EFFECT OF SCANNING RESOLUTION IN DIGITAL PHOTOGRAMMETRIC WORK

A thesis presented for the degree

of

Ph.D. in Surveying Engineering

by

NAGI ZOMRAWI MOHAMMED YOUSIF

B.Sc. in Surveying Engineering (First Class Honours)

Department of Surveying Engineering

June 2005

بسم الله الرحمن الرحيم

(و ما أوتيتم من العلم الا قليلاً)

صدق الله العظيم
الاية(85) سورة الاسراء

DEDICATION

Dedicated…

to my father,

the first one who taught me a letter.

To my mother,

from whom I knew the meaning of life.

To my brothers, Nadir, Eltayeb, and Albasheer,

the light of my way.

To my little family, Maysoon and Nazar

whom I love.

ACKNOWLEDGEMENTS

My primary thanks to Allah, the most beneficent, the most merciful.

Thanks to Dr. Mohammed Ahmed Gorani, my supervisor, for his help, advices and continuous encouragement through this research work. Thanks also to all the staff of the Surveying Engineering Department of the university of Khartoum

I am grateful to Dr. Elshami Mohammed Masaad, head of Khartoum University Consultant Corporation, and Dr. Ali Hassan Fagir, Sudan University of Science and Technology, whom continuously encourage me through this research work.

Finally, I am indebted to all people who gave me their time, advice, and support and helped me in various aspects of this study.

Acknowledgements are extended to my teachers and colleagues at Sudan University of Science and Technology and to all members of Sudan Survey Department.

خلاصة

تعتبرالمساحة التصويرية من فروع المساحة التي استفادت من التقدم الذي طرأ علي تكنولوجيا الحاسوب في مختلف مراحلها. ابتداءً بعملية تسجيل البيانات ثم معالجة الصور مروراً بعمليات الضبط المختلفة وحتي عملية إنتاج الخرائط.

تعتبر أجهزة الرسم التصويري الرقمية المتكاملة(Digital photogrammetric workstations) إحدي ثمار هذا التطور في مجال المساحة التصويرية والتي بدأت بدورها تحل تدريجياً محل أجهزة الرسم التماثلية والتحليلية.

كما تعتبر قوة وضوح الصور الرقمية من العناصر الاساسية التي تؤثر علي دقة النتائج النهائية في المساحة التصويرية الرقمية بصورة عامة و أجهزة الرسم الرقمية المتكاملة بصورة خاصة.

في هذا البحث تمت مناقشة العديد من المواضيع المرتبطة بعملية إعداد الخرائط من خلال إستخدام أجهزة الرسم الرقمية المتكاملة والتي تضم:

- الكاميرات الرقمية:-

حيث أنها وسيلة جمع المعلومات الرقمية المباشره لاعداد الخرائط وتمثل الان البديل لكاميرات التصوير الجوي التقليدية.

- الماسحات:-

حيث يتم استخدام ماسحات ذات دقة عالية لتحويل الصور الجوية إلي صور رقمية.

- معالجة الصور الرقمية:-

هذه البرمجيات أصبحت البديل لمعامل التصوير الفوتوغرافي سواء كانت في عمليات التصغير و التكبير أو في عمليات تحسين مظهر الصورة أوخلافه من العمليات المختلفة وذلك قبل البدء في عمليات القياس.

تم في هذا البحث اجراء اختبارين , الاول في منطقة جبلية و الثاني في منطقة مستوية. أستخدم في الاختبار الاول نموذج جوي لمنطقة جبلية في Switzerland بمقياس رسم 1:40000 مأخوذ بكاميرا ذات رؤية عريضه تم تحويله الي شكل رقمي بإستخدام دقة وضوح مختلفه من خلال ماسحه تصويرية.

أستخدمت الة الرسم الرقمية المتكاملة (Digital Workstation) لضبط النموذج الارضي الرقمي و من ثم قياس احداثيات عدد من نقاط الضبط المستخدمة في الدراسة.

حُسب الخطأ المعياري للاحداثيات المقاسة للنقاط مقارناً مع إحداثياتها الصحيحة لكل دقة وضوح علي حِده.

تم إستخدام برنامج ERDAS في عملية تقويم الصور الرقمية المستخدمة في الدراسة ومن ثم قياس الاحداثيات الأرضية من الصور المقومة و حساب مقدار الأخطاء المعيارية الناتجة. دعت هذه النتائج إلي إجراء إختبار ثاني لعملية تقويم الصور الرقمية. تم في هذا الاختبار إستخدم نموذج جوي لمنطقة مستوية في وسط الخرطوم بمقياس رسم 1:20000 مأخوذ بكاميرا ذات

رؤية عريضه تم تحويله الي شكل رقمي من خلال ماسحه تصويرية و تقويمه ثانية بإستخدام برنامج ERDAS.

خلُصت هذه الدراسة الي أن دقة القياس في المساحة التصويرية الرقمية تتناسب تناسباً طردياً مع دقة وضوح الصور الرقمية المستخدمة في كلٍ من القياسات الأفقية و القياسات الرأسية. كما تم إستنتاج نماذج رياضية لتقدير دقة النتائج المتوقعة ومن ثم أنسب مقياس رسم أفقي و أنسب مقياس رسم رأسي لاعداد الخرائط مقابل دقة وضوح الصور الرقمة الستخدمة.

كما خلصت الدراسة إلي أن إعداد الخرائط إعتماداً علي برامج تقويم الصور الرقمية مثل برنامج ERDAS لا يصلح إلا في المناطق ذات الطبيعة المستوية. غير أن أجهزة الرسم الرقمية المتكاملة هي البديل لإعداد الخرائط في المناطق ذات الطبيعة الجبلية و المناطق ذات الطبيعة المستوية علي حدٍ سواء.

ABSTRACT

Photogrammetry is one branch in surveying that has largely been affected by the development in computer technology in data acquisition, image development and processing, adjustment and further in mapping of data.

Digital photogrammetric workstation is one of the yields of these developments in photogrammetry, which is gradually replacing analogue and analytical plotters.

Pixel resolution is one of the main factors that affect the final results in digital photogrammetry in general and in digital photogrammetric work station in particular.

In this research work, various subjects relevant to the process of digital mapping using digital photogrammetric work station were discussed. Theses subjects include:

- Digital camera:

  The present alternative of the conventional camera and by which direct digital photogrammetric data can be acquired.

- Scanners:

  Special precise photogrammetric scanners are used to transform hard copy images into a digital form.

- Digital image processing:

  Image reduction and enlargement, image enhancement, edge sharpening, and so on, are now at the dispose of user's fingertips

using special softwares, rather than spending a long time in traditional manual manipulation.

Two experiments were carried out in this research work, one in a mountainous area, and the other in a flat one. In the first test an aerial wide-angle hard copy stereopair at scale 1:40,000 of mountainous terrain in Switzerland was transformed to a soft copy using a different scanning resolutions by a special photogrammetric scanner.

A digital photogrammetric workstation was used to measure a number of control points of known ground coordinates.

The root mean square error of the measured ground coordinates of these points and their actual coordinates were computed for each scanning resolution.

ERDAS software package was used to digitally rectify the scanned images using the same pixel resolution used above. The coordinates of points were measured and the root mean square errors were computed again. The result of digital rectification is required to be supported by another test in a flat terrain. In this test an aerial wide-angle hard copy stereopair at 1:20,000 scale of a flat terrain, in the center of Khartoum, was transformed to a soft copy and rectified.

The results of these investigations proved that the accuracy of the measurements in digital photogrammetry is nonlinearly proportional to the scanning pixel resolution in both horizontal and vertical measurements. Mathematical models were developed to estimate the accuracy against

scanning resolution and suitable plotting scales in both horizontal and vertical mapping.

Production of maps using digital image rectification using software packages such as ERDAS is suitable only in a flat terrain. On the other hand, a digital photogrammetric workstation is a productive way for mapping in both flat and mountainous terrains.

LIST OF CONTENTS

LIST OF TABLES

LIST OF FIGURES

CHAPTER 1

INTRODUCTION

CHAPTER 1

INTRODUCTION

1.1 OVERVIEW

Photogrammetry, as classically defined, is the art, science and technology of abstracting useful quantitative and qualitative information about physical and man-made objects by measurements and observations on photos and/or images of these objects. Digital photogrammetry is the science that concerned with digital automation of this process or part of it.

It is very difficult to conceive planning, without the aid of photogrammetry, of any engineering projects covering considerable areas of terrain, such as constructions of roads, railways, dams, reservoirs, pipelines, and large housing developments. Certainly there is no other method of survey which will generate the required data about the terrain surface in the form of accurate plans, maps, photomaps, elevation models, profiles and contours in a timely and economic manners as is required for the planning of all large engineering projects.

However, photogrammetric methods also have their limitations. For example, they have a little or no part to play in the work of setting out roads, buildings, bridges, tunnels, and other structures in the field and of controlling the construction of these structures, nor does it make any sense to use aerial photogrammetric methods for the survey of an

individual building site; the cost and complexity of taking suitable aerial photography, establishing ground control points, carrying out stereoplotting in photogrammetric instruments and verifying and completing the plotted detail in the field would make the whole process uneconomic as compared to field survey methods. As soon as the area to be surveyed or mapped becomes larger than can be covered by one or two pairs of aerial photographs, the situation changes drastically. There is no way in which ground survey methods, whether employing mechanical, optical, electronic or combination methods of measuring distances and angles, can compete with photogrammetric methods of surveying and mapping. This is especially the case in rough or rugged terrain where there is no possibility of ground survey procedures, for producing detailed data about the terrain within a reasonable time frame.

Digital photogrammetry has offered the possibility of capturing or generating terrain data in computer-compatible form for the purpose of digital mapping, terrain modeling, and computer-aided design. Furthermore, the advent of automated, semi-automated and digital methods of collecting highly accurate terrain elevation data in pre-programmed patterns using photogrammetric plotting instruments under computer control gives a method of data collection for extensive areas and speeds up the process of map production so as to shorten the period between the initial data collection from the field and the availability of the resulting map in digital or hard copy form.

Digital photogrammetry is rapidly emerging as a new sub field of photogrammetry. While digital photogrammetry has its roots in the 1950s, major research activities began only in the 1980s, sparked by significant advances in electronic and computers, such as digital cameras, parallel processing, and increased storage capacity. Considerable progress has been made during the last few years. Several digital photogrammetry products are now commercially available, such as digital photogrammetric workstation, automatic digital elevation models software, and digital orthophotos products.

1.2 OBJECTIVES AND BACKGROUND

Digital photogrammetric workstation probably is the most significant product of digital photogrammetric instruments. It represents one of the yields of computer technology applications in photogrammetry. Considering the dynamic nature of this field, digital photogrammetric workstations undergo constant changes, particularly in terms of performance, ease of use, components, cost, and vendors.

The main objectives of the research are to investigate:

- The technology of digital plotters that are termed to be called Digital Photogrammetric Work Stations (DPWs), which are gradually replacing analytical and analogue photogrammetric plotters.

- The study of new methods of digital data capturing, including different types of electronic or digital cameras. The methods that can be used to transform the traditional hard copy data into a digital form.
- Highlight different aspects that support digital photogrammetry such as; digital image processing and image matching procedures that are used in digital photogrammetry.
- Investigate the precision that can be attained using different scanning resolutions for a particular image.
- Examining and discussing the main factors that affect the precision in digital photogrammetric measurements.
- The possibility of generating planimetric and contour maps using different scanning resolutions.
- Suitability of scanning resolution via the required mapping scales.
- Testing the precision of rectified digital image using ERDAS package.
- Comparing precisions that result from DPW with those derived from ERDAS software.

1.3 THESIS LAYOUT

The work carried out in the research is presented in the following lines:

Chapter 2 gives a background of conventional photogrammetric plotters and their theory of work. It includes the analogue systems with its three

branches, optical, mechanical and optical/mechanical projection systems and how these generations of plotters can be upgraded to use digital data acquisition techniques. Also, this chapter gives a detailed discussion of analytical plotters with their different types and methods of computations that can be used.

Chapter 3 discuses the new technology of imaging systems, from the use of the video camera in the data acquisition up to the Charge Coupled Devices (CCD) and push broom scanner camera which is now wide spread.

Chapter 4 outlines, in general, the method of transferring hard copy images into soft copy using photogrammetric scanners; their components and sources of error.

Chapter 5 gives a short discussion about digital image processing. This includes the description of the digital image and some methods of image enhancement that can be applied before taking measurements from the digital image.

Chapter 6 highlights the image matching techniques, the methods, and the problems facing its applications. This is useful in finding conjugate points in stereopairs in photogrammtric problems. .

Chapter 7 concentrates on the digital photogrammetric workstations, its main components and applications.

Chapter 8 reflects the results of photogrammetric measurements carried out in this research, when using different image resolutions and different

methods. Also this chapter is devoted to discuss and analyze the results of the tests carried out.

Chapter 9 includes the conclusions drawn from the research and suggestions for further work.

Finally, six appendences are included. Appendix A represents a contour map of the study area while appendix B contains a three-dimensional representation of the study area. Each of appendences C, D, E, and F represents a contour map of the study area compared with the derived one using the tested resolution.

CHAPTER 2

ANALOGUE AND ANALYTICAL PHOTOGRAMMETRIC SYSTEMS

CHAPTER 2

ANALOGUE AND ANALYTICAL PHOTOGRAMMETRIC SYSTEMS

2.1 STEREOPLOTTING INSTRUMENTS

The approach taken in all stereoplotting instruments is the use of a pair of overlapping photographs to form a three dimensional reduced-scale model of the terrain in the instrument. Then measuring this model of the terrain very accurately to produce the required map or coordinate information instead of measuring the terrain directly using field surveying instruments. The type of model of the terrain, which may be formed in the instrument, can be either optical or mechanical in nature. The photogrammetric procedures carried out using a stereoplotting instrument based on such a model constitute an analogue process where the terrain being measured is simulated by another physical system (the optical or mechanical model), which is measured instead. This is the origin of the descriptive term ‘analogue’, where the *analogue* type of stereoplotting instrument is differentiated from *analytical* type of photogrammetric instrument in which the solution is purely mathematical and the model is wholly numerical.

2.2 ANALOGUE PHOTOGRAMMETRIC INSTRUMENTATION

The analogue photogrammetric instruments can be divided into optical, mechanical and optical mechanical projection instruments.

2.2.1 OPTICAL PROJECTION INSTRUMENTS

Basically, an instrument of this type comprises two identical projectors with the same geometric characteristics (format size, focal length, angular coverage) as the camera, which took the photography. Positive transparent copies (film or glass diapositives) of the pair of overlapping photographs, which cover the area of interest, are placed in the two projectors so that the optical axis of the projector lens, passes through the principal point of the photograph –***inner orientation***- and are illuminated from above so that the images are projected downwards into the space below the projectors. Through the procedure of ***relative orientation*** by which the photogrammetrist rotates and shifts the two projectors in an orderly manner, the two photographs are set in the same relationship to one another as they occupied in the air at the time of exposure. When this has been done successfully, the two bundles of corresponding rays from each projector will meet in the space below the projectors and so form an optical model of the terrain. This optical model can easily be viewed stereoscopically (in three dimensions) by the user, and measurements can readily be carried out on this model.

The actual measurements of the correct stereomodel of the terrain are carried out accurately using a free-moving measuring device, which has a platen with a white surface and a small measuring mark at its center. This device can be used to plot a map from the stereomodel. The observer following the edge of the road, field boundary, forest or other feature precisely with the measuring mark, the correct position being given by a plotting pencil located directly below the mark. If the ground rises or falls, the measuring mark is continuously adjusted by the observer to the correct height in the model as the plotting of the feature continues. This means that continuous measurements of the heights of each ground feature are being made and these relate directly to the actual height present in the terrain.

Alternatively, the measuring mark can be set to a predetermined height and the observer can keep the mark continuously in contact with the optical model of the terrain at that height, so producing a plot of that particular contour on the map sheet. Each required contour can be measured in the same manner, the measuring mark being set to the corresponding height in the model in each case.

The prerequisite for these operations of plotting out the map detail and contours is that the orientation of the optical model be such that it is in the correct relationship with the terrain system – an operation called ***absolute orientation***, carried out by the photogrammetrists. This entails the scaling of the model so that the positions of certain ground control

points, when plotted from the model, fit the corresponding positions of these points already plotted on the map at the desired scale. In addition, the model is rotated as a whole so that correct heights will be measured in the model i.e. brought to a level datum. These operations must be carried out prior to the commencement of the detailed measurements required to produce the map.

2.2.2 MECHANICAL PROJECTION INSTRUMENTS

The basic concept of mechanical projection is to duplicate mechanically all the optical components of the optical projection type of instruments. In the latter, there were photographs, projection lenses, projected rays, and an optical model. In the equivalent mechanical projection instruments, each photograph is duplicated mechanically (as the mechanical photo plane). The projected rays are duplicated mechanically by their equivalents (known as space-rods); the projection lenses are duplicated mechanically as the center of a free-moving gimbal system; and the specific point in the optical model where a pair of intersecting optical rays would meet is the position where the corresponding pair of space-rods meet and forms the mechanical model point.

Thus the basic measuring system in this alternative type of instruments is now wholly mechanical instead of being purely optical as in the previous type of instrument. Thus the terms '***mechanical projection instrument***' and '***mechanical model***' apply to it. However, it must be realized that

these terms apply only to the projection or measuring system. It is still necessary for the observer to view the photographs optically and stereoscopically if three-dimensional measurements are to take place. This is achieved by a mechanical linkage, which ensures an exact correspondence between what is being measured (using the mechanical projection system) and what is being viewed in three dimensions by the operator using the instrument's optical system. The latter is -in principle- a form of mirror stereoscope, by which the basic requirement that the observer's left eye sees the left photo only and his right eye sees the right photo only, is actually achieved. In this way, the observer or operator of the instrument can view and measure the model of the terrain stereoscopically, that is, in three dimensions; in much the same manner as was done in the optical projection type instrument.

The actual measurement of the mechanical model may be carried out by the operator using a free-moving measuring device of the same basic design as that employed in the optical projection instrument. Again, this may have a pencil attached to it to allow direct plotting of the details required for a topographic map. As before, since the mechanical model being measured is a correctly scaled representation of the terrain, the details plotted and the heights measured in this model relate directly to the actual positions and heights present in the terrain.

An alternative to the free-moving measuring device moving over the map sheet is to mount the intersection point (mechanical model point) of the

space rods in a three-dimensional coordinate measuring system which comprises two rails and cross-slide to allow the planimetric (***X***/***Y***) movements to take place, plus a telescopic movement in the vertical (***Z***) direction to allow heights to be measured. This whole system can be moved freely by hand or it can be driven mechanically using hand-wheels and lead screws to any point in the model which has to be measured. By coupling drive shafts and gears to the lead screws, a coordinatograph can be attached to the stereoplotting instrument, so permitting the final map to be plotted at a scale different to that of the actual model in the instrument.

2.2.3 OPTICAL MECHANICAL PROJECTION INSTRUMENTS

A few stereoplotters have projection systems, which are partly optical and partly mechanical, but theses instruments are not as common as those of purely mechanical projection (Wolf 1985). With these instruments, the diapositives are centered in the two projectors and illuminated from above. Corresponding images are optically projected through the projector objective lenses and come to focus on a pair of reference mirrors. The rays are reflected by the mirrors into two optical trains and are viewed by an observer through binoculars. A special mechanical linkage aligns the mirrors so that the reflected rays are received in the optical trains regardless of the area of the diapositives being viewed. Reference half

marks superimposed at each reference mirror fuse into a floating mark that appears to rest exactly on a model point when the half marks are set on corresponding images.

2.3 DIGITAL DATA ACQUISITION USING ANALOGUE STEREOPLOTTING INSTRUMENTS

Besides the graphical plotting discussed in the previous section, it is also possible to record all the measurements made in a stereoplotting instrument in a numerical digital form for subsequent processing in a computer based mapping or information system or in a Computer Aided Design (CAD) system. This approach is one which is being implemented to an ever- increasing extent, and many existing analogue stereoplotting instruments have been converted for this purpose.

All the three dimensional (***X***, ***Y*** and ***Z***) measurements made in a stereoplotting instrument may be ***digitized*** by mounting the measuring mark on a suitable cross-slide system and encoding each of the axes individually using linear or rotary encoders Figure (2.1). Alternatively, a tablet digitizer may be mounted on the base surface of the instrument to give positional (***X***, ***Y***) information while the terrain heights (***Z***) are obtained in digital form by adding a linear or rotary encoder to the height-measuring device. The former arrangement is preferred, since the use of cross-slides can easily allow measuring resolutions or accuracy of 5-10μm, whereas the tablet digitizer is limited to 25-50 μm at best (Kennie and Petrie 1993).

A variety of ***digitizing units*** can be attached to the encoders mounted on an analogue type of stereoplotting instrument. These provide coordinate display, allow the selection of different measuring models (such as point or stream digitizing) and allow headers, feature codes, and descriptions to be entered into the unit.

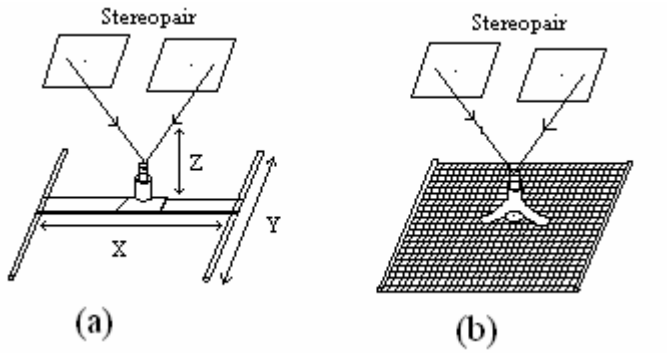

Figure (2.1) Encoders, after Petrie(1997)

(a) Linear encoders attached to cross slide system,

(b) Tablet digitizer mounted on the base surface

Hardware-based and software-based units are all used. Hardware include a stand alone electronic box which decodes and counts the signals coming from the linear or rotary encoders mounted on the stereoplotting instrument and convert them to ***X***, ***Y*** and ***Z*** model coordinate values which can be viewed on a Liquid Crystal Display (LCD). It records them on magnetic tapes, cassettes, cartridges or compacted disks. Software-based units are, as the name suggests, based on the use of an on-line computer which, not only performs the data recording but, can give prompts and

assistance to the operator during the setting up of the stereomodel, as well as carrying out checks on the measured coordinate data.

Essentially, all of these systems are carrying out the blind digitizing technique also used widely for the digitizing of the detail and contours shown on existing maps. Checking must be carried out using hard-copy plots generated at the end of a digitizing session. However, in a few cases a computer-driven plotting/drafting table has been attached on line, which can plot out all the terrain detail and the elevation or contour data measured by the photogrammetrist for his inspection and possible correction during the actual measuring operations.

2.4 ANALYTICAL PHOTOGRAMMETRIC INSTRUMENTATION

The alternative and increasingly important type of photogrammetric instrumentation is that based on the use of analytical photogrammetric procedures in which the optical or mechanical methods of the analogue approach are replaced by purely numerical models based on analytical mathematical solutions which are implemented in suitably programmed computers. From the instrumental point of view, there are several alternative ways in which these solutions may be implemented in practice. These may be classified into three main groups:

i. The use of a comparator as the measuring device and the execution of the analytical photogrammetric solution as an off-line process carried out later in a computer,

ii. The use of a comparator as the measuring device but with the numerical computational solution executed as an on-line process and

iii. The construction and operation of an analytical plotter in which the computer is totally integrated into the design of the instrument and the numerical solution is always an on-line process, executed in realtime and resulting in a continuously oriented stereomodel.

2.4.1 COMPARATOR AND OFF-LINE SOLUTION

The basic arrangement is shown in Figure(2.2), the measuring device may be a mono-comparator in which the individual photographs comprising a stereopair are measured separately. The x, y image coordinates of each point on the first photograph are measured in the instrument, encoded using digitizers and then recorded in a computer-compatible form. When the corresponding points on the second photograph of the stereopair have been measured and recorded, the two sets of measured coordinates data can then be merged together to implement the analytical photogrammetric solution. It will be seen that if a stereopair is being measured and a stereomodel formed, the use of a monocomparator as the measuring device always result in an off-line computational solution since the measurement of the points whose positions and heights have to be determined takes place separately and sequentially on the individual photographs of the stereopair.

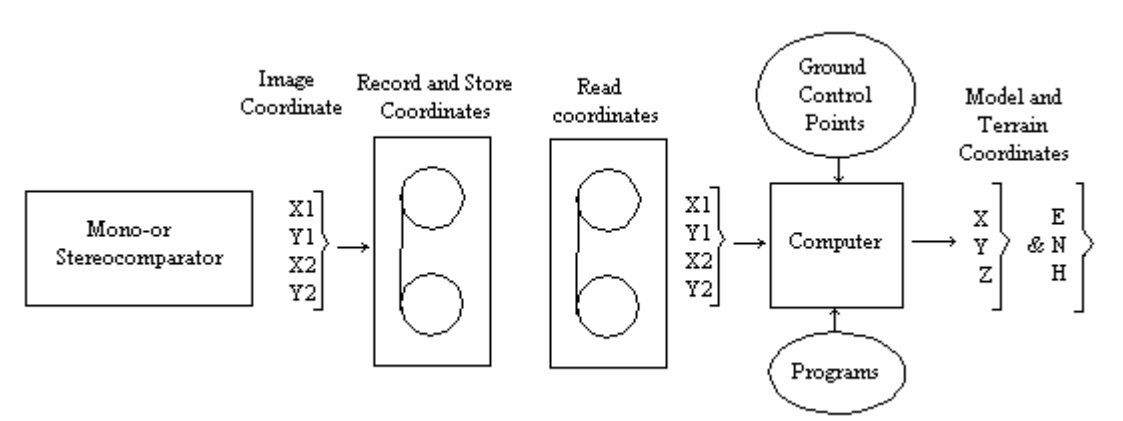

Figure (2.2) Comparator and off-line solution, after Petrie(1997)

Alternatively, the measuring instrument can be a stereocomparator, in which stereo viewing is possible and the measurement of both photographs takes place simultaneously. The image coordinates - in this case x1, y1 for the left photograph and x2, y2 for the right photograph - are again stored and recorded. Later, the numerical computational solution is implemented to determine the terrain coordinates of all points measured in the stereocomparator.

2.4.2 COMPARATOR AND ON-LINE SOLUTION

In this arrangement, the comparator is attached on-line to a computer Figure (2.3). The basic measuring process and computational procedure is the same as that for the off-line solution but, obviously, this arrangement allows the model to be formed and the terrain coordinates to be calculated as soon as minimum number of points needed to implement the analytical solution has been measured. Once this has been achieved, then the

measurement of any other additional points in the model will of-course result in the computation of their corresponding terrain coordinates.

While a monocomparator may be attached directly to the computer to implement this solution, there is little advantage in doing so if a stereomodel has to be measured, since the plates would have to be changed before the second set of measurements can be obtained and the computational solution takes place. A development of this on-line approach is the digital monoplotter, in which a monocomparator, or even a low-cost tablet digitizer, is attached on-line to the computer in which a file of existing digital terrain model (DTM) coordinate data is held. The orientation of the photograph is executed analytically by space resection and a continuous plotting of detail on the photograph may then be carried out monocularly, for instance for map revision purposes.

If a stereomodel has to be measured using a comparator in conjunction with an on-line computational solution, it is almost suitable to use a stereocomparator where the simultaneous measurement of both photographs comprising the stereopair can take place. Quite a number of stereocomparator on-line computer combinations exist. In practice and in many cases, the attachment of the computer to the stereocomparator coordinate output device and the writing of the necessary software have been carried out by the users themselves.

A direct development of this approach is the so-called image space plotter in which the computed terrain coordinates are plotted out graphically in

form of points or lines as soon as they have been determined. This procedure may be characterized or described as being an on-line, open loop solution. In contrast to the third approach of the analytical plotter, there is no oriented stereomodel nor there is a need to implement the formation and solution of the mathematical model in real-time.

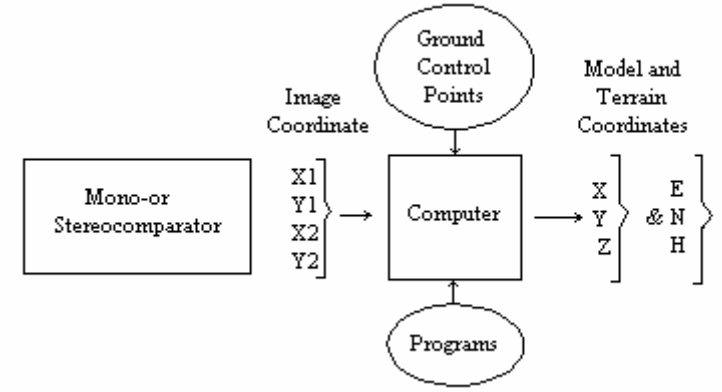

Figure(2.3)Comparator and on-line solution, after Petrie(1997)

2.4.3 ANALYTICAL PLOTTERS

The basic arrangement of an analytical plotter is similar to a stereo-comparator. However, an analytical plotter also features a closed-loop system in which the computer provides a real-time solution of the analytical photogrammetric equations (i.e. it forms the necessary mathematical and numerical model), and issues control signals to motors and driving elements, which also move the plates to the required positions in real time. The result is that an oriented stereomodel is formed and continuously maintained, and the photogrammetrist can measure the

planimetric detail and carry out contouring in exactly the same manner as in an analogue type of stereoplotting instrument.

As will be seen later, two different computational solutions are possible, based on the use of image or object coordinates respectively. The decision as to which of these solutions is used has a profound effect on the design of the analytical plotter and its eventual capabilities. In turn, these affect, in a fundamental manner, the provision of the software required to implement the analytical plotter concept. This includes:

i. The orientation programs which carry out numerically and mathematically the same or similar inner, relative and absolute orientation procedures to those which are used mechanically or optically in analogue instruments
ii. The real-time program which computes image or object point coordinates from the measured input data.
iii. The application programs which perform the digital data acquisition and processing of several operations; mapping, terrain modeling, aerial triangulation, the control of automatic image correlation, and the processing of measurements of deflection, deformation or dimensions in non-topographic photogrammetry.

2.5 ALGORITHMS FOR USE WITH ANALYTICAL PHOTOGRAMMETRIC INSTRUMENTATION

From the algorithmic point of view, there are two basic approaches to implementing analytical photogrammetric procedures- the first involves the measurement and input of image coordinates as the raw data to the computational process, and the second is based on the use of object (model or terrain) coordinates in a corresponding but different computational process.

- Image coordinates primary.
- Object coordinates primary.

2.5.1 IMAGE COORDINATES PRIMARY

The first approach is one in which the inputs are the x, y, coordinates of points measured on the photographs, i.e. the comparator coordinates, and the outputs are the X, Y, and Z model coordinates of these points. In turn, these model coordinates of each point can be transformed into the corresponding easting (E), northing (N), and height (H) coordinates of the terrain system. This approach is the one followed when the points have been measured in a comparator, whether a monocomparator in which each photograph is measured individually or a stereocomparator in which both photographs constituting a stereopair are measured simultaneously. It is also the approach implemented in certain types of analytical plotters.

In practice, one or the other of the two alternative solutions may be adopted within this general approach. In the first, the coordinates of each

camera station and the tilts present on each photograph are determined using the method of space resection. The measured x, y image coordinates and the known E, N, and H coordinate values of the ground control points required for their computation are linked together by the collinearity equations. Once the projection center coordinates and tilts of each photograph have been determined using these equations, the terrain coordinates of all other points measured on the stereopair may be computed using the space intersection technique, again based on the collinearity equations.

The alternative, mathematical solution involves the coplanarity approach. The corresponding x, y image coordinates measured for common point in the stereopair of photographs are used to generate parallaxes from which the tilts of each photograph may be calculated i.e. an analytical relative orientation is achieved. Once these tilt values have been determined, it is then possible to compute the values of the X, Y and Z model coordinates from the measured image coordinates (x, y) of any point, again using specific forms of the collinearity equations. The computed X, Y, and Z model coordinates are then converted by a simple three-dimensional linear conformal or affine transformation into the corresponding E, N, and H terrain coordinate value.

2.5.2 OBJECT COORDINATES PRIMARY

The second approach is the inverse of the first in which the inputs to the analytical photogrammetric solution are the X, Y and Z model coordinates of the measured points. From these, the corresponding image coordinates (x, y) of each point may be computed for each of the component photographs of the stereopair. Simultaneously the X, Y and Z model coordinates of each measured point may also be transformed into the corresponding terrain coordinate values (E, N, H). The use of object coordinates (model or terrain coordinates) as the primary input to the solution is perhaps less obvious to the non-expert, but in fact it is the more straightforward and easier solution to implement in analytical plotters, especially if there is a requirement to produce contours or to generate a digital terrain model in which the measured points have to be located at predetermined positions in the terrain coordinate system under computer control. Thus the majority of analytical plotters follow the object coordinates primary approach.

In mathematical terms, this approach is once again implemented using the colinearity equations with the terms rearranged so that the input values to the computational process are the measured or given object coordinate values (i.e. X, Y, Z) or (E, N, H) coordinates, and the output values are the corresponding x, y image or plate coordinates. These latter values are the positions to which the plates (photographs) are being driven to by the motors and feedback control mechanisms of the analytical plotter to

maintain an oriented, parallax-free stereomodel in which the photogrammetrist can carry out the stereoplotting of line detail or the measurement of individual elevation points or continuous contours or height profiles.

2.6 ANALYTICAL STEREOPLOTTING INSTRUMENTS

Two main types of analytical plotters may be distinguished; one implements the image coordinates primary approach discussed above, while the other is based on the alternative object coordinates primary approach.

2.6.1 ANALYTICAL PLOTTERS WITH IMAGE COORDINATES PRIMARY

The general layout of this type of instrument is given in Fig(2.4). The measuring part of the instrument is, in all major respects, akin to that of a stereocomparator. The two hand wheels, which are operated manually by the photogrammetrist, physically move the left plate to each point being measured or plotted. In this way, the x- and y-coordinates of the left-hand image (x_1 and y_1) are generated. The foot wheel, again operated by the photogrammetrists, imparts the required height value (H) by displacing the right photograph in the x-direction, i.e. it imparts the corresponding x-parallax (px_2) to the right hand image. The final manual input is the y-parallax movement (py_2), which can be input by the operator during the

initial orientation phase of the operation when the instrument is being set up before plotting of the maps or measurement of individual points.

All four possible manual inputs are sent to the computer as digital image coordinates values (x1, y1, px2, py2) using encoders. Once the orientation phase has been completed, the small additional corrections Δpx2 and Δpy2 required to maintain a fully oriented model are generated continuously and in real time by the computer for every position being measured by the operator. The actual physical shifts of the right-hand plate corresponding to these corrections are carried out using stepping motors.

At the same time, the computer is continuously calculating the model (X, Y, Z) and terrain (E, N, H) coordinates of each measured point, which can be transferred and recorded on a tape or a disc. In addition, the co-responding positions (Xt, Yt) of the plotting device on an attached drawing table or coordinatograph can be continuously computed and plotted in the form of points, symbols and lines. The required movements being made by digital stepping motors operating under the control of the analytical plotter's computer.

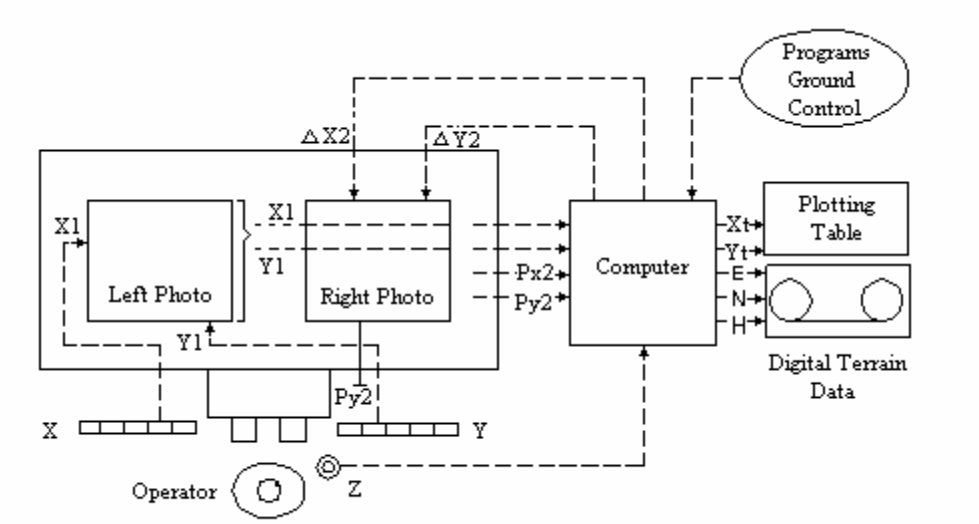

Figure (2.4) Analytical plotter with image coordinates primary, after Kennie and Petrie(1993).

However, a limitation is that, since the terrain coordinates are not a primary input (they are output values), it is impossible to be driven to specified positions under computer control. This can be important in some applications, for example the measurements of elevations at specific points as required for digital terrain modeling.

2.6.2 ANALYTICAL PLOTTERS WITH OBJECT COORDINATES PRIMARY

The basic layout of this type of instrument is shown in Figure(2.5). Again the measuring part of the instrument corresponds closely to that of stereocomparator. However it will also be seen that the movements of the ***X*** and ***Y*** hand wheels and the ***Z*** foot disc made by the operator are encoded and go directly to the control computer. In this way, the object coordinates ***X***, ***Y***, and ***Z*** are input to the computer. This is a major

difference to the arrangement used in the previous type of analytical plotter, where the hand-wheel directly drives the left-hand plate of the instrument. In the 'object coordinates primary' type of instrument, the computer outputs are, in first place, the four-image coordinates x_1, y_1, (for the left photograph) and x_2, y_2 (for the right photograph). These values are applied continuously to the stepping motors of each plate and ensure that the correct positions corresponding to the input coordinates are being viewed and measured by the operator, and that, simultaneously, the stereo-model is being maintained in an oriented, parallax-free condition. In addition, the control computer will also calculate and send, in real time, the required table coordinates position (X, Y) to an automated drawing table or to a graphics terminal to ensure continuous plotting or display of the measured detail or contours. Alternatively or simultaneously the model (X, Y, Z) or terrain (E, N, H) coordinate data can be recorded on a magnetic media or disk.

It will be seen that this particular design approach leads to the most capable and flexible form of an analytical plotter. Unlike the previous type of analytical plotter and although it requires more control mechanisms (motors and drives), it is easier to carryout contouring on this type. It is easy to ensure that the instrument can be positioned at prespecified or predetermined points under computer control. As a result of these considerations, most of the larger photogrammetric manufacturers have adopted this approach.

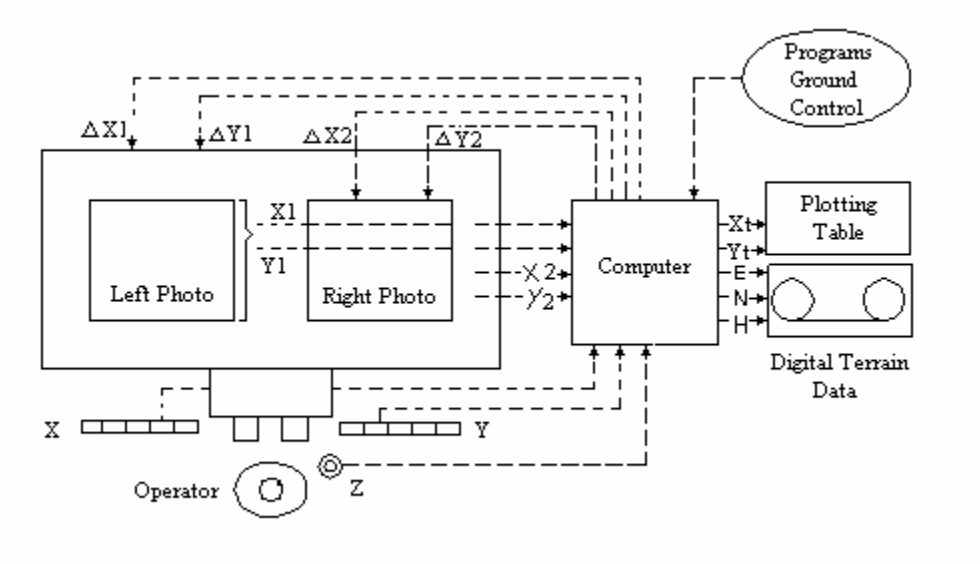

Figure (2.5) Analytical plotter with object coordinates primary, after Kennie and Petrie(1993).

All of these instruments address the conventional aerial photogrammetric marketplace; in that they can accommodate standard 23X23cm format aerial photography and can carry out aerial triangulation for the provision of additional control points to allow the stereoplotting of individual models for topographic map compilation. In addition, most manufactures can provide softwares for the acquisition of digital terrain model (DTM) data. This allows the instrument to be driven to pre-defined points in the terrain coordinate system (***E***, ***N***, ***H***), including, in some cases, the implementation of progressive sampling by which the density of the sampling on a grid basis is varied according to the local roughness of the terrain surface.

2.7 ADVANTAGES OF ANALYTICAL PLOTTERS

Utilizing an analytical plotter instead of the analogue type of stereo-plotting instrument presents various advantages. These may include:

1. The very high measuring accuracy (1 to 3 μm in the most accurate instruments), allied to the possibility of correcting for systematic errors such as lens distortion and film deformation by numerical methods. Also the analytical solution using least squares techniques produces better results than those obtained in analogue plotters. In addition, in analytical plotters there are no mechanical parts, so this can reduce the systematic errors produced from these parts. All these advantages mean that ***more accurate determination of position and height can be achieved***.
2. It is possible to form and measure stereo-models using photography taken with cameras with focal length values, format size and tilts which are ***beyond the range of normal analogue stereo-plotting instruments;*** such as the use of a long focal lengths (***f***=30 cm to 120 cm) and enlarged format sizes (23X46 cm) used in space borne cameras. The direct plotting of vertical or high or low oblique photography taken with non-metric reconnaissance cameras, including panoramic cameras; and the measurement and plotting of metric or non-metric terrestrial photography for industrial purposes.

3. It is also possible to use analytical plotters to measure images, plot maps and form terrain models from the non-photographic ***remotely sensed imagery*** such as the measurement of stereo-models formed from overlapping side-looking radar images and from the stereo-imagery produced by the spot pushbroom scanner.
4. The analytical plotter offers the possibility of ***automating*** substantial parts of the photogrammetric procedure so that certain tasks can be carried out more rapidly and efficiently. In turn, productivity is increased and can be achieved with much less effort on the part of the operator.

CHAPTER 3

THE DIGITAL CAMERA

Chapter 3
THE DIGITAL CAMERA

3.1 INTRODUCTION

Images in a digital form can be obtained either by using scanners to convert analogue photography, such as diapositives or negatives, taken with a film based frame camera, to digital imagery or by using an electronic camera as shown in Fig(3.1).

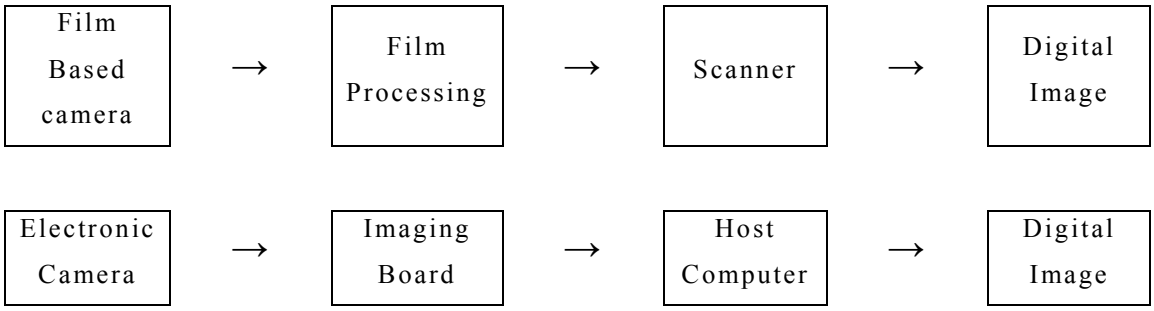

Fig(3.1) Data acquisition, after Kennie(1993).

The early-developed electronic imaging system had quite limited applications. Vidicon tube cameras were not very accurate, proprietary hardware and software increased the cost and offered little flexibility. The appearance of solid-state cameras in the early eighties eliminated these shortcomings. Electronic cameras based on charge-coupled device (CCD camera) greatly changed electronic imaging systems ranging from consumers, electronic still cameras, document scanners, machine vision and scientific cameras.

3.2 GENERAL FUNCTIONALITY OF ELECTRONIC IMAGING SYSTEMS

An electronic imaging system can be employed in different ways depending in the basic functionality of each. The basic functions of an electronic imaging system are:

1. **Image capture:** Refers to the process of obtaining an image during the time of exposure. This corresponds to the latent image of film-based cameras.
2. **Analogue to Digital (A/D) conversion:** Since these images are inherently analogue, an analogue to digital conversion must take place at some stage. The result is a raw digital image
3. **Low-level signal processing:** A raw digital image is processed by a low-level signal processing first.
4. **Further processing and analysis:** This is done by the main processing unit depending on the application at hand.

As shown in Fig(3.2). The functionality can be divided into several modules:

1. The first module represents the traditional electronic imaging system comprising an electronic camera, e.g. solid-state camera where the frame grabber provides for the A/D conversion, processing and a host computer.

2. The second consists of a digital camera. The digital camera performs the A/D conversion and the output is a digital signal.

3. In the third module the processing power of the frame grabber increases due to new signal processing chips, fast memory and miniaturization of microprocessors. This type of frame grabber is known as imaging board.
4. The camera on a chip is an extreme case of miniaturization. It basically consists of a signal chip and a lens, supplemented with a signal processing chip for image compression, colour interpolation, and interface function.

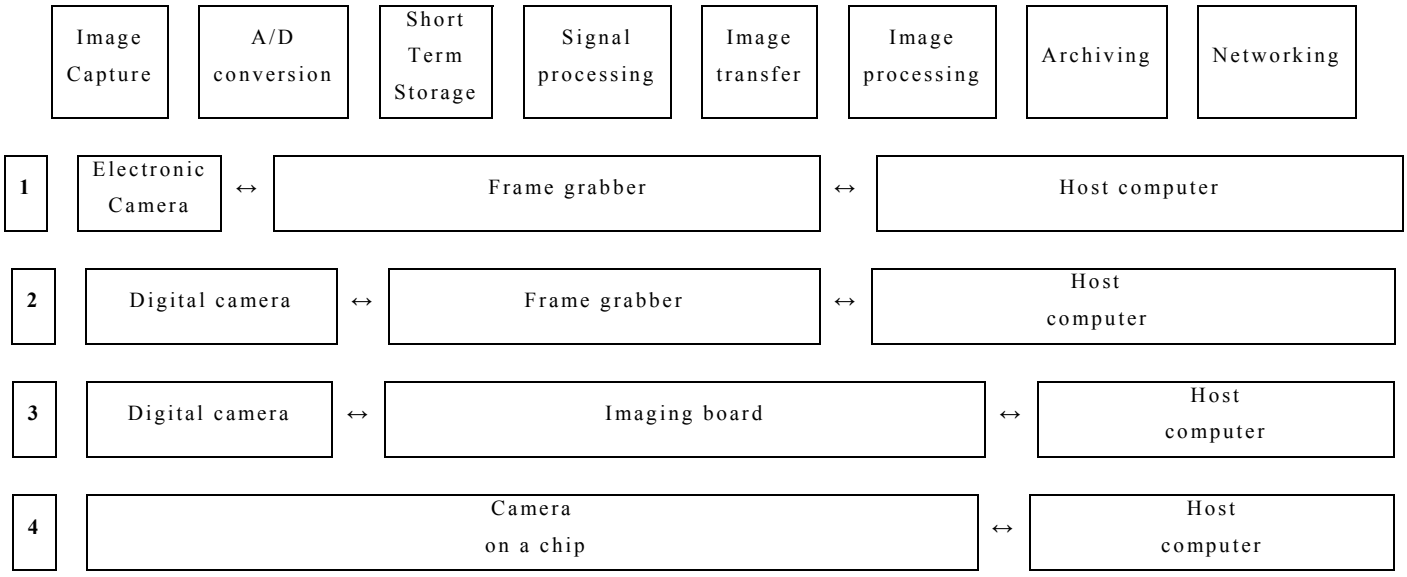

Fig(3.2) General functionality of an electronic imaging system, after Schenk(1999)

3.3. VIDEO CAMERAS

Video cameras mounted on an aerial platform have been used for a number of engineering applications, including the monitoring of traffic flow (Schenk 1999), the recording of stages in the development of

engineering projects, and the assessment of the impact of construction activities such as pipelines on the terrain.

The imaging system used in a video camera is based on a conventional lens and shutter arrangement. However, unlike photographic methods, the video image is formed by recording the charge falling on to a photosensitive screen (Fig3.3) rather than on to a silver halide emulsion. Incoming light falling on to the charge face of the vidicon tube induces a positive charge proportional to the brightness of the incoming radiation, and hence a latent image is performed on the charge face. In order to develop this latent image, an electron beam scans the charge face in a raster fashion, and in so doing discharges the initial positive charge.

The lenses used in video cameras normally have very short focal lengths (typically 8-35mm) and the image format size is also very small in comparison with conventional photographic methods. Successive frames of imagery are recorded at rates which are typically between 25 and 30 Hz on to either magnetic tape or video tape.

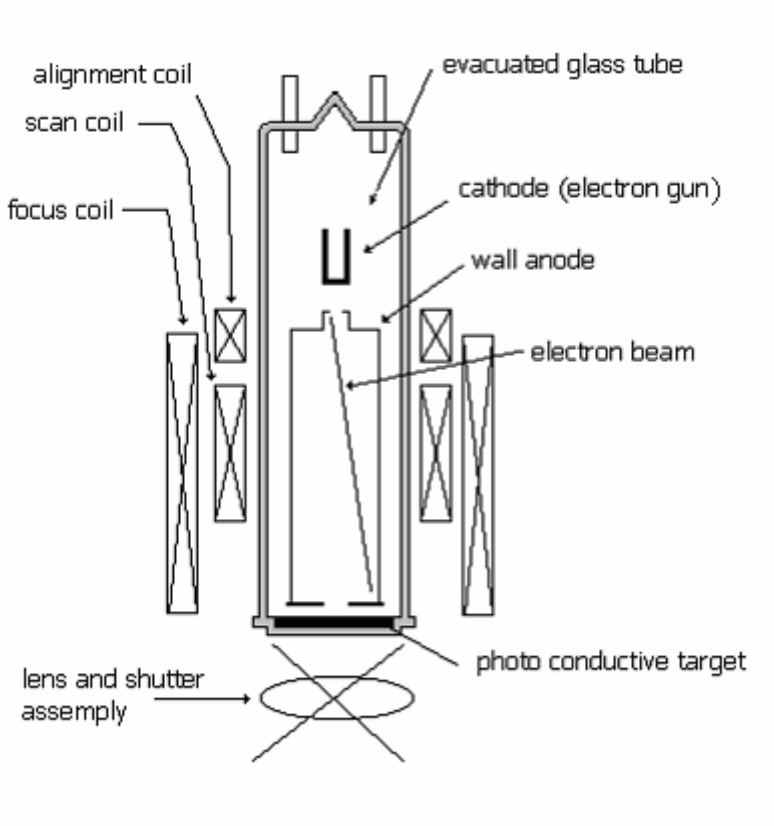

Figure(3.3) Principle of operation of vidicon, after Schenk(1999)

3.3.1 RETURN BEAM VIDICON (RBV) CAMERA

RBV camera operates in a manner similar to the more common vidicon. However, unlike the vidicon, the signal is continuously reflected back to the aperture of the electron gun. The main advantages of this design are:

1. The ability to produce higher- resolution images, and
2. The ability of the photoconductive surface to remain in focus for longer periods.

The best –known example of an RBV camera system is that which is operated on board Landsat 3. Two RBV cameras with a spectral range of 0.505-0.750μm (green to near infrared) were operated, and had a ground pixel equivalent to 30m.

3.4 CHARGE COUPLED DEVICE (CCD) SENSORS

3.4.1 THEORY OF WORKING

The basic building block of a CCD is a *semiconductor capacitor,* which is usually silicon and the *insulator* is an oxide (MOS capacitor) as shown in Fig(3.4) below.

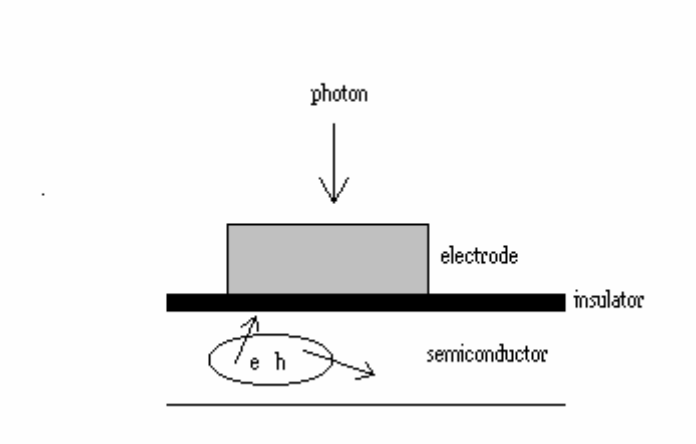

Fig(3.4) principle of a semiconductor capacitor, after Schenk(1999)

The metal electrodes are separated from the semiconductor by the insulator. Applying positive voltage at the electrode, forces the mobile holes to move towards the electric ground. In this fashion, a region (depletion region) with no positive charge is formed below the electode, on the opposite side of the insulator.

If Electro Magnetic Radiation (EMR) is incident on the device, photons with an energy greater than the band gap energy of the semiconductor may be absorbed in the depletion region, creating an electron-hole pair. The electron, referred to as photon electron, is attracted by the positive-charge of the metal electrode and remains in the depletion region while the

mobile hole moves towards the electrical ground. As a result, a charge is accumulating at the opposites side of the insulator. The maximum charge depends on the voltage applied to the electrode. The actual charge is proportional to the number of absorbed photons under the electrode.

The band gap energy of silicon corresponds to the energy of photon with a wavelength of 1.1 μm. According to Blanck's quantum theory of electromagnetic radiation.

$$Q_\lambda = \frac{h.c}{\lambda} \text{----------(3.1)}$$

Where,

Q_λ is the energy,

λ is the wave length,

c is the speed of light and

h represents Blanck's constant

Equation (3.1) can be thought of as providing the correspondence between the wave nature of light and its particle nature (wave-particle quantity) of EME.

Lower energy photons (but still exceeding the band gap) may penetrate the depletion region and be absorbed outside. In that case, the generated electron-hole pair may combine before the electron reaches the depletion region. It is realized that not every photon generates an electron that is accumulated in the wall. Consequently, the quantum efficiency is less than unity.

3.4.2 THE CCD ARRAY

An ever-increasing number of capacitors are arranged to what is called a CCD array. It is costumary to refer to these capacitor sites as detector pixels, which can be arranged in different ways such as:

1. Linear array,
2. Frame transfer,
3. Interline transfer,
4. Time delay and integration transfer.

3.4.2.1 LINEAR ARRAY WITH BILINEAR READOUT

On this case on both sides of the single line of detectors is another line array (CCD shift register) as shown in Fig (3.5). Since these two CCD arrays are also light sensitive, they must be shielded. After integration the charge accumulated in the active detectors is transferred to the two shift registers during one pixel clock. The shift registers are read out in a series fashion. If the readout time is equal to the integration time, then the sensor may operate continuously, without a shutter. This principle is known as *pushbroom* which is put to advantage in line cameras mounted on moving platforms to provide a continuous coverage of the object space.

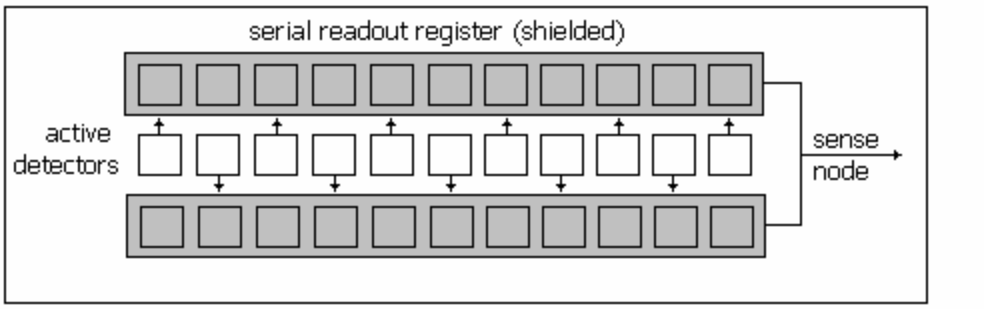

Fig(3.5) Linear array with bilinear readout, after Schenk(1999)

3.4.2.2 FRAME TRANSFER

If we assume that, the frame transfer image as consisting of two identical arrays. The active array accumulates during integration time. This charge is then transferred to the storage array, which must be shielded since it is also light sensitive. During the transfer, charge is still accumulating in the active array, causing a slightly smeared image.

The storage array is readout serially, line by line. The time necessary to readout the storage array far exceeds the integration. Therefore, this architecture requires a mechanical shutter. The shutter offers the advantage that the smearing effects are suppressed.

3.4.2.3 INTERLINE TRANSFER

The concept of interline transfer array is that, the columns of active detectors (pixels) are, separated by vertical transfer registers. The accumulating charge in the pixel is transferred at once and then readout

serially. This allows again an open shutter operation assuming that, the transfer registers can be readout during integration time.

Since the CCD detectors of the transfer register are also sensitive to irradiance, they must be shielded. This in turn, reduces the effective irradiance over the chip area. The effective irradiance is often called *fill factor*. The interline transfer imager as described here has a fill factor of 50%. Consequently longer integration times are required to capture an image. To increase the fill factor, a micro-lens may be used. In front of every pixel is a lens that directs the light incident on an area defined by the adjacent active pixels to the (smaller) pixel, (T.Schenk 1999).

3.4.2.4 TIME- DELAY AND INTEGRATION (TDI) TRANSFER

This type of CCD array resembles closely what is known in photogrammetry as forward motion compensation for aerial cameras. The idea of TDI transfer is to subdivide the integration time in *n* intervals and to transfer the charge accumulated during one such interval to the next column of pixels where it continues to accumulate during the next interval. Consequently, this approach corresponds to moving the film by an amount proportional to the distance the object traveled during exposure time, which is called Image Motion Compensation (IMC) in conventional photogrammetry.

3.4.3 NOISES IN CCD

In CCD sensors, not all of the electrons being measured in the drain are generated from incident radiant flux. The detectors, including the electronic component, also produce nonsense electrons, (collectively called noise). These, may be:

1. Systematic noise, or
2. Random noise.

3.4.3.1 SYSTEMATIC NOISE

The systematic component of noise often produced by instrumental error and can be determined, by measuring the unexposed array and subsequently eliminated from the signal (like systematic errors).

3.4.3.2 RANDOM NOISE

Random noise originates from different sources. These may be due to:

1. Thermal motion of charged particles and thermal current fluctuations in the detector and other electronic components of the CCD sensor cause what is called *dark current,* which is affected by temperature. Dark current doubles with every 8°C temperature increase (T. Schenk, 1999)
2. The discrete nature of electromagnetic radiation,
3. Incident flux on the CCD sensor which has a random component (Radiation noise),

4. The generation of electrons by photons (photoelectrons) in the detector is random.

3.4.4 SPECTRAL SENSITIVITY OF CCD

The reflected radiation is usually detected by Silicon Photodiodes(SP), which are sensitive to wavelengths from 0.4 μm to 1.1μm (including emitted thermal infrared) radiation, is usually detected by photon detectors, either made from Mercury Doped Germanium (MDG) which is sensitive to wavelength from 3 μm to 14 μm or Indium Antimonite (IA) which is sensitive to wavelengths from 3 μm to 5 μm and Mercury Cadmium Telluride (MCT) which is sensitive to wavelengths from 8 μm to 14 μm (Harris 1987) as shown in table (3.1).

CCD Type	**Notation**	**Spectral sensitivity μm**
Silicon photodiode	*SP*	0.4-1.4
Mercury doped germanium	*MDG*	3-14
Indium antimonite	*IA*	3-5
Mercury cadmium telluride	*MCT*	8-14

Table(3.1) Spectral sensitivity of the CCD Detectors.

3.5 SOLID STATE CAMERA

Solid-state cameras, based on CCD sensors, (termed CCD cameras), are predominantly used in digital photogrammetry. Traditionally, the

output of a solid-state camera is an analogue video signal. Recently, cameras with a digital output have become available. These are generally termed '*digital cameras'*.

The chief advantages of the solid-state camera over the classical film based camera are:

- The instant availability of images for further processing and analysis, which is essential in real time photogrammetry.
- The increased spectral flexibility.

3.5.1 COMPONENTS OF A SOLID-STATE CAMERA

The major components of a solid state camera are shown in Fig(3.6) below. These are:

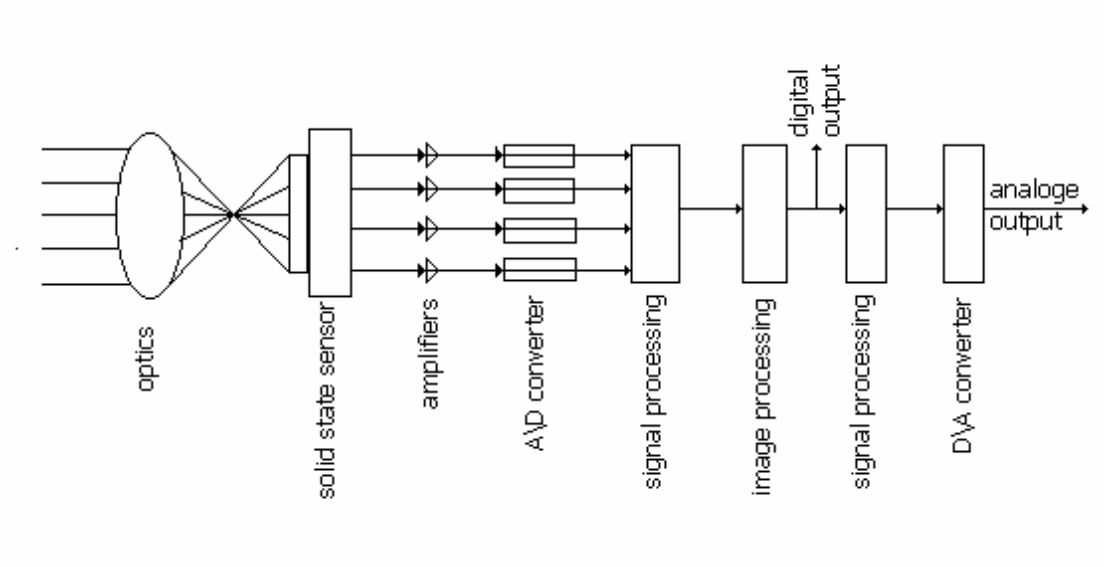

Figure(3.6) The major components of a solid state camera, after Schenk(1999).

1. The optics components: includes lens assembly and filters such as infrared blocking filter, to limit the spectral response to the visible spectrum. As an option, the optics subsystem may comprise a shutter.
2. The solid-state sensors: these are positioned in the image plane, and are either arranged in a linear array or a frame array. Linear arrays are used for aerial cameras while close range applications, including mobile mapping systems, employ frame array cameras. The accuracy of a solid state camera depends, to a great deal, on the accuracy and stability of the sensing elements, such as:
    i. The uniformity of the sensor element spacing,
    ii. Flatness of the array.
3. Amplifiers: the voltage generated by the sensor readout mechanism must be amplified for further processing.
4. Further processing: further processing begins with converting the analogue signal into a digital signal (A/D converter). This is not only necessary for producing digital output but also for signal and image processing.

3.5.2 LINE CAMERA

For a solid state camera to have a resolution comparable to a classical frame camera it must have sensing elements of the order of 20,000 X 20,000. Such image sensors do not exist and will not likely become available commercially in the near future (schenk, 1999). An alternate solution of frame cameras, are the so-called *line cameras*.

Line cameras use linear arrays, which are considerably cheaper than large staring arrays. Moreover, they can be put together more easily to increase the number of sensing elements and the readout is much shorter. Such cameras are used in SPOT imagining system.

Fig (3.7) sketches the principle of acquiring data with a line camera. A linear CCD array is placed in the camera's focal plane, which accumulates charges during the integration (exposure) time from a narrow strip on the ground (generally referred to as a line). The charge is transferred to an adjacent register and readout serially.

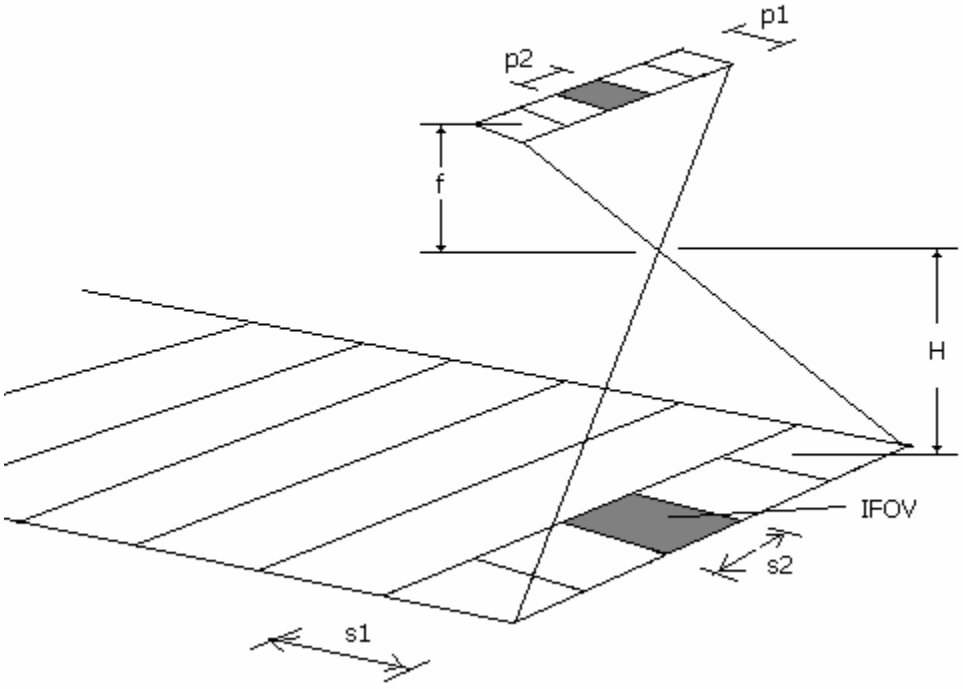

Fig(3.7) Principle of data acquisition with a line camera, after Kennie and Petrie(1993).

The projection of an array pixel on the ground is called Instantaneous Field Of View (IFOV) ant its dimensions are $s_1 x s_2$ where,

$$s1 = \frac{H}{f} p_1 \text{ --------(3.2)}$$

$$s_2 = \frac{H}{f} p_2 \text{ -------(3.3)}$$

p_1 and p_2 are the pixel dimensions of the CCD array,

H is the flying height and

f is the camera focal length.

If n is the number of pixels of the array, we obtain the width, L_w and the length, L_l of the line as follows:

$$L_w = s_1 \text{ ----------} (3.4)$$
$$L_l = s_2.n \text{ ----------} (3.5)$$

During integration time, t_i the platform moves by

$$\Delta s = v.t_i \text{ ----------} (3.6)$$

where v is the velocity of the platform.

Therefore, the effective IFOV is smaller for all practical purposes. Assuming a line width of $L_w = \Delta s$.

$$L_w = s_1 \approx \Delta s = v.t_i$$

Since the charge accumulated during the integration time is transferred very quickly to the shift registers, the array is immediately ready for a new integration cycle. This important property of CCD linear arrays, ensures continuous ground coverage.

For obtaining ground coverage of equal scales (in the direction of flight and perpendicular to it) we require $\Delta s = s_2$ *or*

$$v = \frac{H}{f.t_i} p_2 \text{ ----------} (3.7)$$

3.5.3 EXTERIOR ORIENTATION OF A LINE CAMERA

If the condition for the velocity, expressed in equation(3.7), is not satisfied then an unequal ground coverage results. Fig(3.8) depicts several conditions. The top row shows the lines on the ground while the bottom row is a sequential representation of the recorded irradiance by the CCD array.

The ideal situation is reached if the velocity condition (equation (3.7)) is satisfied and if the camera axes remain parallel from line to line. In

that case, the ground pattern should be covered by a number of lines as sketched in the figure. Fig(3.8a) demonstrates the case of $v_a=2v$, that is the ground pattern is covered in half the time. Fig(3.8b) is an example of an irregular velocity across the ground pattern. The result is a distorted image. However, an apparent change in velocity may be caused by a rotation of the camera axis, due to pitch and roll, for example. If we imagine a rotation about the longitudinal axis of the platform carrier, known as roll in case of airplanes, or as ω- rotation to photogrammetrists, the consequence is a lateral displacement of the lines, as illustrated in Fig(3.8c). An interesting situation occurs when a rotation perpendicular to the carrier is present (pitch or φ- rotation). Now, the apparent velocity may even become negative as in Fig(3.8c). The resulting image is highly distorted and does not resemble the ground pattern any more. Finally, (Fig.3.8d) shows the effect of crab (κ-rotation).

These distortions represent a fundamental problem of line cameras, namely the determination of the exterior orientation of every line.

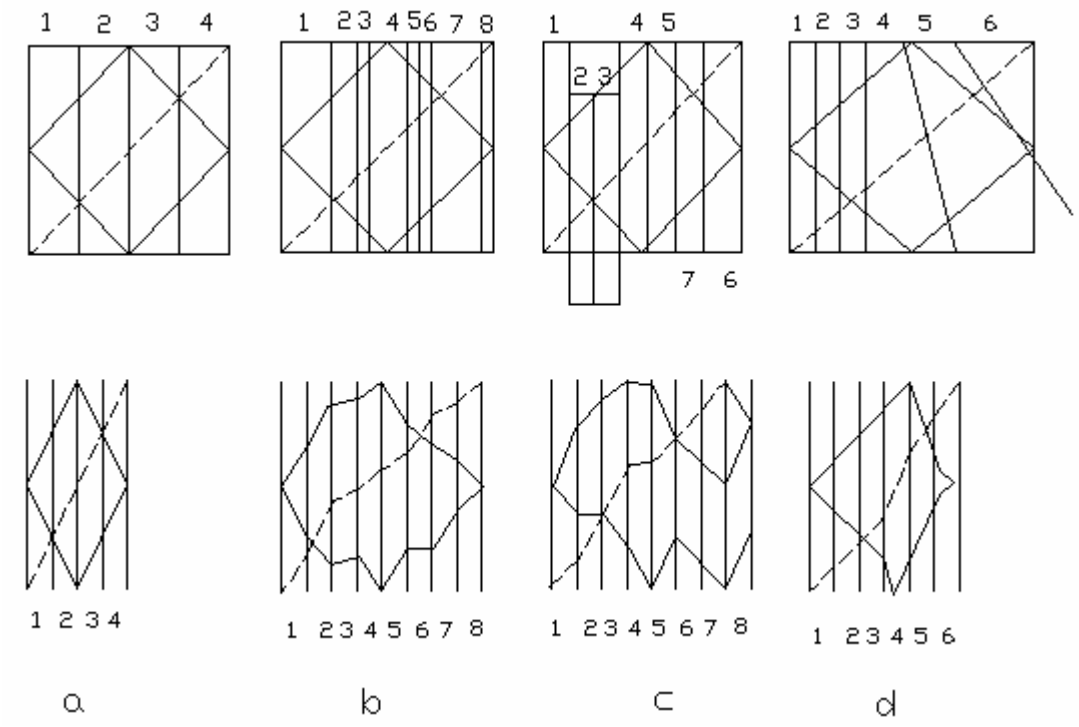

Fig(3.8) Unequal ground coverage by a linear array camera, after Schenk(1999).

3.5.4 ADVANTAGES OF LINE CAMERAS

The advantages of the line camera can be summarized in:

1. Relatively simple design,
2. Low cost for the linear sensor array
3. Coloured imagery can be acquired by adding additional linear arrays with different spectral sensitivity.

3.5.5 ANALOGUE OUTPUT

The concept of interlace presented in Fig(3.9) shows a frame of 525 scan lines consisting of two fields, (called odd and even fields). To provide time for vertical retrace, only 485 lines are displaced, however. That is,

every field has 242.5 active lines. The first line of the odd field begins in the left upper corner. After a horizontal retrace, the procedure repeats itself until 242 lines are displayed. Now the remaining half line is displayed at the bottom, followed by a vertical retrace to the center of the very top scan line where the display of even field begins.

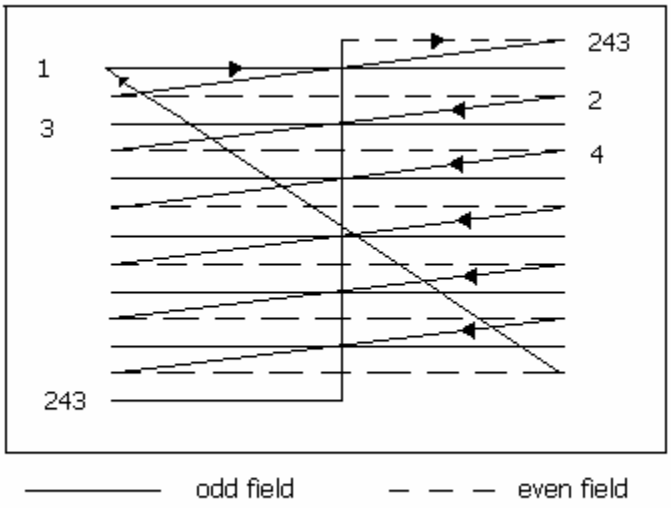

Figure(3.9) The concept of interlace, after Schenk(1999).

3.5.6 A/D CONVERTER

The principle task of the frame grabber is to convert the analogue video signal into a digital form. This is accomplished by sampling the signal into n^2 equal intervals, where nxn is the resolution of the camera, that is, the number of pixels. Fig(3.10) shows a video signal. The horizontal synchronization (h-sync) signal marks the beginning of a frame. The time

interval, Δt, for one frame is about 33 milliseconds (ms). Consequently, one pixel has a time interval of $\Delta t_p = 33\text{ms}/n^2$. We realize that for high-resolution images the clock that generates the sampling interval must be very precise. Moreover, the synchronization with the video signal becomes crucial.

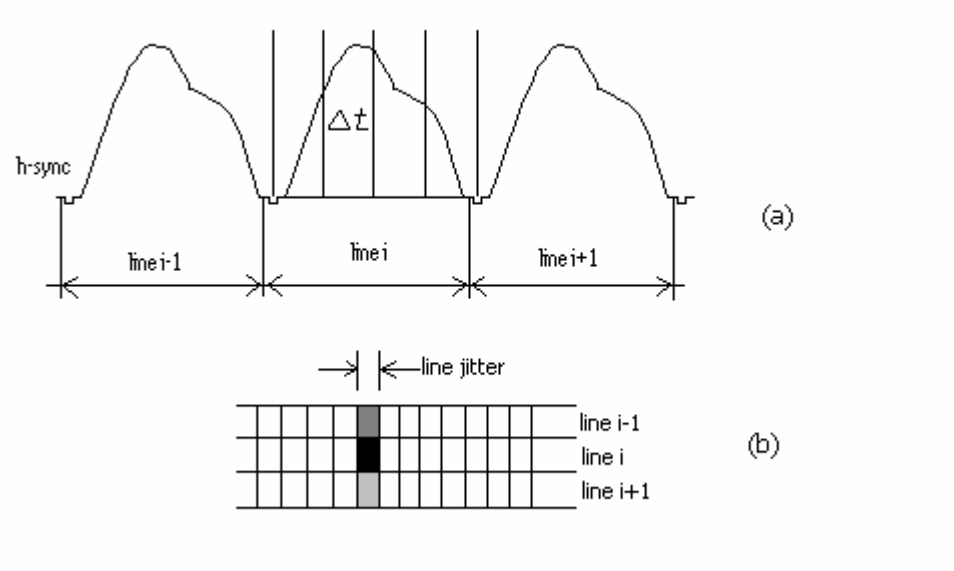

Fig(3.10) Video signal digitized by dividing the time interval between the two h-sync signals, after Schenk(1999)..

CHAPTER 4

PHOTOGRAMMETRIC SCANNERS

CHAPTER 4

PHOTOGRAMMETRIC SCANNERS

4.1 INTRODUCTION

Until now (2005), film based camera remains the main data acquisition source for aerial applications. Modern aerial cameras are an engineering feat. They provide, together with the film's impressive geometric and radiometric resolution, high quality photographs. Scanners convert hard copy documents into a digital form. In addition to digitize / scan aerial and satellite photography, scanners are also employed to convert line maps of all sorts into digital form. The requirement for converting such documents can be stated as follows:

1. Format Size:

Common size of aerial photographs is 9x9 inches (23X23cm) and 12x18 inches (30.5X45.7cm) for satellite photography.

2. Geometric Resolution and Accuracy:

This depends on the type of application. For accurate work, such as aerial triangulation a 15μm pixel size and 2μm pixel accuracy are required.

3. Radiometric Resolution:

The density range is 2.5 for panchromatic and up to 3.5 for colour photography.

4.2 TYPES OF SCANNERS

The scanners or raster scan digitizers are fully automatic devices capable of producing and storing a file of raw coordinate data for all images appearing on the photograph. Till recently (2005), most of these devices were ***drum scanners***, but nowadays, ***flat bed*** types are available. Figure(4.1) below shows the two types of scanners.

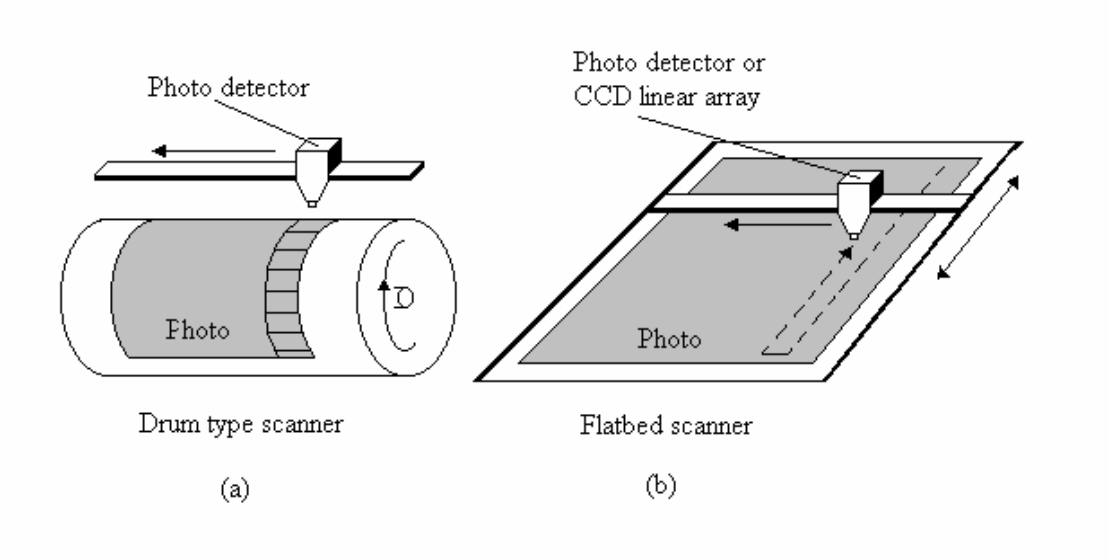

Figure(4.1) Types of scanners, after Kennie(1993)

4.2.1 DRUM TYPE SCANNER

In this type of scanner the photograph is wrapped around a drum, which is rotated at a constant speed below a photodetector head. This is moved, continuously, forward in steps along the axis of the drum Fig (4.2). The step size defines the width of the scan line. With these devices, it is possible to digitize either black and white (monochrome) or full colour photographs. In the former case a single photodetector is used (Fig(4.3)); in the later, different filters are used to perform colour

separation of the details contained in the photo (Fig(4.4)). Each colour-separated channel is being sensed for the presence or absence of data by its own individual photodetector.

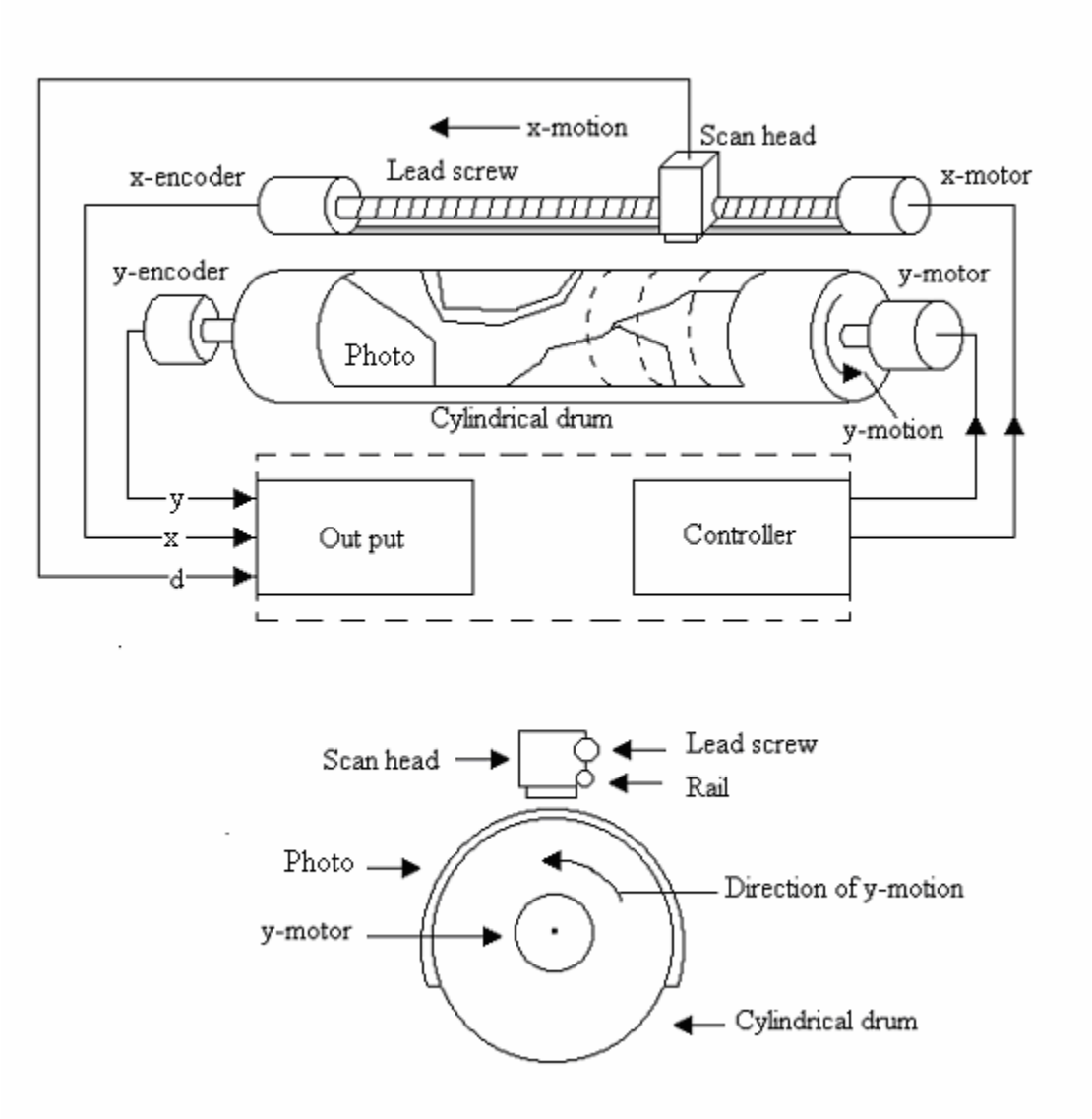

Figure(4.2)Drum type scanner, perspective view(upper) and cross-section(lower), after Kennie(1993)

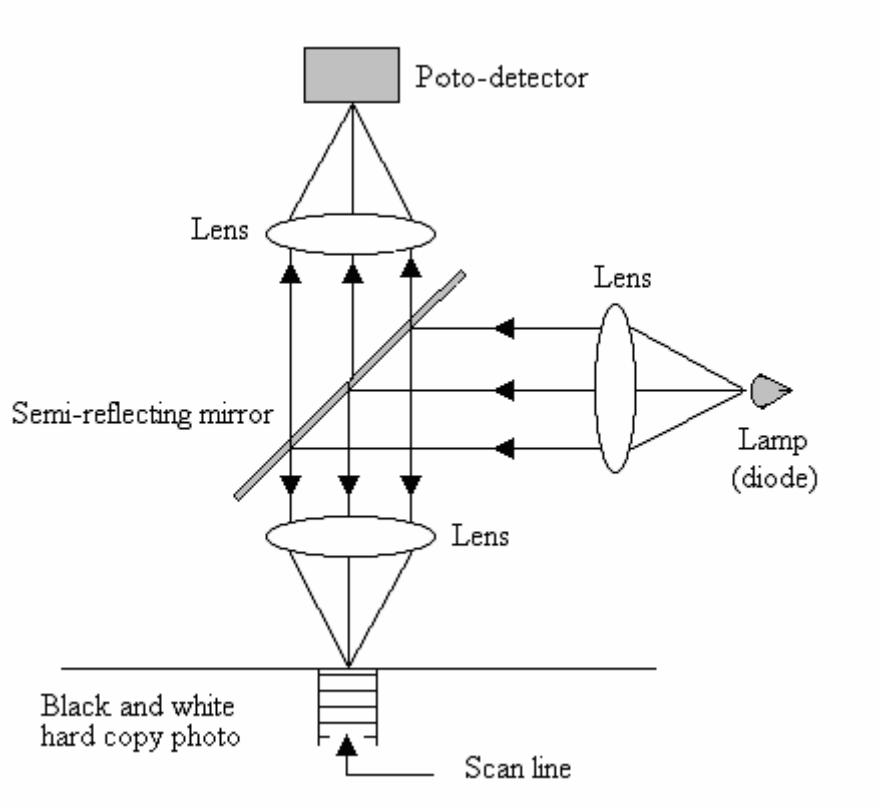

Figure(4.3)Scan head for monochrome image, after Petrie(1993).

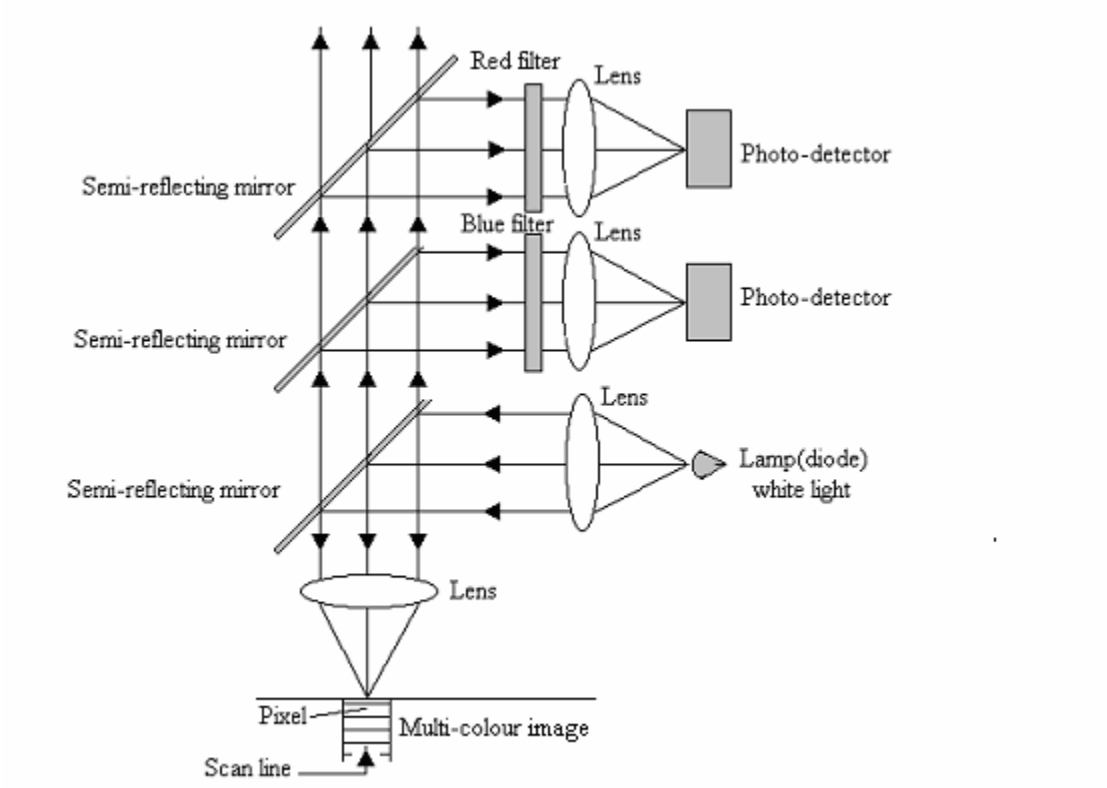

Figure(4.4) Scan head for colour image, after Petrie(1993).

4.2.2 FLAT BED TYPE

The alternative type of scanner is called flat bed. In this device the photograph is laid flat on a baseboard and is then scanned by a cross-slider or gantry which rapidly traverses the photo from top to bottom. Alternatively, the gantry may be held fixed and the sheet passed below it. The elements, which sense the image, are array of solid-state photodiodes. The coordinate data is read out continuously on a line by line basis and stored on disc or tape as in the drum type.

4.3 DRUM SCANNER VIA FLAT BED SCANNER

As impressive as the radiometric resolution fidelity of drum scanners is, their use is hampered by geometric problems, these are:

(i) Uneven drum surface,

(ii) Difficulty to press the film firmly against the drum,

(iii) Differences in rotating speed,

(iv) Calibrating drum scanners poses an additional problem because a high precision glass plat cannot be mounted.

Today's scanners are predominately flat bed type. The devices are in a solid-state sensor, such as increased number of sensing elements per chip and decreased size of the elements, account for the wide spread use of flatbed scanners.

4.4 PRINCIPLE COMPONENTS OF A PHOTOGRAMMETRIC SCANNER

The principle components of a flat bed scanner demonstrated are:

1. Illumination and an optics system,
2. Photo-carrier,
3. Sensor, and
4. Electronic components.

4.4.1 ILLUMINATION AND AN OPTICS SYSTEM

Illumination and an optics system is affected by different factors, such as:

1. **The light source:** must be stable and sufficient so that the flux incident on the light sensor is solely a function of the film density. Typical light sources are halogen lamps with a power of 100 to 300 watts, or fluorescent lamps. Such lamps may cause considerable heat diffusion, which, in turn may affect the sensor and the film stability. To prevent these undesirable effects, the thermally insulated lamp is positioned as far from the sensor and film as possible and a fiber optics cable guides the light to the illumination position. For compensating any variation in the light source, its energy must be measured directly and the corrections can be applied accordingly to the produced energy from the sensor.

2. **The dynamic scanning process:** the saturation energy of the sensor is the product of integration time with the incident flux. To keep the integration time as short as possible the light source must radiate enough energy. **Lighting method:** two possibilities in scanner design can be adopted; either diffuse or direct light.
   (a) In the case of diffuse illumination, a light scattering-glass plate is placed on top of the film. The advantages of this are:
      i. Small blemishes on the base of the emulsion, such as dust particles or scratches, will not be imaged.
      ii. In addition that diffuse light produces a smaller image noise than direct light sources.
   (b) Direct illumination requires a condenser lens. Its function is to generate coherent light from a point light source. This provides the advantage of the large depth of focus (due to the rather narrow bundle of light rays emanating from the light source), alleviating problems associated with defocalization.
3. **Colour wheel:** it contains the necessary filters for scanning colour film. With this solution, the film is scanned three times. Another solution to scanning colour images is using

three separate line sensors, each sensitive to a primary colour. In that case all thee colours are scanned in one pass.(figure 4.4)

4. **The lens system:** must be corrected for radial distortion and aberration. A critical issue is to ensure that the film patches are precisely imaged in the plate containing the sensor elements. Moreover, the relative position of the objective lens, film, and line sensor must remain constant during the sensing process.

4.4.2 PHOTO-CARRIER

The photo carrier of photogrammetric scanners is usually a modified version of the analytical plotter carrier stage. Thus, a high reliability and geometrical accuracy of about 2 μm can be expected. The photo carrier sits on two axes cross slide. Motion is controlled through a servo system through function device, for example. Linear encoders with an accuracy of 1 μm, or less, provide the positional feedback. The maximum speed is typically between 10 to 20mm/Sec.

Some scanners provide an option for scanning film rolls. Conceptually, the solution is similar to that employed in aerial cameras, except that for scanners, no vacuum is applied to press the film firmly against the glass plate. With this option, the manual loading of film is circumvented and it is conceivable that the scanning of an entire film

roll containing several hundred frames is carried out without the assistance of an operator.

As the photo carrier moves the film across the line sensor, a small strip, called ***swath***, is digitized. Its width is determined by the physical dimension of the sensor, multiplied with the magnification of the optical system

Swath width = sensor width × magnification

At the end of the swath, the carrier first moves perpendicular to the scan direction by the swath width and only then resumes the scanning operation. To prevent overlaps or avoid gaps between adjacent swaths, the shift must be very accurate. Moreover, a smooth movement at a constant speed in the scanning direction is essential as this determines the pixel size in the scan direction.

4.4.3 SENSORS

The sensor function is to measure the film density. The incident flux Q_i interacts with the film, where it is either absorbed, reflected or transmitted. The ratio of transmitted flux to the incident flux is the transmittance t

$$t = Q_t / Q_i$$

The density, D, is defined as the logarithm of the reciprocal of transmittance, or;

$$D = log\ (1/t)$$

A density scale of equal steps is perceived **linear**. It follows that the density range of a film should be digitized in equal steps. The density of black and white aerial films range from of 0.2 to 2.5, and colour films from 0.3 to 3.5.

Almost every flat bed scanner employs a ***CCD line sensor.*** One of the reasons of using the CCD line sensor instead of arrays is the increased sensitivity of line sensors.

Photo multipliers are the most sensitive and accurate sensing elements. They virtually count signal photons. It does not surprise that drum scanners, equipped with photo multipliers, provide linearity across the full density range of photographic material – a numerous problem with CCD sensor.

4.4.4 ELECTRONIC COMPONENTS

The scanner electronics consists of several components providing the following essential functionality

1. **A/D conversion:** The charge accumulated in the CCD sensor element is read out and converted to an analogue video signal. The output of the scanner is a digital signal containing the gray value of all the pixels. The A/D conversion module quantities the amplitude into 2^n equal steps (gray levels), where n is the number of bits required to represent the gray values. Although most scanners output 8 bits, the internal quantization is sometimes performed at a

high level, for example, with 10 to 12 bits. In that way some of the problems with low sensitivity in dark areas are alleviated. To accommodate fast conversion and individual corrections to every pixel, the technique of Look-Up-Tables (LUT) is used. For every analogue input value they contain the corresponding digital output. LUTs are generated during an internal calibration procedure.

2. **Sensor control:** A line sensor must be controlled, for example the sensor plane must coincide with the image plane. If colour sensitive elements are used, the control unit is responsible that all three line sensor receive light from the same film area.
3. **Carrier control:** Provides the necessary circuitry for the DC motors deriving the cross-slide system.
4. **Memory:** the digital signal may be temporarily stored in an internal memory.
5. **Output interface:** Provides the link to the host computer or a mass storage device. Ideally, the data transfer rate should correspond to the scanning speed.
6. **Host computer:** The host computer plays an important role. It provides:
    i. The graphical user interface for the operator to communicate with the scanner, and

ii. Controlling and monitoring the scanning process, application software may analyse scanned image for completeness and consistency.

4.5 THE CONCEPT OF PIXEL SIZE

There are different types of pixels that exist in digital photogrammetry; these are:

1. **Sensor pixel:** refers to one sensor element. Its size is determined by the type of the line scanner. Typical sizes are between 10 and 15μm.
2. **Scan pixel:** refers to the projected area of the sensor pixel onto the film. It is what the scanner outputs to the interface.
3. **Photo pixel:** refers to the film resolution. This is not a physical pixel; it is more a conceptual realization.
4. **Refined pixel:** this is the final result of the scanning and post processing procedures. This pixel is stored and eventually processed further by digital photogrammetry methods. If no post processing is performed on the host computer (such as enhancements) then the refined pixel is equal to the scanned pixel.

4.5.1 SENSOR PIXEL AND SCANNED PIXEL

Assume for a moment that the photo carrier does not move. The sensor elements are projected through the lens onto the film. In that

case the size of the scan pixel would be equal to the size of the sensor pixel multiplied with the magnification of the optical system.

If the photo carrier moves, the sensor pixel is projected onto the moving film during the exposure time. The pixel size ***s*** in the scan direction is now a function of the scanning speed and exposure time. The pixel size along the scan direction S_y is equal to

$$S_y = v.\Delta t \text{ ----------(4.1)}$$

where

v is the scan velocity,

Δt the integration time.

And the pixel size along the line sensor S_x is equal to

$$S_x = S_s.m \text{ ----------(4.2)}$$

Where

S_s is the sensor pixel size,

m is the magnification of the optical system.

Therefore, we can say that the size of the scan pixel is controlled by the optical magnification of the sensor pixel in one direction and by the velocity of the photo carrier and integration time of the sensor element in the other direction.

4.5.2 SCAN PIXEL AND PHOTO PIXEL

Before the scanning procedure takes place, one should think of how large should the scan pixel be so that the original document (film) is

represented as faithfully as possible. This is the same as to ask for the minimum size of the photo pixel, or the resolution. Film resolution is often expressed by the number of line-pairs per millimeter, which is still used. An alternative method of describing resolution is the Modulation Transfer Function (MTF), which employs a bar chart with progressively closer spacing of the bars (Floyd 1999). From these values it can be found that the size of the photo pixels is 10 to 20 μm for black and white and 15 to 25 μm for colour emulsions. According to the sampling theorem, the pixel size should be half the highest frequency, or half the spread function width in this case.

4.6 SOURCES OF ERRORS

The majority error sources can be either geometric errors or radiometric errors.

4.6.1 GEOMETRIC ERRORS:

The repeatable accuracy of the high quality photogrammetric scanners is 2 μm over the entire format. Even this accuracy is maintained, potential problems may arise from:

a) **Misaligned line sensors**, which result in;

(i) a skewed image coordinate system,

(ii) small gaps between adjacent swaths,

b) **Wrong scale perpendicular to the scan direction**, caused by a wrong optical magnification, which results in

(i) an overlap between swaths, or

(ii) gaps between swathes

c) **Scale errors along the scan direction**, caused by an uneven speed or poor synchronization between the sensor and the photo carrier, results in

(i) a rectangular pixel shape, and/or

(ii) pixels of the same row in adjacent swaths do not match exactly.

4.6.2 RADIOMETRIC ERRORS

This may include:

a) Emulsion of aerial films have a large dynamic range and, more or less, linear characteristic of the density as a function of exposure. On the other hand CCD sensors are not linear in high-density areas.

b) Other radiometric problems may arise from colour miss-registration, due to chromatic aberration or positional offsets of the image path projected to the colour sensitive line sensors. Proper colour balance may be difficult to achieve because the CCD sensor sensitivity is quite

different in the visible portion of the spectrum. Blue has a much lower sensitivity than red and green.

c) The radiometric resolution is further reduced by electronic noises, such as thermal noise and blooming. A measure to reduce electronic noise is to cool the sensor and to average multiple measurements. Also, slower integration and readout time help in reducing the noise.

CHAPTER 5

DIGITAL IMAGE PROCESSING

CHAPTER 5

DIGITAL IMAGE PROCESSING

5.1 INTRODUCTION

Digital image processing is central to the effective use of modern digital photogrammetry and remote sensing data. Although a limited amount of information can be gleaned from the interpretation of a photographic image produced from aerial photography, for example, the full potential of the data can only be realized if the original data, edited and enhanced to remove systematic errors, are used with a suitably programmed image processing system.

5.2 DIGITAL IMAGE

Any scene in the real world can be mathematically expressed by a two-dimensional light intensity function $g(x, y)$ where x and y denote spatial coordinates and the value of g at any point (x, y) is proportional to the brightness or the gray-level of the image at that point.

A digital image is the representation of the scene, which has been digitized, both in spatial coordinates and in brightness. Hence, the image can be considered as a matrix whose rows and columns indices identify a point in the image and the corresponding element of the matrix represents the gray-level at the point, as shown in Eq(5.1). The elements of the

matrix are usually referred to as image elements or picture elements or pixel.

$$f(x,y)=\begin{bmatrix} g(0,0) & g(0,1) & .... & g(0,n-1) \\ g(1,0) & g(1,1) & .... & g(1,n-1) \\ .... & .... & .... & .... \\ g(n-1,0) & g(n-1,1) & .... & g(n-1,n-1) \end{bmatrix} ----(5.1)$$

5. 3 SAMPLING AND QUANTISATION

In order to be in a form suitable for computer processing, a continuous image function *g(x,y)* must be converted to discrete values, both in spatial coordinates and in amplitude. Spatial coordinates digitization is usually called image ***sampling*** while amplitude digitization is, commonly, spatial coordinates read to as gray-level ***quantisation***.

5.4 IMAGE DESCRIPTION

The most important methods that are used to describe a digital image are either mathematically by an average and standard deviation or graphically, by a histogram.

5.4.1 AVERAGE AND STANDARD DEVIATION

The average $\breve{g}_a$ of the gray level of the digital image reflects the overall brightness of an image as shown in Eq(5.2).

$$\bar{g}_a(x,y)=\frac{1}{n.m}\sum_{x=0}^{n-1}\sum_{y=0}^{m-1}g(x,y)----------(5.2)$$

on the other hand the standard deviation of the image gray level reflects the contrast of the digital image as in Eq(5.3) below.

$$\sigma = \sqrt{\frac{1}{n.m}\sum_{x=0}^{n-1}\sum_{y=0}^{m-1}(g(x,y)-\overline{g_a})^2} \text{ ----------(5.3)}$$

5.4.2 HISTOGRAM

Let $p_i(z)$ denotes the relative frequency with which the gray levels z occurs in an image $f(x,y)$ and let [$zl,\ldots,zu$] be the rang of gray levels. Assuming that the gray levels are normalized in the interval [0,1] it follows that the histogram is the probability density function $p_i(z)$ of image i. For equalized gray levels we have for the cumulative density function

$$h_i = \sum_{z=l}^{u} p_i(z) \text{ --------(5.4)}$$

5.5 DIGITAL IMAGE PROCESSING

Digital image processing techniques are used to improve the visual appearance of images to a human observer and to process pictorial information suitable for machine perception (Gonzalez 1993). It can be divided into the following areas:

Acquisition: deals with the ways of how to acquire images. For example, by using a digital camera or by digitizing analogue images (photographs).

Storage and compression: are concerned with suitable techniques to store digital images.

Enhancement and restoration: these techniques are used to improve the visual appearance of images or to recover degraded images.

Segmentation: deals with partioning the image into meaningful regions.

Visualization: These are techniques used for presenting images on a variety of media, including monitors, printers, and film recorders.

Some of these are discussed in this chapter.

5.6 ENHANCEMENTS AND RESTORATION

The main objective of the image enhancement techniques applied to a digital image is to bring that image to be suitable for a particular application. Different operations can be adopted on the digital image for the purpose of enhancing or restoring. These are:

Point operations: the result of point operation depends only on the input gray level at the same point. Typical point operations include stretching and threshold of a gray level.

Local operations: here, several input pixels in the neighborhood contribute to the resulting output pixel.

Global operations: the entire input image contributes to the output.

Geometric operations: the result of geometric transformation depends on gray levels from different positions in the input image such as scaling, rotating, translating, and rectifying images.

Image enhancement techniques can be classified according to application to:

***Contrast stretching*:** To improve the contrast of the image.

Sharpening: To make certain features of an image more pronounced, e.g. edges.

Smoothing: includes techniques that render an image of smoother appearance, e.g. by removing noise or suppressing details.

Correcting defects: To correct image defects such as removal blunders in the gray levels.

Few of theses operations are highlighted hereafter.

5.6.1 CONTRAST STRETCHING

The stretch operation redistributes values of an input image over a wider or narrower range of values than the original. Stretching can, for instance, be used to enhance the contrast in the image when it is displayed. The two important stretch methods are linear stretch and histogram equalization (nonlinear stretch).

5.6.1.1 LINEAR STRETCH

In a linear stretch Fig(5.1) the gray levels of the image is modified by the following equation,

$$g_2(x,y) = \left[(g_1(x,y) - g_1 \min) * \left(\frac{g_2 max - g_2 min}{g_1 max - g_1 min} \right) \right] + g_2 min \text{ ------(5.5)}$$

Where,

$g_1(x,y)$ and $g_2(x,y)$ are the input and output values of the gray level,

$g_1 min$ and $g_1 max$ are the lower and upper ***'stretch from'*** boundaries,

$g_2 min$ and $g_2 max$ are the lower and upper ***'stretch to'*** boundaries.

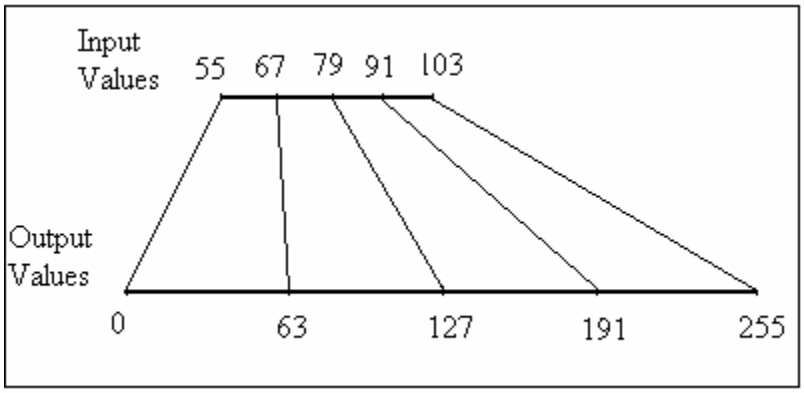

Fig(5.1) Schematic representation of a linear stretch, after Janssen(2000).

5.6.1.2 HISTOGRAM EQUALIZATION

Histogram equalization or histogram linearization defines a transformation from a gray level g_1 to a gray level $g2$ so that distribution of $g2$ becomes even. That is, the histogram of $g2$ is uniform as shown in figure (5.2) below.

Lower and upper boundaries of the ***'stretch from'*** range are determined in the same way as with linear stretching. The ***'stretch to'*** values are determined from the number of specified output intervals. When 256 intervals are specified, the output values will range from 0 to 255. Then the following procedure is adopted:

The histogram of the input image is calculated. The total number of pixels with values is calculated (undefined values are not considered).

The total number of pixels with values, is divided by the number of required output intervals, in order to get a threshold, for the number of pixels that ideally should end up in each interval.

For the first interval, in the histogram of the input image, when the cumulative number of pixels reaches the 'threshold' value, the input value in the histogram closest to this 'threshold' is selected and all input pixel values equal or smaller than this value are assigned the first output value.
For the next intervals, whenever a next factor the threshold is reached in the input histogram, the value closest to the this threshold is selected and all input pixel values equal or smaller than this value but larger than the previous interval boundary value are assigned the next output value.
In this way all output intervals are filled with input values.

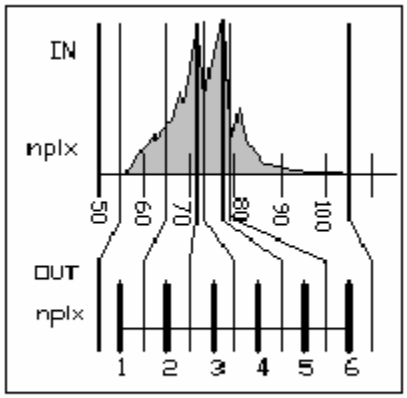

Fig(5.2) Histogram equalization, after Janssen(2000).

5.6.2 IMAGE SMOOTHING

Smoothing operation is primarily used for:

1. removing or reducing noise, and
2. reducing resolution.

Different operators can be used for image smoothing such as neighborhood averaging, median filtering.

5.6.2.1 NEIGHBORHOOD AVERAGING

The averaging for a digital image ***f(x,y)*** of ***N×N*** dimension, is to produce a smooth image ***g(x,y)*** the gray levels of which at any point is obtained by taking the average gray level of the neighboring pixels by the equation,

$$g(x,y) = \frac{1}{M}\sum_{i=1}^{n} f(x,y) \text{----------(5.6)}$$

Where,

x, y =1, 2, ..., n

n is the total number of pixels in the operator.

To reduce the aberration produced by the averaging operator a threshold T can be used according to the following equation,

$$g(x,y) = \begin{cases} \frac{1}{M}\sum f(x,y) if \left| f(x,y) - \frac{1}{M} \text{.....} \right| < T \text{----(4.7)} \\ f(x,y) otherwise \end{cases}$$

Where ***T*** is a positive threshold.

This method reduces the distortion or effacement since it does not change the area of a large difference compared with T; this area usually represents the edges. Therefore, this equation smooths the image and preserves the edges.

5.6.2.2 MEDIAN OPERATOR

The choice of threshold T above in the averaging filtering to preserve the edges depends on a trial and error method. Therefore, median filtering is used as an alternative solution. Here, the pixels in the neighborhood are ranked according to brightness. Then the gray level *f(x,y)* of the central pixel is replaced with the median gray level of the neighboring pixels.

5.6.3 IMAGE CORRECTION

Image corrections (or image restoration) goal is to remove image defects. These errors may be radiometric distortions or geometric distortions. Different mathematical models are developed according to the particular error whether it occurs randomly or systematically recalling that smoothing operators can eliminate noises.

5.6.3 IMAGE SHARPENING

Image sharpening or edges sharpening techniques are important tools to emerge the edges in the digital image. Different methods are available; some of them are discussed here.

5.6.3.1 SHARPENING BY DIFFERENTIATION

Gradient is the most spread method used in digital image processing in which the gradient of the function *f(x,y)* is defined as follows,

$$G[f(x,y)] = \begin{bmatrix} \frac{\partial f}{\partial x} \\ \frac{\partial f}{\partial y} \end{bmatrix} \text{-------(5.8)}$$

Then the magnitude of the gradient express the rate of change per unit distance in the direction of the vector. The magnitude is expressed as,

$$|grad[f(x,y]| = \left[\left(\frac{\partial f}{\partial x} \right)^2 + \left(\frac{\partial f}{\partial y} \right)^2 \right]^{1/2} \text{-------(5.9)}$$

Substituting the derivatives by the differences

$$\left.\begin{aligned} \frac{\partial f}{\partial x} &\cong \frac{\Delta f(x,y)}{\Delta x} = \frac{f(x+1,y) - f(x,y)}{(x+1) - x} = f(x+1,y) - f(x,y) \\ \frac{\partial f}{\partial y} &\cong \frac{\Delta f(x,y)}{\Delta y} = \frac{f(x,y+1) - f(x,y)}{(y+1) - y} = f(x,y+1) - f(x.y) \end{aligned}\right] \text{-----(5.10)}$$

Then,

$$grad[f(x,y)] = \left[(f(x+1,y) - f(x,y))^2 + (f(x,y+1) - f(x,y))^2 \right]^{1/2} \text{---(5.11)}$$

Sometimes, this is further approximated by,

$$grad[f(x,y)] \cong |f(x+1,y) - f(x,y)| + |f(x,y+1) - f(x,y)| \text{---(5.12)}$$

f(x,y)	***f(x,y+1)***
F(x+1,y)	

From the above discussion, it follows that the gradient operator windows are defined by

$$G_x = \begin{vmatrix} 0 & -1 & 0 \\ 0 & 1 & 0 \\ 0 & 0 & 0 \end{vmatrix} \qquad G_y = \begin{vmatrix} 0 & 0 & 0 \\ -1 & 1 & 0 \\ 0 & 0 & 0 \end{vmatrix}$$

Robert's operator approximates the gradient by taking the differences along diagonals.

$$grad[f(x,y)] = \left[[f(x,y) - f(x+1,y+1)]^2 + [f(x+1,y) - f(x,y+1)]^2\right]^{1/2} ---(5.13)$$

or taking the absolute value;

$$grad[f(x,y)] \cong |f(x,y) - f(x+1,y+1)| + |f(x+1,y) - f(x,y+1)| ---(5.14)$$

f(x,y)	***f(x,y+1)***
f(x+1,y)	***F(x+1,y+1)***

Note that the gradient approximated above is proportional to the difference between the neighboring pixels therefore, it takes a large magnitude at the edges and small value at the smooth areas and zero at constant gray level areas.

After choosing a suitable gradient method, the new image can be represented by different ways. The most simplest one is to make the gray level *g(x,y)* at the point equal to the gradient of *f* at that point;

***g(x,y)=G[f(x,y)]*----------(5.15)**

The problem here is that the smooth areas becomes darker because of the smaller difference. To overcome this problem, the value of ***g*** can be taken as:

$$g(x,y) = \begin{Bmatrix} G[x,y] if G[f(x,y)] \geq T \\ f(x,y) otherwise \end{Bmatrix} ---(5.16)$$

Where, ***T*** is a positive threshold correctly chosen to represent the edges and to preserve the smooth background.

Moreover, the edges can be represented with a particular gray level as follows;

$$g(x,y) = \begin{Bmatrix} L_G if G[f(x,y)] \geq T \\ f(x,y) otherwise \end{Bmatrix} ---(5.17)$$

To study only the changes in gray level of the edges we can use;

$$g(x,y) = \begin{cases} G[f(x,y)] if G[f(x,y)] \geq T \\ L_B otherwise \end{cases} ---(5.18)$$

Where, L_B is a particular gray level for the background.

Finally, if only the edges are required to study, then

$$g(x,y) = \begin{cases} L_G] if G[f(x,y)] \geq T \\ L_B otherwise \end{cases} ---(5.19)$$

This produces an image representing only the edges and the background with specified gray level or colour.

Operations based on taking differences between immediate neighbors are quite sensitive to noise. To reduce this effect different windows has been proposed, such as ***Sobel*** operator which performs better for noisy images

because it takes differences between every other row or column. Moreover, the direct neighbor has a higher weight

$$s_x = \begin{vmatrix} 1 & 2 & 1 \\ 0 & 0 & 0 \\ -1 & -2 & -1 \end{vmatrix} \qquad s_y = \begin{vmatrix} 1 & 0 & -1 \\ 2 & 0 & -2 \\ 1 & 0 & -1 \end{vmatrix}$$

Sobel operator

5.7 SEGMENTATION

Segmentation is the process by which the image can be divided into the different objects, which compounds the image. Segmentation is one of the most important process in automated image analysis.

The algorithm of image segmentation depends on either;

- **Discontinuity of gray level**: here image segmentation uses change detection in a gray level by detecting isolated points, lines, or edges.
- **Similarity:** here the algorithm depends on the threshold region growing and region splitting and merging.

5.7.1 THE DETECTION OF DISCONTINUITIES

The detection of discontinuation of points, lines or edges generally uses a small window such as that in figure(5.3)below.

W_1	W_2	W_3
W_4	W_5	W_6
W_7	W_8	W_9

Figure(5.3) 3×3 window.

If, w1, w2, …,w9 represents the elements of the window;

x1, x2,…, x9 are the gray levels of the image elements under the window.

Then, the elements and gray levels can be represented in a vector form as;

$$w = \begin{bmatrix} w_1 \\ w_2 \\ \vdots \\ w_9 \end{bmatrix},$$

$$x = \begin{bmatrix} x_1 \\ x_2 \\ \vdots \\ x_9 \end{bmatrix} \text{-----(5.20)}$$

The inner product of w and x is equal to,

$$w'x = w_1x_1 + w_2x_2 + \cdots + w_9x_9 \text{------(5.21)}$$

5.7.2 POINT DETECTION

The problem of an isolated point detection is useful in noise elimination. Figure (5.4) shows the basic window used for this application.

-1	-1	-1
-1	8	-1
-1	-1	-1

Figure(5.4) Basic window used for isolated point detection.

The center of the window is moved through the image, and inner product (vector product) is computed at each position

$$w'x = -x_1 - x_2 - x_3 - x_4 + 8x_5 - x_6 - x_7 - x_8 - x_9 \text{ ----------(5.22)}$$

In the area of the same gray level the product will equal to zero. On the other hand, if the center of the window moves over an isolated point the result will be greater than zero.

Practically, a threshold T will be selected to define a point as an isolated point. Or

$$|w'x| \rangle T \text{ --------(5.23)}$$

5.7.3 LINE DETECTION

In the case of line detection, four windows are used as shown in figure (5.5) below.

-1	-1	-1
2	2	2
-1	-1	-1

(a)

2	-1	-1
-1	2	-1
-1	-1	2

(b)

-1	2	-1
-1	2	-1
-1	2	-1

(c)

-1	-1	2
-1	2	-1
2	-1	-1

(d)

Fig (5.5) Edge detection windows.

The vector product of the window in (a) is sensitive to a horizontal line where the window in (b) is sensitive to a line inclined by 45˚. The third window in (c) is sensitive to a vertical line, and the final window in (d) is sensitive to a line inclined by –45˚.

To detect the direction of a line, the four windows will be applied to the line and the more sensitive is selected.

5.7.4 EDGE DETECTION:

The edge can be defined as the boundary between two regions of a different gray level property. Edge detection techniques, basically, depend on gradient operation as discussed before.

5.8 DETECTION OF SIMILARITY

Dividing the image into different regions can be done through psudo-colour classification either by density slicing or transformation.

The use of colour in representing and enhancing digital image has a great advantage in the interpretation of an image compared with a gray one,

remembering that, the eye can distinguish between thousands of different colours compared with a limited range of gray level.

5.81 DENSITY SLICING

Dividing the gray level into different ranges is a simplest technique in colour image processing. In this method different planes are taken parallel to the x, y-image plane intersecting the image density. Figure (5.6) represents a single plane intersecting an image density at f(x,y)=Li to divide the image into two different colours. Elements of a gray level above the plane will then take one colour, while the elements of gray level below the plane will take the other colour. The elements on the plane itself can be related to either colour. The result of this operation is the production of a new image with two different colours. It is appearance, can be controlled by rising or lowering the intersecting plane in the direction of gray level axes.

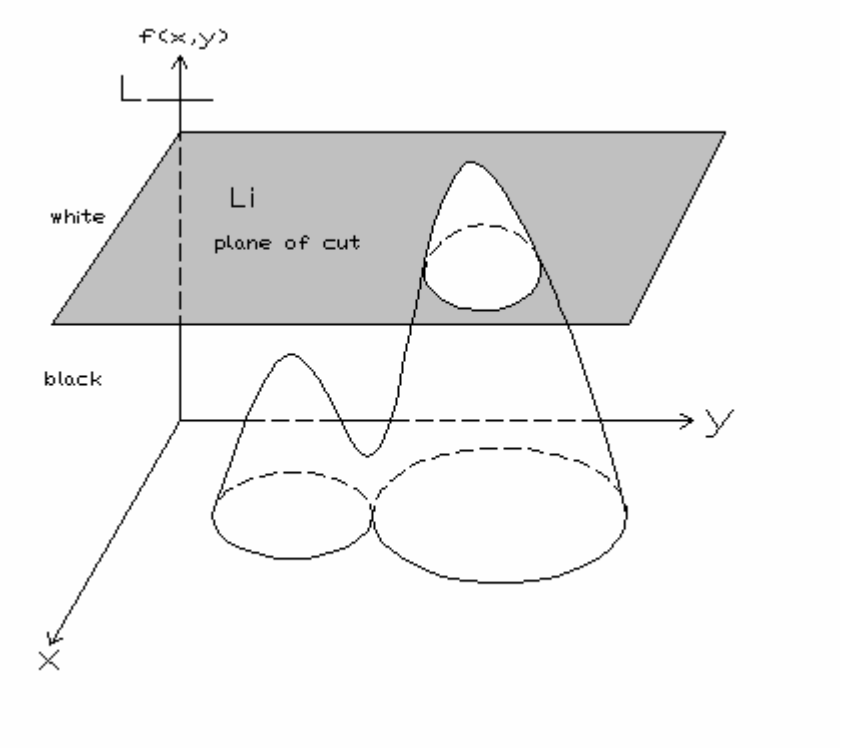

Fig (5.6) Gray levels divided into different ranges,

after Gonzalez(1993).

In other words, f(x, y)= ck if f(x ,y) € Rk

Where

ck is a colour required for the area,

Rk is the plane of cut.

5.8.2 GRAY LEVEL TO COLOUR TRANSFORMATION

Other transformation methods can be used for colour image processing as shown in Fig(5.7)in this method three independent transformations are applied to each element of gray level. The three results are then applied independently to the three (blue, green, red) cathode ray tube guns.

This method can be enhanced, by using a different filter for each colour.

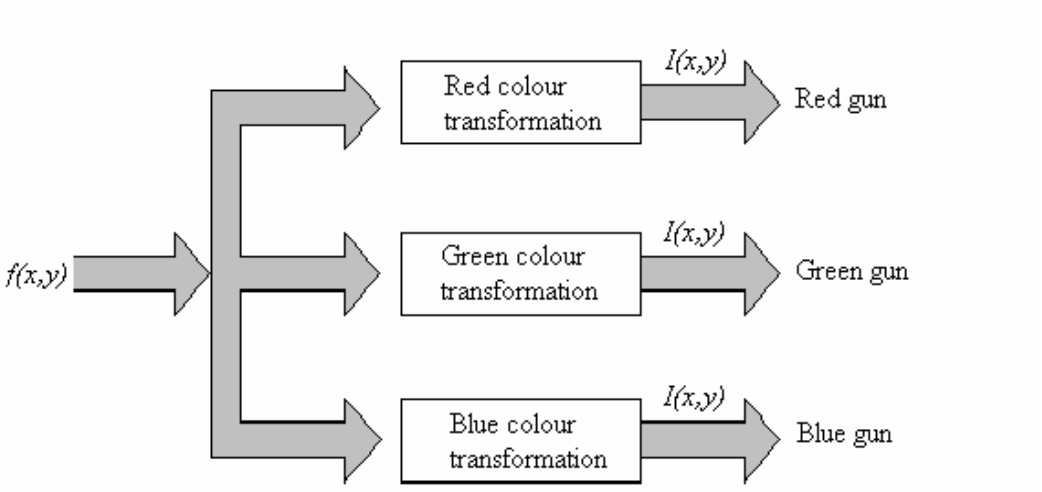

Figure(5.7) Gray level to colour transformation diagram, after Gonzalez(1993).

CHAPTER 6

PRINCIPLES OF IMAGE MATCHING

Chapter 6

PRINCIPLES OF IMAGE MATCHING

6.1 INTRODUCTION

One of the most fundamental processes in photogrammetry is to identify and measure conjugate points in two or more overlapping photographs. Stereo photogrammetry relies entirely on conjugate points. In analogue and analytical photogrammetry the identification of conjugate points is performed by a human operator. In digital photogrammetry the problem is solved automatically using a process known as ***image matching.***

Image matching or correlation, sometimes called automatic stereo-matching or correspondence problem in computer vision, consists of some components. These are:

1. Conjugate entity: is a more general term than conjugate point. Conjugate entities are the images of object space features, including points, lines and areas.

2. Matching entity: is the primitive, which is compared with primitives in other images to find conjugate entities. Primitives include gray levels, extracted features, and symbolic descriptions.

3. Similarity measure: is a quantitative measure of how well matching entities corresponding to each other. Generally, the degree of similarity is measured by a variance cost function. In its simplest form

this may be the cross-correlation coefficient or the standard deviation in least squares matching.

4. Matching method: performs the similarity measure of matching entities. The methods are usually named after the matching entity, for example area-based matching, feature-based matching, and relational (symbolic) matching.

1. **Matching strategy:** refers to the concept of the overall scheme of the solution of the image-matching problem. It encompasses;
   - **i.** The analyses of the matching environment,
   - **ii.** The selection of the matching method, and
   - **iii.** The quality control of the matching.

Matching Method	**Similarity Measure**	**Matching Entities**
Area-based	Correlation, least-squares	Gary levels
Feature-based	Variance cost function	Edges, regions
Symbolic	Variance cost function	Symbolic description

Table (6.1) Relationship between matching methods and matching entities

As shown in table (6.1), the first column lists the three best-known matching methods. Area-based matching is associated with matching grey levels. That is, the grey levels distribution of small areas of two images which is called ***image patches***, is compared and the similarity is measured by correlation or least squares techniques. Area- based matching using

correlation is often simply called ***correlation***. Likewise, area-based matching with a least-squares approach for measuring similarity is known as ***Least Squares Matching*** **(LSM).** Area based matching is quite popular in photogrammetry- presumably because of the long practice.

Feature-based matching is predominantly used in computer vision. Here, edges of other features derived from the original images are compared to determine conjugate features. The similarity, for example, the shape, sign and strength of edges, is measured by the cost variance function.

The third method, ***symbolic matching***, refers to methods which, compare symbolic descriptions of images and measure the similarity by a cost function. The symbolic descriptions may refer to grey levels or derived features.

6.2 PROBLEM STATEMENT

The problem of image matching can be stated as follows:

1. Select a matching entity in one image
2. Find its conjugate (corresponding entity) in the other image(s)
3. Compute the three dimensional location of the matched entity in object space
4. Assess the quality of the match.

Obviously, the second step is the most difficult to solve. Although the other steps appear trivial at first sight, there are still interesting issues involved. Take a typical stereopair as an example, possible questions

that may arise: which one of the two images should the matching entity is selected. What entity should be selected and how is it determined in the first place.

6.3 FUNDAMENTAL PROBLEMS OF IMAGE MATCHING

The problems that must be addressed and solved by different matching method are:

1. Search space,
2. Geometric distortions.

6.3.1 SEARCH SPACE, UNIQUENESS OF MATCHING ENTITY

Without restricting the search space, the process of finding conjugate points in a stereo-pair, facing two problems:

1. **Combinatorial explosion:** occurs if the similarity measure between the matching entities is computed over the ***entire*** image (model).
2. **Ambiguity:** occurs if the matching entity is not characterised (unique enough).

A solution to the first problem is to restrict the search space for finding conjugate entities. The second problem must be tackled by selecting more unique matching entities.

6.3.2 CONSTRAINTS AND ASSUMPTIONS

A problem is said to be well-posed if:

i. A solution exists

ii. The solution is unique

iii. The solution depends continuously on the initial data.

Otherwise, the problem is said to be ill-posed.

Image matching is an ill-posed problem, because it violates several if not all of the conditions of a well-posed problem are not met. For example, no solution (occlusion) or no unique solution (ambiguity) must exist. Image matching belongs to the class of inverse problems, which are known for their ill-posed nature. A crucial question is how image matching is made well-posed. The approaches range from complete ignorance to sophisticated regularisation methods.

A straightforward way to make image matching well-posed is to restrict the space of possible solution. For example by setting bounds. The underlying function of the similarity measure is non-monotonous and rather flat around peaks and troughs. As illustrated in Fig(6.1) it must be in the image matching process with rather close to the true solution otherwise we may end up with a secondary minimum or too many iterations are required. Consequently, we need very good approximation to assure convergence. The convergence radius is also called ***pull-in-range***. Area-based methods must be in the search process as close of a few pixels from the true conjugate location. Feature-based matching and symbolic matching has a much larger convergence radius. Approximations

and search space are closely related; the better the approximations the smaller the search space.

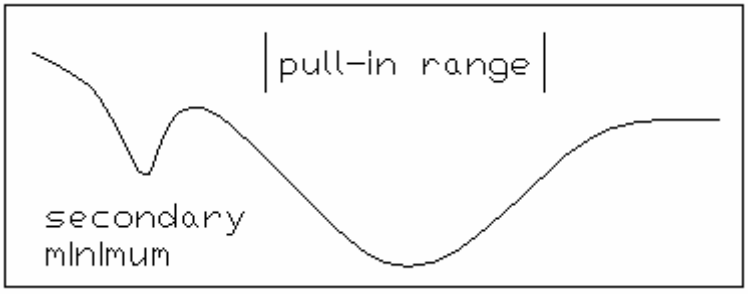

Fig(6.1) The ill-posed nature of image matching, after Schenk(1999).

A bold step toward making image matching well posed is to introduce constraints. An example of strong geometrical constraints is the fact that the prespective centres, the conjugate points and the corresponding object point all must lie in one plane (the epipolar plane).

Assumptions about the matching problem are another source restricting the solution space. As in aerial stereopairs where we safely assume that the forward overlap is about 60%. This is useful because it permits to predict the conjugate location fairly well. As long as we work with aerial images there is nothing wrong with this kind of assumptions.

In summary, the problem is to obtain good enough approximations and to strike a fine balance between assumptions made and constraints imposed on the solution on the one hand, and on maintaining generality on the other hand.

6.3.3 GEOMETRIC DISTORTIONS OF MATCHING ENTITIES

The compelling conclusion from the discussion above is to make the matching entities as unique as possible so that only one solution (match) exists. Instead of comparing the grey level of one pixel, several pixels must be considered in similarity measure. Thus, the grey levels of an image patch, size $n \times n$ pixels, are compared with those of the patch in the other image. Suppose for a moment that both image patches are centred on their true conjugate locations. The similarity measure yield a maximum if the grey levels of every pixel compared are identical. This is an ideal situation, which will never occur in reality. **Noises**, changing illumination and reflection properties between two consecutive images cause differences in the grey levels. Another source that causes two image patches to appear different, even in their true conjugate location, are **geometric distortions** due to the central projection and due to relief.

Referring to Fig(6.2) which depicts an stereopair and two image patches, size 5×5 pixels, central at the conjugate location. The most ideal case refers to the situation where every pixel pair corresponds to the same spot in object space. That is, every pixel in the image patches must be conjugate. ***The geometrical conditions for this ideal case are that both images and the surface patch must be parallel to the base***. Any departure from this condition causes *geometrical distortions*.

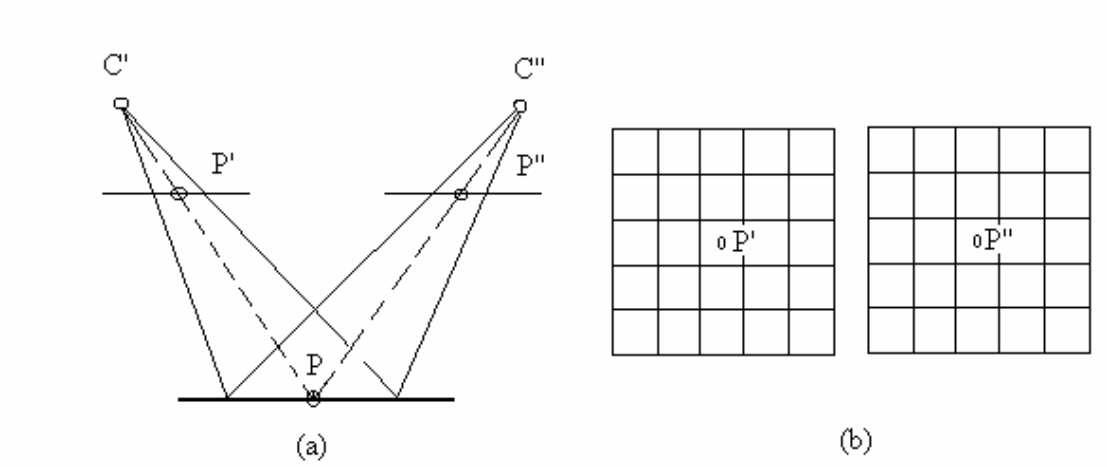

Fig(6.2) Two image matches in their conjugate position, after Schenk(1999).

Geometrical distortions may be caused by:

1. **Orientation parameters.**
2. **Scale difference between the two images.**
3. **Different rotation angles between the two images, and**
4. **Effect of tilted surface on geometrical distortion.**
5. **Effect of relief on geometrical distortion.**

6.3.3.1 GEOMETRICAL DISTORTION DUE TO ORIENTATION PARAMETERS

Fig(6.2) illustrates the situation of a true vertical stereopair, of horizontal airbase and horizontal and flat surface. Consider a real stereopair and a flat surface patch with its surface normal parallel to the camera axes of the left image. The impact of scale and rotations of the right image is of interest. This configuration corresponds to a dependent relative orientation.

It should be stressed that the cases examined here refer to un-oriented stereopairs. If the orientation is known then the images can be transferred and resampled into a normalized position analogous to the ideal situation of Fig(6.2). Since in photogrammetry we begin usually with un-oriented stereopairs it is important to be aware of geometrical distortions caused by the orientation parameters.

6.3.3.2 SCALE DIFFERENCE BETWEEN THE TWO IMAGES

A stereopair with different scale caused by different flying heights is shown in Fig(6.3a). The projection of two conjugate image patches Fig(6.3b) onto the flat surface reveals that the pixels within the image patches are now longer conjugate because they refer to different locations in object space. To demonstrate the case the left upper pixel of both patches are dark shaded. The further we move from the centre the larger the discrepancies. Consequently, the similarity measure will be affected.

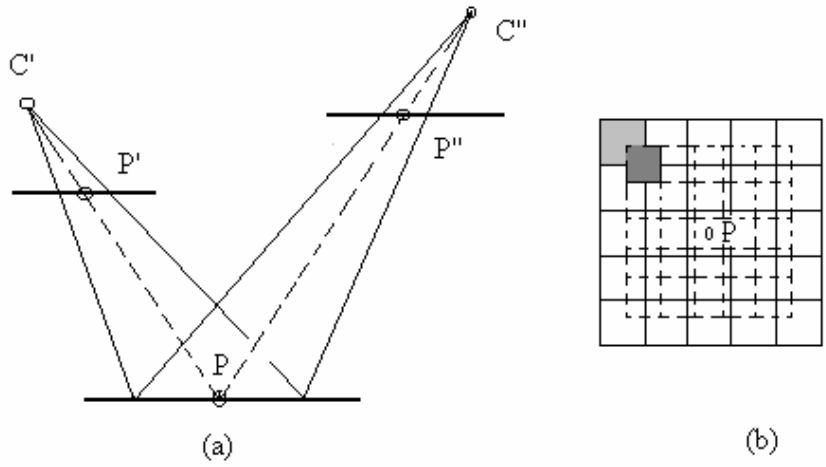

Fig(6.3) Stereopair with different scale, after Schenk(1999).

.

6.3.3.3 DIFFERENT ROTATION ANGLES BETWEEN THE TWO IMAGES

The effect of differences in rotation angles is represented in Fig(6.4). Considering the case of dependent relative orientation, the rotation angles of the right image are with respect to the fixed position of the left image. Fig (6.4a) depicts the effect of a rotation of the right image about the x-axis (ω). The right image patch appears in its projection on the flat surface as a rectangle. The effect of a φ-rotation (rotation about the y-axes) is shown in fig (6.4b). Finally, the κ-rotation has an effect as illustrated in fig (6.4c).

It is evident from Fig(6.4) that the pixel-to-pixel comparison is wrong because the same pixel in the two image patches refers to a different position in the object space. Again compare for example, where the pixel of the left upper corner appear in object space.

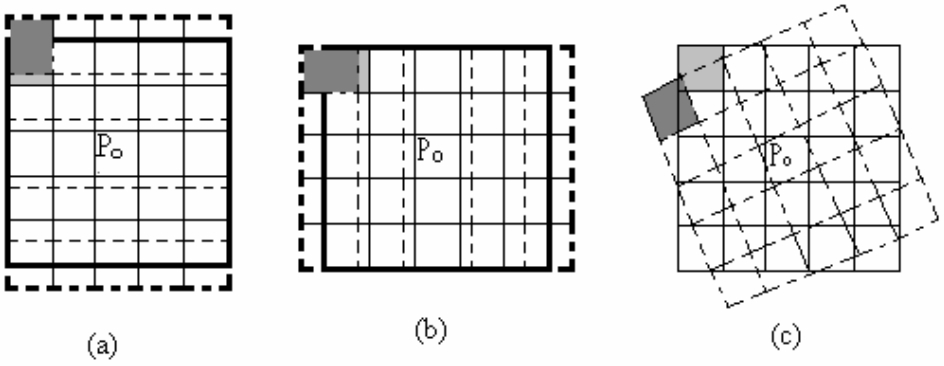

Fig(6.4) The effect of rotation differences between left and right image of a stereopair, after Schenk(1999).

6.3.3.4 EFFECT OF TILTED SURFACE ON GEOMETRICAL DISTORTION

As mentioned before the assumption is that the flat surface patch in object space is parallel to the left image. This is why the left image patch always appeared as a perfect square for a true vertical stereopair than a tilted surface in Fig(6.5a). The surface is rotated about the air base B in Fig(6.5b) reveals that this is an ideal situation because every corresponding pixel is still conjugate. The geometric distortion is identical in both images.

If the surface is tilted about an axis perpendicular to the airbase, as shown in Fig (6.5c), the effect is very different. Fig(6.5d) shows that the surface appears as a small rectangle in the right image. This situation is referred to as foreshortening. If the surface is tilted further then a critical angle is reached where it is no longer visible in the right image.

A closer examination of Fig(6.5) reveals another consequence of a tilted surface, namely the decreased resolution in the direction perpendicular to the rotation axis. In the second case discussed, the resolution of the foreshortening image is smaller in x-direction.

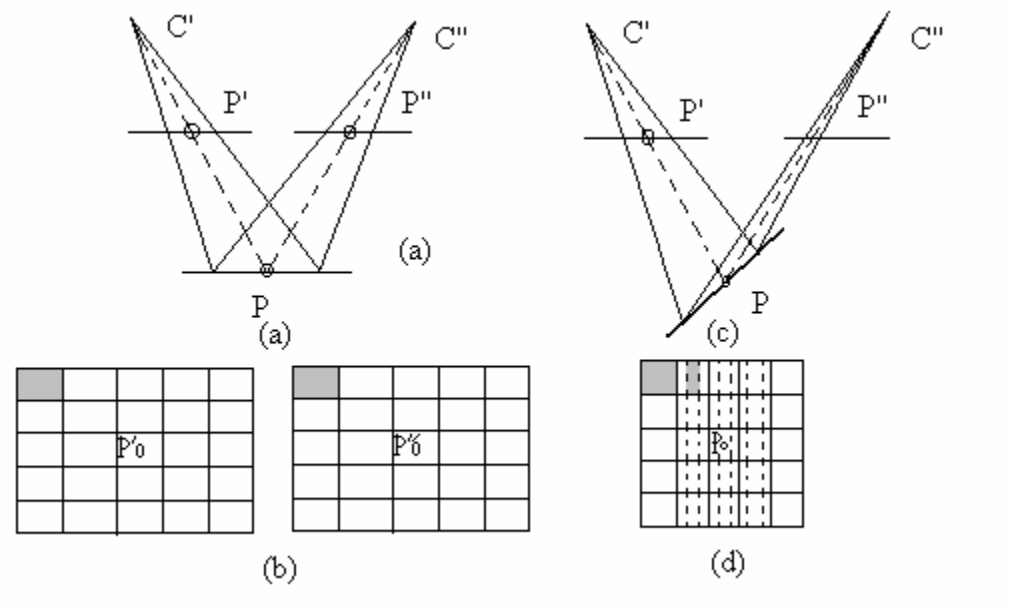

Fig(6.5) The effect of tilt surface on the similarity measure in area based matching, after Schenk(1999).

6.3.3.5 EFFECT OF RELIEF ON GEOMETRICAL DISTORTION

Unlike all previous cases the assumption now is that a real surface patch with elevation differences. As before, the image patches at their conjugate location are projected onto the 'mountainous' surface patch.

As Fig(6.6) demonstrates, the individual pixels are not conjugate even in the case of a perfectly vertical stereopair.

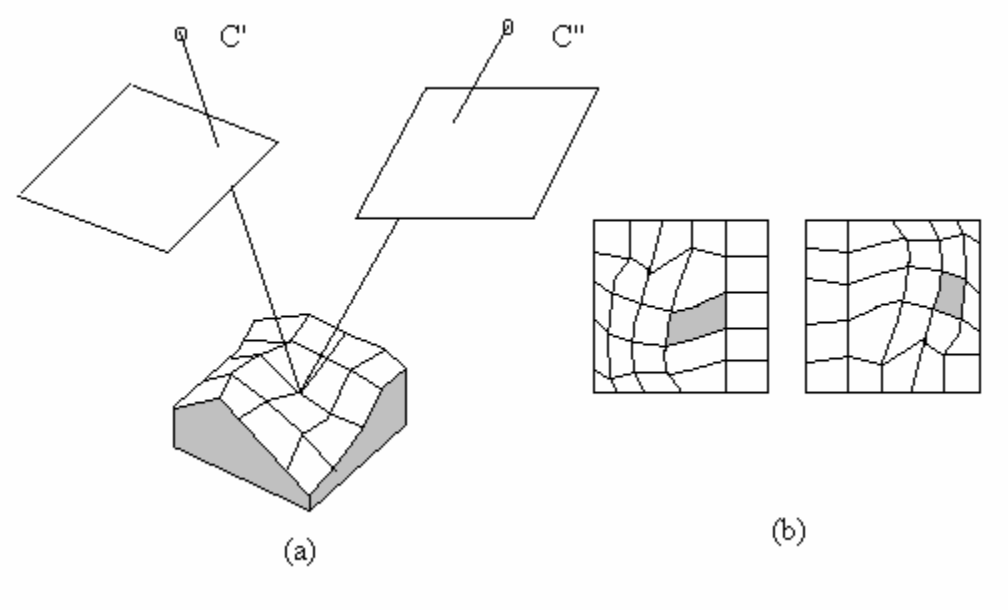

Fig(6.6) The effect of relief on the similarity measure

In area based matching, after Schenk(1999).

.

6.4 SOLUTION TO FUNDAMENTAL PROBLEMS

6.4.1 SEARCH SPACE AND APPROXIMATIONS

The blind search approach of taking the entire image as the search space, insurmountable computational problem. Moreover, the search space is far too large because the ill-posed nature of image matching requires very good approximations. This is particularly true for area-based methods. Consequently, the search space must be limited to a rather small area, which is called the pull-in-range. This limitation, can be done by applying some geometrical conditions such as:

i. Epipolar line

ii. Vertical line locus.

iii Hierarchal approach.

6.4.1.1 EPIPOLAR LINE

A powerful constraint for conjugate entities is epipolar lines. Fig(6.7) illustrates the concept. The epipolar plane is defined by the two projection centres C′, C″, and the object point P. The epipolar lines e′, e″ are the intersections of the epipolar plane with the image planes. The epipolar plane contains the conjugate points, which must lie on epipolar lines.

Epipolar lines reduce the search space dramatically. If a matching entity in one image is chosen then the epipolar line in the other image can be computed, provided the stereopair is oriented.

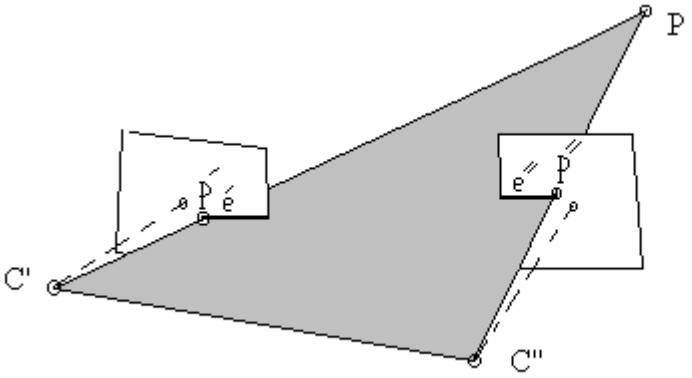

Fig(6.7) Epipolar geometry of a stereopair, after Schenk(1999).

Usually, the epipolar lines are not parallel to the x-axis of the photo coordinate system. Quite often it is desirable to transform the images in

such a way that epipolar lines become parallel to the rows of the digital images i.e. the x-axes. Such stereopairs called normalised images

For the following discussions normalized images are assumed. Suppose we pick the matching entity P′ in one image, then the search space is restricted to the same row in the other image. We can certainly predict the conjugate locations. Fig(6.8) shows bundle ray C′P′ where P is the feature in the object space with an estimated elevation Zp. This bundle ray intersects the true space at point S. In an oriented model some elevations exists (from the orientation process). Thus, reasonable approximation of Zp is obtained, for example, by taking the average of all known elevations. With Zp and the orientation parameters, the conjugate feature P″ is computed as the image of the estimated object feature P.

Next, the uncertainty Δz of the predicted elevation must be estimated. This may turn out to be more difficult than predicting Zp. Usually, some a previous knowledge about the area is available, e.g. mountainous, or flat. Also, the maximum and minimum values of the existing orientation points may serve as a basis to estimate Δz.

For near vertical stereopair, the following equations can be used to determine the approximate location x″p of the conjugate feature.

$$x''_p = x'_p - px_p \text{ ------(6.1)}$$

$$px_p = \frac{B}{H_D - Z_p} f \text{ ----(6.2)}$$

Substituting the air base B in the above equation by $b_0 \frac{H_D}{f}$, the following expression for the location of the conjugate entity is obtained

$$x''_p = x'_p - b_0 \frac{H_D}{H_D - Z_p} \text{--------(6.3)}$$

Where:

B the air base,

b0 the image base, and

pxp the x-parallax of point P.

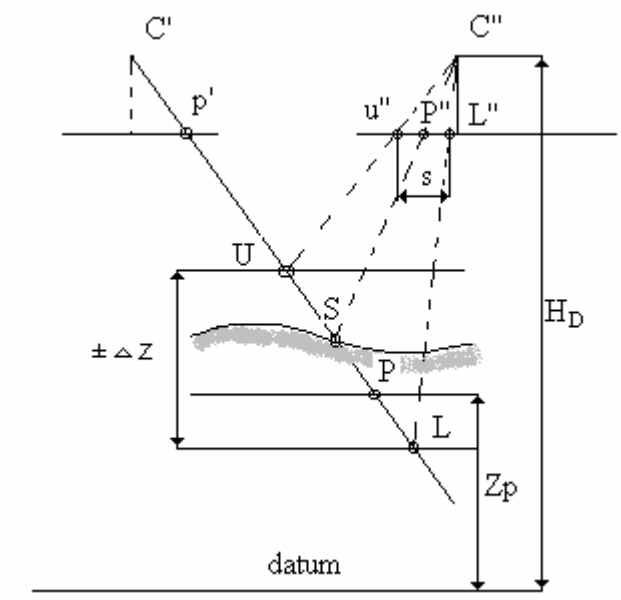

Fig(6.8) Estimating the matching location and the search space on the epipolar line.

Now we determine the search interval S and again assume the true vertical images. Referring to Fig(6.8) and Eq.(6.3) we have

$$s = x''_U - x''_L \text{ ----------(6.4)}$$

$$x''_U = x'_U - b_0 \frac{H_D}{H_D - Z_U} \text{ -------(6.5)}$$

$$x''_L = x'_L - b_0 \frac{H_D}{H_D - Z_L} \text{ --------(6.6)}$$

Recognising that x′U = x′L we have for s

$$s = b_0 H_D \frac{\Delta z}{(H_D - Z_L)(H_D - Z_U)} \text{ ------(6.7)}$$

Approximating the denominator in this equation by (HD-Δz/z)2 we have for search interval s the following expression

$$s \approx b_0 \frac{H_D \Delta z}{(H_D - Z_p)^2} \text{ ----------(6.8)}$$

The following procedure describes the essential steps for implementing a matching scheme along epipolar line:

Select matching entity in one image, e.g. P′.

Estimate the elevation, ZP, of the matching entity and its uncertainty range Δz.

Compute approximate location, P″, using Eq.(6.3)

Compute search interval, s, with equation(6.8).

Perform matching within search interval; select matching entity P′ remains constant.

Analyse the similarity measures obtained in step 5 for determining conjugate location P″.

1.4.1.2 VERTICAL LINE LOCUS

Another useful geometrical constraint for the search space is the so-called vertical line locus illustrated in Fig(6.9)

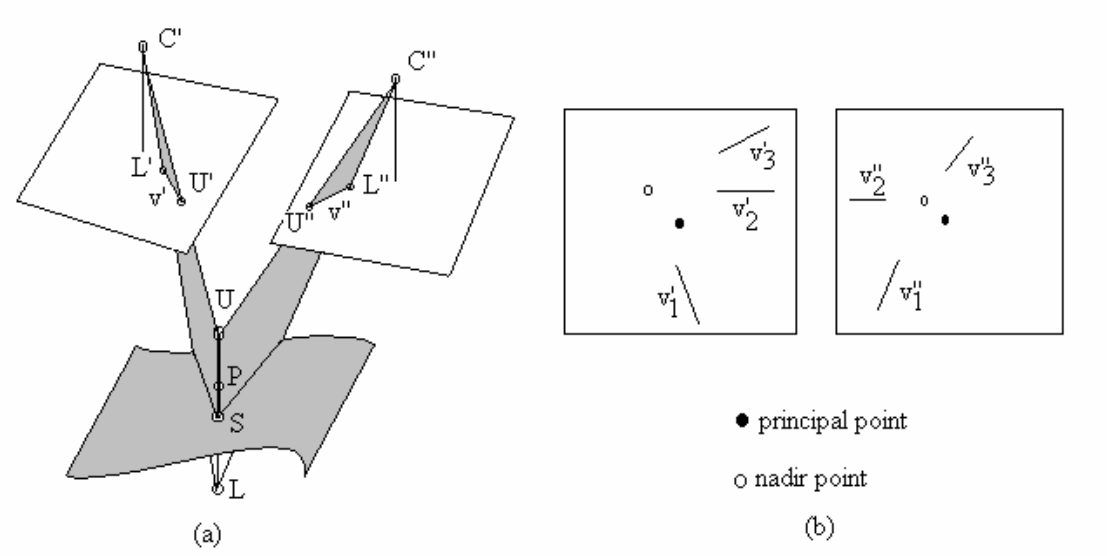

Fig(6.9) Concept of vertical line locus, after Schenk(1999).

.

If P is the estimate of the position of a feature in object space and Δz be the uncertainty range of the initial guess. This determines the lower (L) and upper (U) bounds of P, which are projected back to the images. The distances L′, U′ and L″, U″ are labeled v′ and v″ respectively. The conjugate entities in both images are confined to the two lines v′ and v″ which are found by intersecting the triangles, defined by the projection center and the lower and upper bounds L and U, with image planes. Because the triangles are in plane, which contains also the plumb line from the perspective centers, the projected vertical lines in the images

are radial with respect to the nadir. Moreover, L′ and L″ as well as U′ and U″ are on epipolar lines.

Note that v′ and v″ have different lengths. In fact, they may collapse to a point if the extension of the vertical line U, L passes through a projection center. Fig(6.9b) shows some examples of vertical line locus pairs in the stereopair.

Several approaches exist to implement the concept of vertical line locus scheme. Fig(6.10) illustrates one possibility. Here, the matching begins at the lower bounds where the template and matching window are centered at L′ and L″, respectively. The matching procedure repeats for points between L and U. Of all the positions matched in this fashion, only one is correct, indicated by the maximum response of the similarity measure.

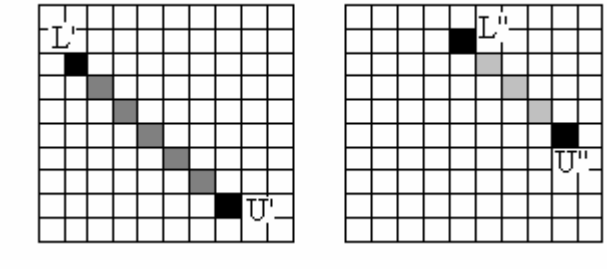

Fig(6.10) Concept of matching along the vertical line loci, after Schenk(1999).

The following procedure may be followed when implementing the concept of the vertical line locus approach:

Select the Xp, Yp-position of a point P in object space and estimate the elevation ZP and its lower and upper bounds ZL and Zu .

Begin the matching process by projecting Xp, Yp, ZL back to both images. Perform a similarity measure at the image positions x′L, y′L and x″L, y″L

Move along the vertical line in suitable steps $\Delta z = (ZU - ZL)/n$. project the object points Xp, Yp, ZL + Δz back to the images and repeat the similarity measures.

Repeat step 3 until ZU is reached.

Analyze the similarity measures obtained in every step and determine the maximum for the conjugate positions.

The vertical line locus method is useful for applications where conjugate entities at certain positions in object space are required. One such application is the automatic generation of DEMs. Where, the X,Y-positions are given by the grid posts.

In contrast to epipolar line method, the matching position in both images is changed (along the images of the vertical line). This may be a disadvantage for certain implementations, because for every matching position, both image patches are new.

The vertical line locus method can also be combined with epipolar line method, to increase the reliability of matching points. Fig(6.11) shows the concept. Suppose the matching begins at L. Before moving to the next epipolar line several matches are performed at the epipolar line through L′ and L″ in Fig(6.11). L″ is kept constant and matching is performed by moving L′. The true match is found at E′L. The true

conjugate position is always to the right of L′ because the true surface is below L in object space. Now we move on to the next epipolar line and repeat the same procedure. When we reach U, the conjugate entity to U″ is in E′U –always to the left of U′ because the true surface is higher as in Fig(6.11). The line of the true matches E′i intersects v′ at the location where U, L pierces the surface- the point we want to find. The analysis of the similarity measure for all matching positions should reflect this situation by maximum response.

It is worth to point out that a combination of vertical line locus and epipolar line may offer advantages. In this schema, the matching at every point along additional matches along the epipolar complements the vertical lines. This will render more data for analyzing the cost function, resulting, in general in a more reliable match.

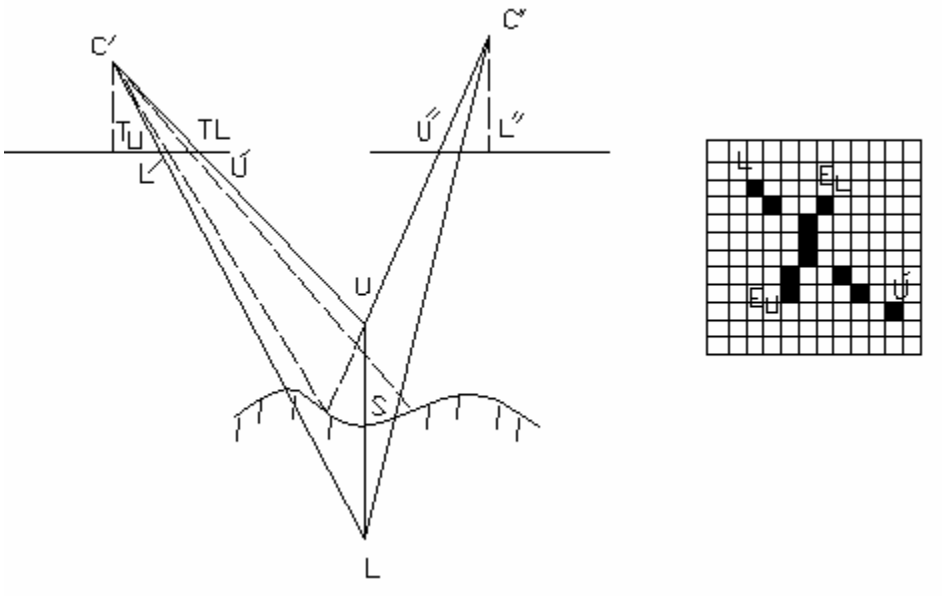

Fig(6.11) Combining vertical line locus and epipolar line method, after schenk(1999)

6.4.1.3 HIERARCHAL APPROACH, (COARSE-TO FINE-STRATEGY)

Another way to reduce the pixel search space is to increase the pixel size. This solution reduces the search space and at the same time improves the approximations (in pixel) by beginning with coarse resolution and then projecting the results to ever-finer resolution images until we are at the original resolution. This is best accomplished by generating image pyramids for the stereopair Fig(6.12).

With images at a resolution of 32kX32k an image pyramid with intermediate levels of 16k, 8k, 4k, ... is generated, for example by smoothing the original image with Gaussian filter of appropriate (σ). The resolution level that we can start with, depends on:

1. The matching method, and
2. The uncertainty of the estimated elevation.

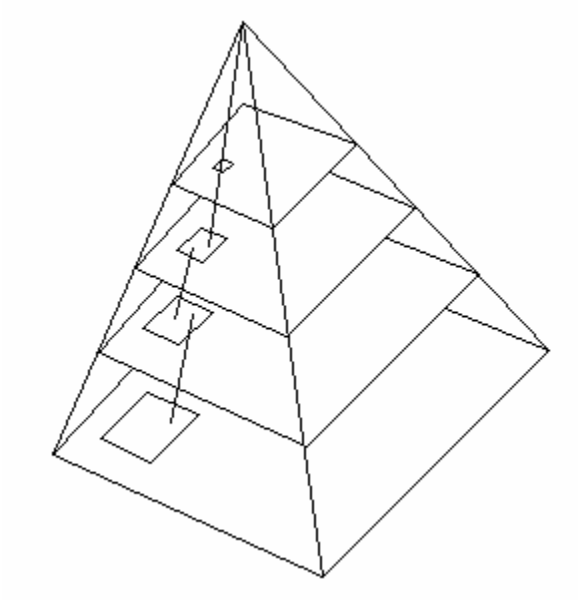

Fig(6.12) Tracking matched entities through the image pyramid, after schenk(1999)

.

To prevent multiple matches, the matching entities must be unique; at least in the search space.

If gray levels are used as matching entities then the uniqueness of the image patches increases with their size, in addition to effect of geometric distortion. The crux is to find a good compromise between these conflicting factors. Obviously, it is desirable to measure the uniqueness so that we do not increase image patch size once it is unique enough. Several methods may be used, such as:

1. Variance,
2. Autocorrelation,
3. Entropy.

1. VARIANCE

Variance $\sigma^2 = \frac{1}{R.C}\sum_{x=0}^{R-1}\sum_{y=0}^{C-1}(g(x,y) - \overline{g_a})^2$ of the image function provides a measure of how different the gray levels are. A small variance indicates a rather flat (homogeneous) image, while a large variance points to a grey level distribution over large intervals.

2. AUTOCORRELATION

Autocorrelation $\rho = \frac{\sigma_{LR}}{\rho_L \rho_R}$ of the image function provides a measure of the image match. A high autocorrelation factor indicates repetitive patterns within the sub-image- something, which reduces the uniqueness. A totally random image function would show no correlation- this is the most unique function, but it does not exist in reality. Real images are more deterministic than random.

3. ENTROPY

Entropy $H = -\sum_{i=0}^{\max} p_i \log_2 P_i$ measures the randomness of the image function. High entropy indicates more randomness than low numbers one.

The uniqueness of the gray level function depends on the location in the image. It should be determined for every new location.

1.5 AREA BASED MATCHING

The entities in the area-based matching are gray levels. Here, the idea is to compare the gray level distribution of small sub-image, called image patch, with its counterpart in the other image. Fig(6.13) illustrates the concept and introduces a frequently used terminology.

- The template, is the image patch, which usually remains in a fixed position in one of the images.

The search window (some times called matching window) refers to the search space within which image patches are compared with the template. The two best-known criteria are cross-correlation and least squares matching.

The position and size of the search window can be determined with the methods described in section (6.4.1).

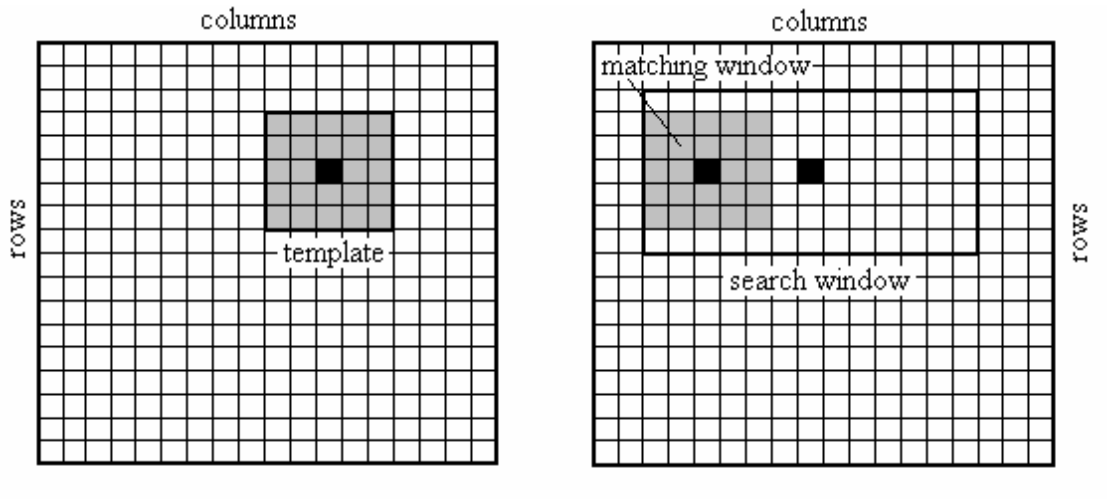

Fig(6.13) Area based matching, after Schenk(1999).

A number of issues must be addressed independently of the similarity measure method. These issues are:

1.Location of template

2.Size of template

3.Location and size of search window

4.Acceptance criteria

5.Quality control.

a. Location of template:

Theoretically, the template's center can be placed within an area, which is half the template size smaller than the image. On closer examination we probably want to be more selective within the accepted boundary.

b. Size of template:

The size of the template and the matching window is an important parameter. With increasing size, the uniqueness of the gray level function usually increases, but so do the geometric distortion problems. A compromise must be found, e.g. by computing a uniqueness measure for different template sizes. This also serves the purpose of checking the usefulness of the template location.

c. Location and size of search window:

Since area based matching requires very close approximations, the location of the search window is crucial. Its size, that is, the search space does not play a role because the close approximations limit shifts

to a few pixels. A hierarchical strategy is usually employed to ensure good approximations.

d. Acceptance criteria:

The factors obtained for measuring the similarity of the template and matching window must be analyzed. Acceptance /rejection criteria often change, even within the same image. Threshold values or other criteria should be locally determined (on the fly).

e. Quality control:

The quality control includes an assessment of the accuracy and the reliability of the conjugate locations. Moreover, the consistency of matching points must be analyzed, including the compatibility with expectations or knowledge about the object space.

Certain condition may causes area-based matching to fail, for example:

i. Placing the template on areas which are not occupied in the other image,

ii. Selecting an area with low SNR, or repetitive pattern,

iii. Selecting an area containing break lines.

6.5.1 AREA BASED MATCHIMG (CORRELATION TECHNIQES)

Correlation techniques have a long tradition for finding conjugate points in photogrammetry. In fact, first experiments with analogue correlation methods were conducted in fifties. The idea is to measure the similarity

of the template with the matching window by computing the correlation factor.

6.5.1.1 CROSS-CORRELATION FACTOR

The correlation coefficient ρ is defined by:

$$\rho = \frac{\sigma_{LR}}{\sigma_L \sigma_R} \text{--------(6.9)}$$

If ρ is normalized then $-1 \leq \rho \leq +1$

Where

σL standard deviation of image patch L (template)

σR standard deviation of image patch R (matching window)

σLR covariance of image patches L and R

Introducing the image function gL(x,y), gR(x,y) for the left and right image patches (or the template and matching window for that matter) and their means ğL, ğR, we have the following defining equations:

$$\bar{g}_L = \frac{\sum_{i=1}^{n}\sum_{j=1}^{m} g_L(x_i, y_i)}{n.m} \text{----------(6.10)}$$

$$\bar{g}_R = \frac{\sum_{i=1}^{n}\sum_{j=1}^{m} g_R(x_i, y_i)}{n.m} \text{----------(6.11)}$$

$$\sigma_L = \sqrt{\frac{\sum_{i=1}^{n}\sum_{j=1}^{m} (g_L(x_i, y_i) - \bar{g}_L)^2}{n.m-1}} \text{----------(6.12)}$$

$$\sigma_R = \sqrt{\frac{\sum_{i=1}^{n}\sum_{j=1}^{m} (g_R(x_i, y_i) - \bar{g}_R)^2}{n.m-1}} \text{----------(6.13)}$$

$$\sigma_{RL} = \sqrt{\frac{\sum_{i=1}^{n}\sum_{j=1}^{m} ((g_L(x_i, y_i) - \bar{g}_L)(g_R(x_i, y_i) - \bar{g}_R))}{n.m-1}} \text{---(6.14)}$$

The cross-correlation factor is determined for every position r, s of the matching window within the search window. The next problem is to determine the position u, v that yields the maximum correlation factor.

The maximum correlation factor:

The normalized cross-correlation factor ρ assumes values in the interval ±1. A value of unity is obtained if the template and the correlation window are identical. If there is no correlation between the two image patches, that is to say no similarity at all, then $\rho = 0$. A value $\rho = -1$ would indicate an inverse correlation, such as a diapositive and/or negative of the same image.

If the search window is constrained to the epipolar line then the correlation factors can be plotted in a graph like that in Fig(6.14a). The maximum is found by fitting a polynomial, e.g. a parabola, through the correlation values. Noting that, the maximum only rarely coincides with the integer values of the pixel address.

The next figure demonstrates less ideal cases. Though the correlation factor in the Fig(6.14b) is fairly high, the maximum is not determined very well at all. It corresponds to two image patches with little contrast. The reliability of the conjugate points is low. Fig(6.14c) shows another problem, namely the difficulty of deciding which of the two peaks is the correct maximum.

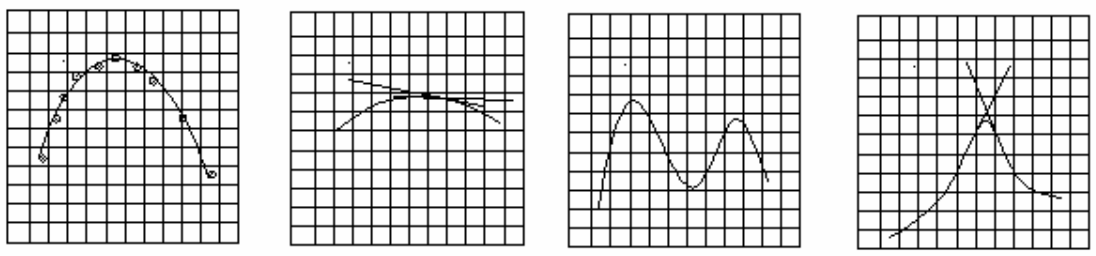

(a) (b) (c) (d)

Fig(6.14) Fitting parabola and typical problems, after Schenk(1999).

A comparison between Fig(6.14a) and Fig(6.14b) suggests to use the 'flatness' of the correlation function as a quality measure for the distinctness of the maximum. The flatness can be measured, e.g. by the angle between the tangents to the parabola and next to the maximum Fig(6.14d).

The following procedure describes the general steps of area-based matching with correlation as a similarity measure:

1. Select the center of the template in one image

2. Determine approximate locations for the conjugate position in the other image as described in section (6.4)

3. For both, the template and the correlation window, determine the minimum size, which passes the uniqueness criteria described before. Select the larger of the two values as the window size for the current matching location.

4. Compute the correlation coefficients $\rho_{r,s}$ with equation (6.9) for all positions r, s of the correlation window within the search window.

5. Analyze the correlation factors. A minimum threshold must be reached for a valid match. A part from the maximum, determine the distinctness as a quality measure.

6. Repeat steps 2 to 5 for a new template location until all positions to be matched are visited.

7. Analyze the matching results on a global base for consistency and/ or compatibility with prior scene knowledge.

6.5.2 LEAST SQUARES MATCHING

The idea of least squares technique is to minimize the gray level differences between the template and the matching window, whereby the position and the shape of the matching window are parameters to be determined in the adjustment process. That is, the position and the shape of the matching window are changed until the gray level difference between the deformed window and the (constant) template reach minimum. While we immediately grasp the idea of moving the matching window until the conjugate position is found, the deforming aspect may be less obvious at first sight. After discussing the various geometric distortions cased by either unknown orientation parameters, tilted surface patch, surface patch with relief, etc., it becomes clear that the shape of the matching window must be changed so that all pixels in the window become conjugate with their counterparts in the template.

CHAPTER 7

DIGITAL PHOTOGRAMMETRIC WORKSTATION

Chapter (7)

DIGITAL PHOTOGRAM METRIC WORKSTATION

7.1 INTRODUCTION

The main characteristics of a digital photogrammetric systems DPS as shown in Fig(7.1) are as follows:

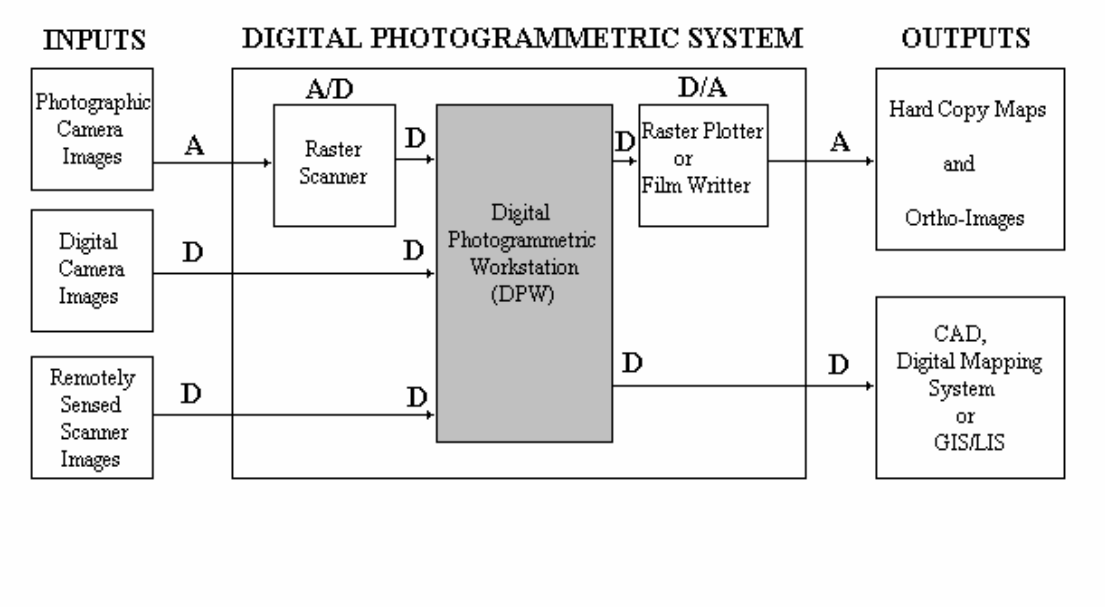

Fig(7.1) Overall Concept of The Digital Photogrammetric System.

1. It is a system combining computer hardware and software that allows photogrammetric operations to be carried out on digital image data.
2. These operations are carried out on sets of image data consisting of picture elements (pixels) of fixed shapes and size. Each individual pixel is assigned a brightness value (BV), which gives the value of

the radiance from the object field falling on each individual element of the imaging sensor.

3. The imaging sensor can take the form of:
    i. Digital camera equipped with an aerial array of charge coupled detectors.
    ii. Pushbroom scanner featuring a linear array of CCDs.

    Each of these detectors gives a direct output of the image data in digital form through analogue to digital (A/D) conversion of the radiance value, which is measured electronically for each individual element of the sensor.
4. For topographic mapping operations, however, digital image data are most often derived from the frame images on photogrammetric film produced by an aerial camera. These film images need to be converted to digital form by using high precision scanners equipped with linear or aerial CCD arrays. In this case the scanner forms a vital and integral part of the DPS.
5. The main element of DPS is the **Digital Plotting Workstation (DPW),** on which the required analytical (i.e. numerically and mathematically based) photogrammetric operation are carried out to produce data for input to:
    - Digital mapping systems
    - CAD systems
    - GIS/LIS systems.

6. These photogrammetric operations include:
    - Manual operations such as the feature extraction involved in map compilation and revision.
    - Automatic or semi-automatic operations such as the generation of digital elevation model (DEM) data and ortho-image data.
7. Final output may take the form of:
    - Vector line maps
    - Digital terrain model (DTM) data
    - Digital ortho-images.

Here, in addition to devices that can record purely digital data, the overall DPS will include devices such as raster-based plotters and film writer, which can produce hard copy maps, prespective views of terrain surface and continuous-tone images from the DPW image data. Essentially, these carryout a digital -to-analogue (D/A) operation.

7.2 HISTORICAL BACKGROUND

The development of digital photogrammetric workstation (DPW) or what is called softcopy photogrammetry, can be thought of in three phases (Schenk 1999):

- The first reasonably detailed concept of a DPW was in 1982, referred to as fully digital stereoplotter. The functionality

resembles strongly that of an analytical plotter, the major difference being the fact that the photographs are replaced by digital images. The idea is to build the digital stereo- plotter on the basis of image processing systems and analytical plotter software. Case 1982 provided another fundamental concept of a digital image exploitation system. Again, the proposed system had the functionality of an analytical plotter with the potential of automating photogrammetric tasks such as digital elevation model DEM generation.

- The second phase in the history of DPWs between 1982-1988. Major efforts were directed towards implementing hardware components and developing low-level system software. The application software was ‘borrowed’ from analytical plotters. The systems of that period were very much characterized by minimal functionality and performance, and it does not surprise that the photogrammetric community met these first soft copy workstations with a healthy doses of skepticism.

- Finally, the third phase of DPW development began with increased activities by researchers, developers, and photogrammetric societies. For example, ISPRS established during the 1988 congress the intercommission working group (I/II) that was charged with the task to define the functionality and performance of digital

photogrammetric system, including a critical evaluation of existing systems. The workstation group provided the following: *"**A digital photogrammetric system is defined as hardware and software to derive photogrammetric products from digital imagery using manual and automated techniques**"*.

In contrast to the first generation systems the recently developed DPWs meet the performance criteria one can reasonable expect for solving photogrammetric tasks efficiently and reliably. It can be used for digital orthophoto production, aerial triangulation, and through to a lesser extent, compilation.

7.3 MAIN COMPONENT OF DPW

The DPW consists of several parts, which enable the system to do the following functions:

1. **Archiving:** store and access images including image compression and decompression.
2. **Processing:** basic image processing tasks, such as enhancement and resembling.
3. **Display and Roam:** display images or sub-images, zoom in and out, roam within a model or an entire project.
4. **3-D measurement:** measure interactively points and features to sub-pixel accuracy.

5. **Super positioning:** measured data or existing digital maps must be superimposed on the display images.

Therefore, the DPW consists of the following components:

1. Central processing unit CPU,
2. Operating system OS,
3. Main memory,
4. Storage system,
5. Graphic system,
6. 3-D viewing system, and
7. Measuring system.

These components should have the following specifications:

1. **The central processing unit CPU:** should be reasonably fast considering the amount of computations to be performed.
2. **The operating system OS:** 32 bit based and suitable for real time processing.
3. **The main memory:** should be sufficient to meet the large amount of data to be processed.
4. **The storage:** requirements in digital photogrammetry can be met through a carefully selected combination of available storage technologies. The options may include:

a) **Hard disk:** is an obvious choice, because of fast access and high performance capabilities. However, the high cost of disk space may make it economically infeasible to store entire project on disk derives. But it typically uses for interactive and real-time applications, such as roaming or displaying spatially related images.

b) **Optical disk:** have slower access time and lower data transfer rate, but at lower cost. The classical CD ROM and CD-R(writable) with a capacity of approximately 0.65 GB can hold only one stereomodel.

c) **Magnetic tape:** offers the lowest media cost per GB. Because of its slow performance due to sequential access type, magnetic tapes are primary mainly used as backup devices.

5. **The graphic display system:** is another crucial component of DPW. The purpose of the display processor is to fetch data such as raster (images) or vector data (GIS), process and to store it in the display memory and update the monitor. The display system also handles the mouse input and the cursor.
6. **3-D viewing system:** this facility is regarded by most photogrammetrists as an absolute necessity, for both measuring the ground control points needed for absolute orientation and subsequently measuring the details (feature extraction). Required

for topographic map compilation and the 3D digital data needed for use in GIS/LIS environment. It is also vital element in carrying out map revision and editing the digital elevation data produced by automatic image matching. It also permits the stereo-superimposition of vector data on the stereo model for accuracy checks and completeness. Thus virtually all DPWs feature stereo-viewing capability.

For human operator to see stereoscopically, the left and write images must be separated. This separation is accommodated in different ways, for example spatially, spectrally or temporally see table(7.1) below.

- **Spatially:**
    i. By using two flat-screen monitors displaying the left and the write images of the stereopairs, respectively. These can be viewed using a mirror stereoscope.
    ii. Alternatively, the two monitors can be set at right angle to each other, one with its axis pointing horizontally, the other pointing vertically upward. One has a horizontal polarization sheet placed in front of it , the other has a vertical polarization sheet. A large semi-reflecting mirror set between the two monitors acts as a beam splitter and allows the two component images to be superimposed on each other. The operator

wears a appropriate spectacle with horizontally and vertically polarizing filters to allow stereo-viewing.

iii. Instead of using two monitors, one split screen monitor can be used to display the left and right images side by side and view these through the mirror stereoscope.

- **Spectrally:**

i. A low-cost solution is simply to superimpose the two component images of the stereopair on the screen of a single colour monitor, with one image displayed in red and the other in green, using the anaglyphic technique familiar to photogrammetrists from early analogue stereoplotting instruments based on optical projection. Users wearing spectacles with the corresponding red/green filters view the resulting stereomodel on the monitor.

ii. Polarization using alternating (left/right) corresponding images on a single monitor screen. In this case, however, each image has a different polarization pattern (clockwise/anticlockwise) introduced by an electronic prism mounted in front of the display monitor. Users viewing the stereomodel, wear spectacles equipped with the corresponding polarizing filters (these are described as ‘passive’ spectacles to distinguish them from the so-called ‘active’ spectacles) acting as alternating shutters on the

crystal eye system. The principle supplier of this type of viewing system is a tectonic subsidiary vision.

- **Temporally:**

This method implement an alternate display of left and right image synchronized by polarization. A commonly used stereo-viewing system on DPWs alternates the left and right component images on a single monitor screen at high speed (e.g. 50 to 60 Hz per image). Viewing is carried out using spectacles equipped with alternating shutters synchronized with the alternating images on the monitor (the left eye sees only the left image and the right eye sees only the right image). Most DPWs using this technology have adopted the Crystal Eye system (from the Stereo Graphics corporation), which is based on the uses of liquid crystal shutters and an infrared emitter.

Separation	Spatial	Spectral	Temporal
Implementation	(1) 2 monitor + stereoscope (2) 1 monitor (split screen) + stereoscope (3) 2 monitor + polarization	(1)Anaglyphic (2)polarization	(1) Alternate display of left and right image synchronized by polarization

Table(7.1) separation of images for stereoscopic viewing

7. **Measuring System:** The analogy to the floating-point mark of analytical plotters is the 3-D cursor that is created by using pattern of pixels, such as cross or circle. The cursor moves in increments of pixels, which may appear as jerky, compared to the smooth motion of analytical plotter. As distinct advantage, cursor can be

represented in any desirable shape and colour. The accuracy of interactive measurements depends on:

i. How well you can identify a feature,

ii. The resolution, and

iii. The cursor size.

7.3.1 ROAMING

Refers to moving, the 3D-pointing device. This can be accomplished in two ways:

i. In the simpler solution, the cursor moves on the screen according to the movements of the pointing device (e.g. mouse) by the operator.

ii. The preferred solution is to keep the cursor locked in the screen center, which requires redisplaying the images. This is similar to the operation on analytical plotters where the floating-point mark is always in the center of the field of view.

Factors such as storage organization, bandwidths, and additional processing are causing delays in the stereo display.

7.4 APPLICATION FUNCTIONALITY

7.4.1 PREPARATION

The preparation phase begins with the project definition, including information about project size, tolerances, average scale, camera calibration data, ground control points, and system parameters. For every

model additional information is usually required, such as the identification of the diapositives and their position on the stages, viewing model (ortho/pseudo), and orientation procedures. By and large, this first phase of entering essential information is identical on analytical plotters and DPWs.

The next preparatory step involves the adjustment of the viewing conditions, accomplished to the analytical plotter with the help of various buttons and dials that are usually arranged in close proximity to the viewer's eyepieces. First, the illumination of the diapositives is adjusted such that they appear equally bright. On DPWs, image enhancement techniques allow for more subtle adjustments. Basically, the hole range of photo lab processing techniques is available at the operators fingertips.

7.4.2 ORIENTATION PROCEDURE

In analytical plotter system after the diapositives are placed on the stages and the viewing control is set the model is ready for orientation. The procedure is essentially the same on the DPW.

7.4.2.1 INNER ORIENTATION

The inner orientation process determines the relationship between the stage coordinate and photo coordinate systems. It determines the exact position of the diapositives on the carrier stage. Accordingly, the inner orientation on a DPW relates the digital image to the digitized diapositives. Therefore, the mathematical model must consider the

scanner geometry and its systematic errors. The transformation parameters, then relate pixel coordinates to photo coordinates.

Like on analytical plotters we expect that the DPW ‘drives’ the cursor into the vicinity of the first fiducial mark. Precise measurement of the fiducial is left to the operator. However, one may expect that pattern recognition software would determine the precise location. Another advantage can be seen in the fact that all fiducial marks can be displayed simultaneously, on the monitor, each in a separate window with a cursor placed on the predicted location.

Although, the time required to measure the interior orientation interactively is very short, it may be justified to perform it automatically, for example immediately after scanning. In that case, the digital image would include the transformation parameters.

7.4.2.2 RELATIVE ORIENTATION

The task of establishing a model is accomplished by measuring a number of conjugate points (parallax points) followed by computing the five orientation parameters. A gain, we expect the analytical plotter to derive to a pre-specified pattern of parallax points, where the parallax is removed by moving one stage with respect to a locked position of the other stage. This same procedure can be accomplished on the DPW by keeping one of the stereo cursors in a fixed position while moving the other one. We may even expect from the DPW that conjugate points are

found automatically, especially when the operator provided good approximation. After having measured enough points, the orientation parameters can be determined. This is the turning point on analytical plotters to switch from stereo-comparator mode to model mode. That is, the orientation elements are now used in the real time loop to maintain the model. The transition between the two models goes almost unnoticed; if every thing went with the first six-parallax points then you have all of a sudden a model established. Now we wonder again on how this all works on a softcopy station. The measurement of points and the computation is indeed very similar, but not the sudden switch to model mode, unless we have a system with centrally fixed cursor and real-time roaming. The majority of existing DPWs must take a deep breath, however, to switch from comparator to model mode, because the images need to be resampled to epipolar geometry. By that we refer to the process of transforming the actual images into a normalized position such that the rows become parallel with the base. In that case, conjugate points lie on the same row. This reduces dramatically the search space resulting in faster matching procedures and makes roaming easier.

The relative orientation can be automated to a degree where it runs as an autonomous batch process. This is particularly appealing because the resampling to epipolar geometry can be allowed immediately after the orientation. Moreover, this batch process can be run a less costly environment.

After the model has been oriented and resampled – the model is already established.

7.4.2.3 ABSOLUTE ORIENTATION

During the process of absolute orientation the relationship between the model and the object space is established. For aerial scenes this requires the measurement of control points. Quite often, the identification of control points poses significant problems, because panels may only be partially visible, or are of low contrast compared to the background. If the identification is difficult for human operators the more difficult it is for computer. As consequence automatic control points recognition is years away from becoming practical.

7.4.3 DIGITAL AERIAL TRIANGULATION

Aerial triangulation is a good example to demonstrate the potential of DPWs to automate photogrammetric process, thereby substantially increasing the price performance ratio. Even though today aerial triangulation is a well-established process its performance and reliability can be considerably improved.

Traditionally, aerial triangulation begins with preparing annotation photographs, whereby a suitable number well distributed points are carefully selected such that they appear on as many photographs as possible. Once the preparation is completed, the points must be

transferred to all photographs. This later phase is quite crucial, particularly the transfer of strip tie points. In fact, the success of an aerial triangulation projects depends largely on the quality of the point transfer. Only after the points are transferred or clearly identified can the measuring process begin.

Automatic aerial triangulation offers significant improvements:

i. The point transfer can be combined with simultaneously measuring conjugate points on all images involved. In the preparation phase, for example, block points can be automatically selected at suitable locations. A distinct advantage is the possibility to simultaneously determine conjugate points that appear on more than two photographs by a procedure known as multi-image matching. In traditional aerial triangulation, an operator can normally only view two images at the same time, conjugate points in multi-images are determined with the help of a point transfer device.

ii. Another advantage of aerial triangulation is the fact that there is virtually no economic limit as far as the number of measured points per photo is concerned. If implemented as a batch process the computation time does not matter a great deal. Increasing the number of points from the typical 9 points pattern per image to say 50 or even 100 points considerably increases the reliability and the accuracy.

7.4.4 AUTOMATIC DIGITAL TERRAIN MODEL GENERATION

One of the major goals of digital photogrammetry has always been, and well continued to be, is the automatic generation of digital terrain models (DTMs) or digital elevation models (DEMs). Considerable progress has been made during the last few years but many problems still persist, such as area with low SNR, break lines, or occlusion.

DTMs for the purpose of orthophoto production are quite successful since high accuracy is not required. The automatic DTM generation is not bounded to DPWs.

The DPW comes in handy for the subsequent quality control – a very important aspect of DTM generation. Unfortunately, problems are not always detected and subsequently reported by DPW programs. For many applications, a visual inspection is inevitable. The manual checking procedures and the interactive editing reduces the savings gained in the automatic DTM generation.

7.4.5 DIGITAL ORTHOPHOTO PRODUCTION

Digital photogrammetry makes an increasing interest in ortho photo production. Automatically generated DEMs are often accurate enough for orthophotos, especially when derived from small-scale imagery. DPWs play a central role in the production of orthophotos because, the image processing capabilities allow for radiometric adjustments and the super positioning of additional information, such as vector data or text.

Moreover, the visualization facilities make DPWs an important component in the production of orthophotos.

Variations of orthophoto production include draping radiometric information on prespective views of surfaces. Another interesting use of DPWs is for generation of animated sequences. An example is the animated view of ghost driver through city (analogous to flight simulation, but with increased demand for true 3-D scenes.

CHAPTER 8

RESULTS AND ANALYSIS

Chapter 8

RESULTS AND ANALYSIS

8.1 INTRODUCTION

The rapid progress in computer technology in the last years has greatly influenced the development of surveying instruments and techniques, in both data acquisition and adjustments and further in mapping and analysis of data.

Digital photogrammetry is one branch, which has largely been affected by this development. Particularly in terms of performance, comfort level components, cost, and vendors.

Digital photogrammetric workstation is one of the yields of this development in photogrammetry, which is replacing gradually the analytical plotters in developed counties, and creeping to replace analogue plotters in underdeveloped countries such as Sudan before starting to cope with analytical plotters.

Therefore, it becomes necessary to study this technology, components, techniques, accuracy, and so on and to be ready for the total replacement of the existing plotters.

A number of field and laboratory measurements have been carried out using different photogrammetric measuring instrument. The main objectives are to investigate:

- The technology of Digital Photogrammetric Work Stations (DPWs) that are gradually replacing analytical and analogue photogrammetric plotters.
- Discuss different processes of digital data acquisition either directly by digital photogrammetric systems, or indirectly from hard copies.
- High light different aspects that support digital photogrammetry such as; digital image processing and image matching procedures that are used in digital photogrammetry.
- The accuracy that can be attained using different scanning resolution.
- Examining and discussing the main factors that affect the accuracy in digital photogrammetric measurements.
- The possibility of generating planimetric and contour maps using different scanning resolution.
- Suitability of scanning resolution via vertical and horizontal mapping scales.
- Testing the accuracy of rectified digital image using ERDAS package.

- Comparing accuracies that can be obtained from Digital Photogrammetric Work Stations (DPW) with that reduced from Erdas imagine software.

8.2 STUDY AREA

An aerial stereopair Fig(8.1) consists of two successive 60% overlapping vertical photographs taken in mountainous terrain in Switzerland with a Wild RC10 universal film camera wide angle of 152.77mm focal length, Kodak plus X aerographic 2402 film emulsion, 230X230mm format, and 6000m flying height was used in this study. See appendices (A) and (B).

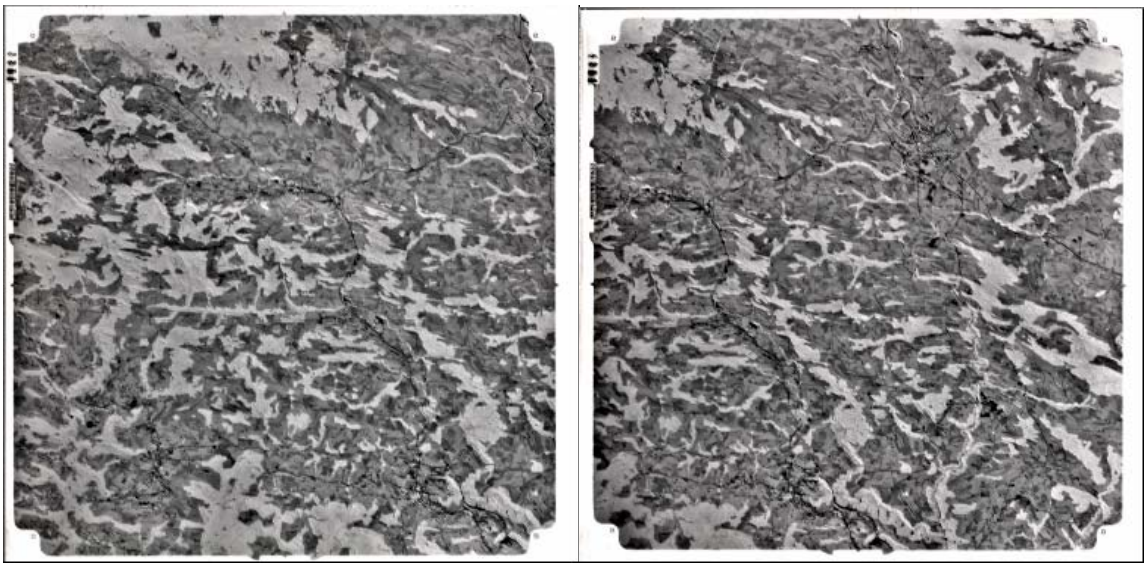

Fig(8.1) A stereomodel of the study area.

8.2 ULTRA SCAN

Ultra scan 5000 was used for transforming the hard copied diapositives of a stereopair into a digital form applying different scanning resolutions. Ultra scan 5000 is a high performance colour flatbed

scanner, which combines both, a supreme geometric performance and high-end radiometric quality. The Ultra Scan 5000 is a state of the art device for digital photogrammetry and graphic art applications.

8.3.1 GENERAL SPECIFICATIONS OF ULTRA SCAN 5000

- **Technology:**

  Flatbed CCD scanner

  Trilinear CCD with 3X6000 elements

  x-y technology with moving CCD-array

- **Geometric specification:**

  Geometric accuracy of ±2µm RMSE.

  Optical resolution from 5µm up to 500µm

- **Radiometric specification:**

  Density range of 0 to 3.4 logD (4.0 log Dmax)

  Uniformity better than 1 DN at 8 bits

  Single pass colour

- **Source material:**

  Colour or black and white images

  Transparent or opaque

  Positive or negative

  Cut film or roll film

- **Scanning area:**

  252X246mm (9.9X9.7 inch) with high resolution

  264X246mm (10.4X9.7 inch) with low resolution

- **Colour depth:**

  3X12 bit at A/D converter

  3X16 bit in software

8.4 SCANNING RESULTS

Ultra scan 5000 was used for scanning the stereomodel with different resolutions. These were selected to be 10, 20, 30, and 80μm. This transform the hard copy images into a soft copy in a digital form to take memory as shown in table(8.1).

Pixel Size (μm)	Memory Size (Mb)			
	Left image	Right image	Stereomodel	Mean
10	1715.2	1664.0	3379.2	1689.6
20	429.0	428.0	857.0	428.5
30	192.0	184.0	376.0	188.0
80	26.8	26.0	52.8	26.4

Table (8.1) Memory Size of digital images.

Now, if a graph is plotted for the pixel resolution used to scan a hard copy of an image via the memory size required for the resultant digital image as shown in figure(8.2) below. Using special statistical software (Microsoft Excel) a mathematical model can be created to estimate the memory size using ultra scan 5000 by the following equation

$$y = 170548x^{-2.0017} \text{ ----------(8.1)}$$

Where,

y is the estimated memory size in Mb,

x is the required pixel size in μm.

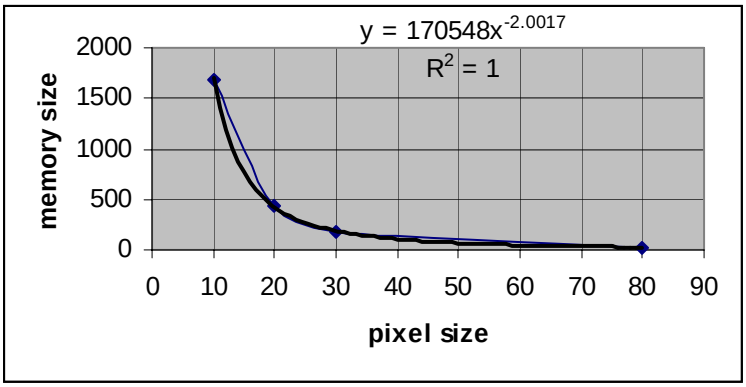

Figure(8.2) Pixel resolution against memory size.

The correlation factor (R)-see chapter 6- of the original graph and the estimated graph was found to be unity (R=1), which means that the estimated graph is totally representing the original data.

8.5 GROUND CONTROL

The Swiss triangulation net provided the base for a vertical and horizontal control network. A certain number of distances were measured with the WILD DI 10 Distomat.

Pre-signalized cross shape control point was used, of 1mX1m central plate and 1mX2m cross arm, which is suitable for different flying height as shown in Fig(8.3).

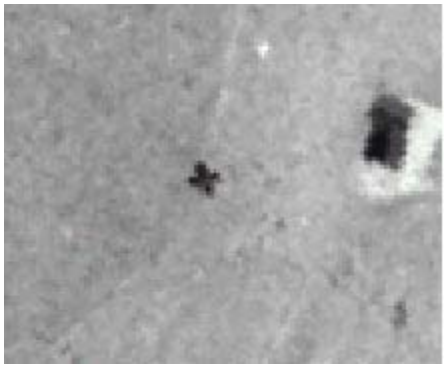

Figure (8.3) Typical pre-signalized control point.

A number of well distributed ground control points of a given *X*, Y, and Z object space plane coordinates whose images appeared in the two overlapping photos were used in this study. Four of these points were fixed as a control. The rest were used as check points. These points are listed in table(8.2).

Point	Actual Ground Coordinates(m)		
	X	**Y**	**Z**
1	752360.22	246244.48	950.65
2	750411.55	244620.42	943.10
3	750941.39	245676.68	958.00
4	751254.82	246531.96	907.81
5	750896.88	247543.96	917.37
6	749788.66	247604.71	1064.58
7	751091.62	249058.47	944.93
8	749251.94	247800.80	1074.74
9	748323.10	247011.39	964.11
10	748458.34	250110.92	918.24
11	747746.58	249305.93	817.64
12	747237.37	249573.26	831.48
13	749251.94	247800.80	1074.74

Table(8.2) Actual ground plane coordinates.

8.6 DIGITAL IMAGE PROCESSING

As mentioned in chapter five digital image processing is central to the effective use of modern digital photogrammetry and remote sensing data.

Here, photographic images scanned from aerial photographs were enhanced before starting any measurement procedure.

The left and right images of any scanned resolution was enhanced using histogram equalization in order to get the best visualization of the images.

Fig(8.4) represents the left image of 80µm resolution before enhancement. The histogram of the image shows that the gray level was extended between 24 and 219.

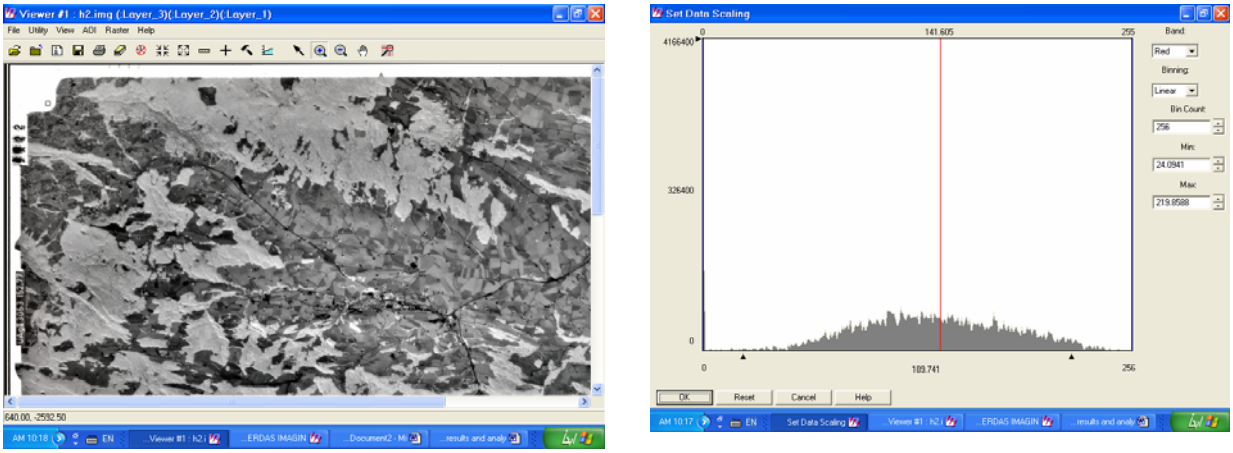

Fig(8.4)The left image and its histogram before equalization.

Fig(8.5) shows the left image after stretching the gray level to be from 0 to 255 using histogram equalization technique to get the best image contrast. Note how sharp is the image now.

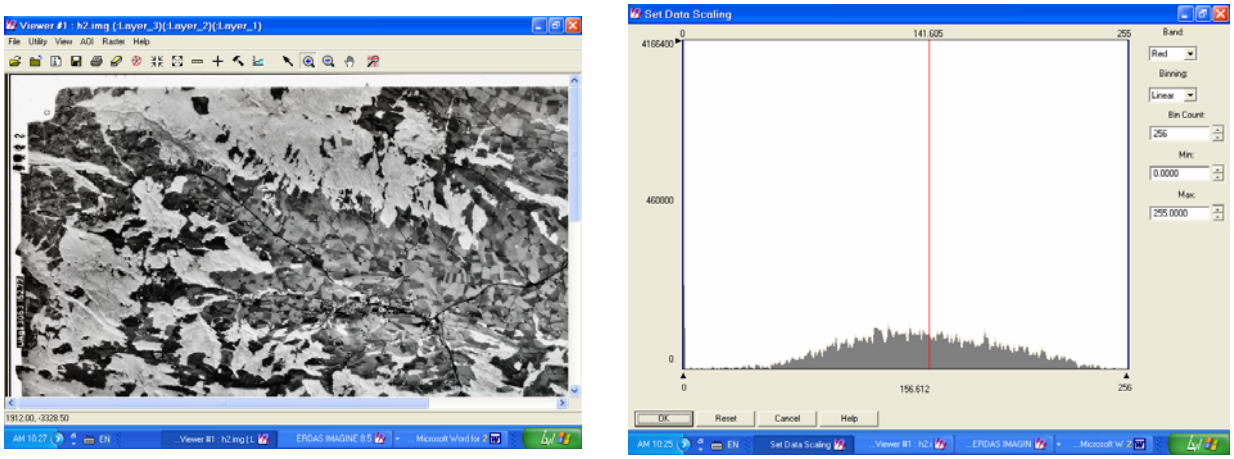

Fig(8.5)The left image and its histogram after equalization.

Before adopting the enhancement to the right image, its gray level was extended from 19 to 198 as shown in fig (8.6).

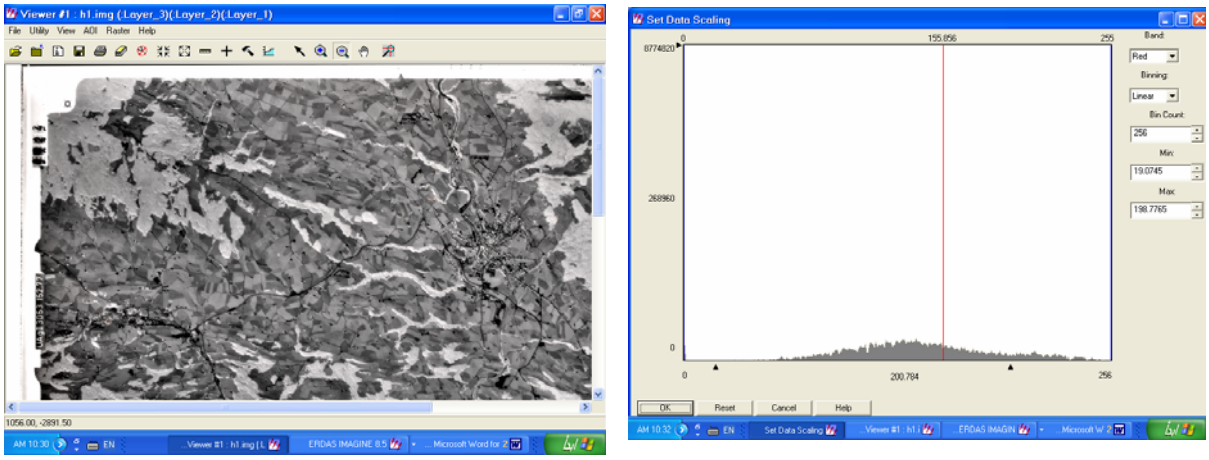

Fig(8.6)The right image and its histogram before equalization.

Now, after stretching the gray level of the right image using histogram equalization the image becomes sharp, and ready for taking measurements as shown in Figure(8.7).

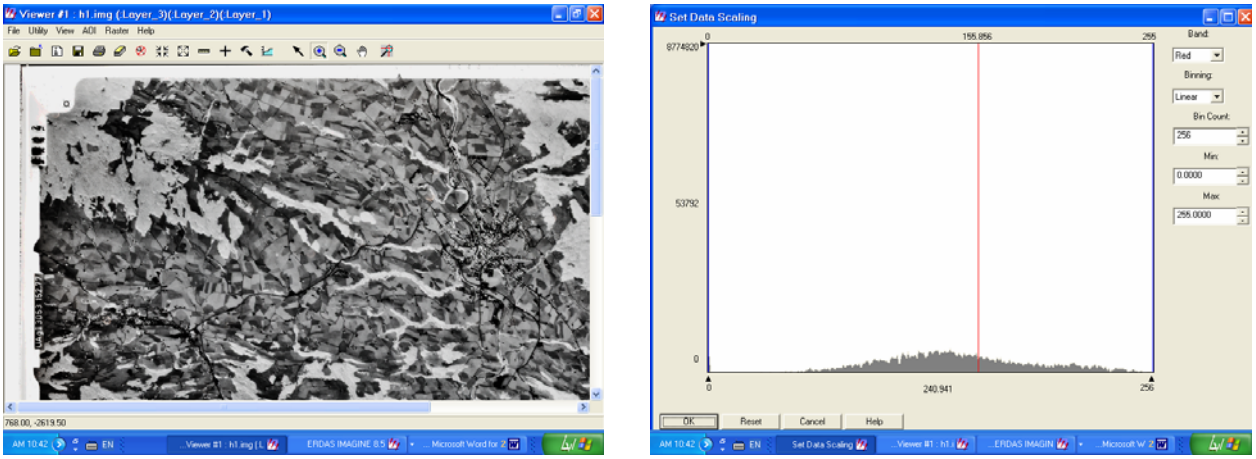

Fig(8.7)The right image and the histogram after equalization.

8.7 PHOTOGRAMMETRIC MEASUREMENTS AND (DPW)

Figure (8.8) demonstrates a typical photogrammetric workstation that was used for taking observations with the following specifications:

1. Flat split screen.
2. Hand-wheel and mouse x, y-movement technology.
3. Foot disk for height measurements.
4. Spatial (one split screen) and temporal viewing system.
5. Geosystem software.

Different sets of measurements were taken for X, Y and Z-coordinates of The points covering the study area using digital photogrammetric workstation. Another sets of measurements were taken for X and Y coordinates using rectified images with ERDAS software package.

Figure (8.8) A typical digital photogrammetric workstation.

8.7.1 RESULT OF THE 10μm SCANNING RESOLUTION

After completing inner and relative orientation of the model using DPW, absolute orientation was carried out using the control points. Then the curser was located at each check point and its coordinates were read out. Table(8.3) below shows the results of measurements taken from a model created from a stereopair of the 10μm scanning resolution.

POINT	DERIVED COORDINATES(m)		
	X	Y	Z
1	752359.72	246244.55	951.83
2	750410.84	244621.08	942.91
3	750941.66	245677.43	958.46
4	751255.42	246531.37	907.14
5	750897.00	247543.89	918.04
6	749788.95	247605.68	1067.04
7	751091.65	249058.02	946.95
8	749253.21	247800.96	1076.18
9	748322.93	247011.47	964.39
10	748457.79	250110.25	919.15
11	747744.17	249306.29	816.18
12	747235.03	249573.65	830.46
13	749251.91	247800.84	1074.65

Table(8.3) Results of the 10μm resolution.

8.7.2 RESULT OF THE 20μm SCANNIMG RESOLUTION

Table(8.4) represents the result obtained from measurement taken for a model created from images of the 20μm scanning resolution.

POINT	DERIVED COORDINATES(m)		
	X	Y	Z
1	752360.29	246244.03	951.78
2	750411.55	244620.74	944.36
3	750941.83	245677.65	960.33
4	751255.08	246532.01	910.46
5	750896.72	247543.71	919.88
6	749788.38	247606.98	1061.88
7	751091.35	249059.35	945.14
8	749252.12	247803.45	1071.78
9	748323.14	247012.42	964.98
10	748456.82	250112.19	916.89
11	747746.64	249304.09	817.28
12	747237.06	249571.71	830.89
13	749251.90	247800.72	1074.88

Table(8.4) Results of the20μm resolution.

8.7.3 RESULT OF THE 30μm SCANNING RESOLUTION

A model constructed from images derived from the 30μ scanning resolution was again measured through the required points. Table(8.5) below shows the result.

POINT	DERIVED COORDINATES(m)		
	X	Y	Z
1	752360.22	246244.80	951.10
2	750410.81	244620.84	941.35
3	750941.21	245678.56	958.03
4	751254.88	246532.28	910.92
5	750896.98	247544.65	917.58
6	749788.71	247607.39	1067.71
7	751091.25	249059.04	946.37
8	749252.87	247802.48	1075.08
9	748323.12	247011.62	962.72
10	748458.87	250110.59	918.93
11	747747.85	249305.06	819.10
12	747239.43	249571.28	833.50
13	749252.06	247800.65	1074.95

Table(8.5) Results of the 30μm resolution.

8.7.4 RESULT OF THE 80μm SCANNING RESOLUTION

Finally, The result of the 80μm is tabulated in table(8.6) below.

POINT	DERIVED COORDINATES (m)		
	X	Y	Z
1	752356.96	246246.64	959.47
2	750411.15	244619.71	939.39
3	750939.84	245678.13	958.65
4	751255.16	246530.84	907.47
5	750897.08	247543.40	915.44
6	749793.92	247603.99	1079.64
7	751091.69	249052.67	956.65
8	749258.21	247798.97	1084.33
9	748320.70	247009.94	962.18
10	748459.55	250107.00	925.56
11	747735.76	249313.08	812.77
12	747227.75	249577.86	831.90
13	749252.12	247801.01	1075.32

Table(8.6) Results of the 80μm resolution.

8.8 ESTIMATION OF PRECISION

In this work, the estimation of precision based on the criteria of the root mean square error RMSE equation(8.2)

$$RMSE = \sqrt{\frac{\sum(\bar{x} - x)^2}{n}} \text{ ----------(8.2)}$$

where,

x is the actual quantity,

$\bar{x}$ is the measured quantity, and

n is the number of quantities.

The root mean square error of the derived coordinates of points was computed for each scanning resolution and tabulated in Table(8.7).

RESOLUTION (μm)	RMSE(m)				
	X	Y	Z	XY	XYZ
10	0.43	0.57	1.23	0.71	1.42
20	0.55	1.05	1.87	1.19	2.21
30	1.50	1.92	2.72	2.44	3.65
80	2.32	2.59	7.58	3.48	8.34

Table(8.7) Estimated precision.

Where, the RMSE of $XY = \sqrt{X^2 + Y^2}$, and that of $XYZ = \sqrt{X^2 + Y^2 + Z^2}$.

It can be seen from the table that the RMSE of X was computed to be 0.43, 0.55, 1.50, and 2.32m for the resolution of 10, 20, 30 and 80μm respectively.

A graph of the pixel size against the precision obtained in the *X*-coordinate was plotted in Fig(8.9) which demonstrates that slight change

in precision is occurred up to 20µm, but from 20 up to 80µm quicker change is noted.

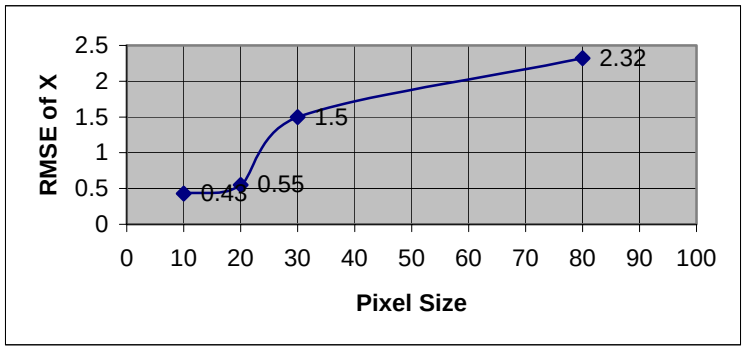

Fig(8.9) The precision of *X*-coordinates.

The RMSE of the y-coordinates was computed to be 0.57, 1.05, 1.92, and 2.59m for 10,20,30, and 80µm pixel size respectively. Again by studying Fig(8.10) the rapid declination in precision of the derived *Y*-coordinates for the pixel size greater than 20µm can be seen .

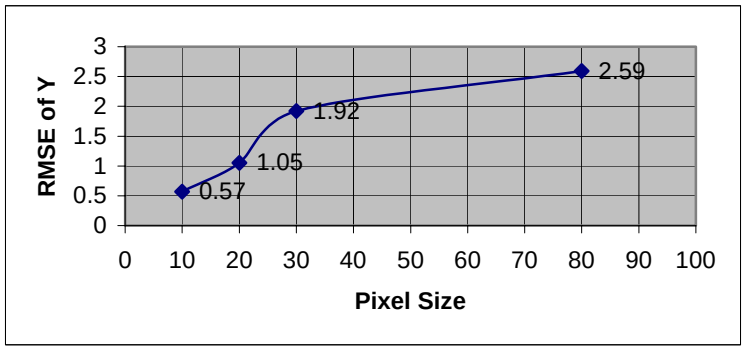

Fig(8.10) The precision of Y-coordinates.

By studying Fig(8.11) which represents the pixel size against RMSE of Z-coordinate, it can be seen that the precision is quickly (linearly) reduced with the increase of pixel size compared with that obtained for *X* and *Y* derived coordinates and this may be due to the fact that the intersection of object rays for the height is more sensitive than *X* and *Y* coordinates specially in a steeper ground.

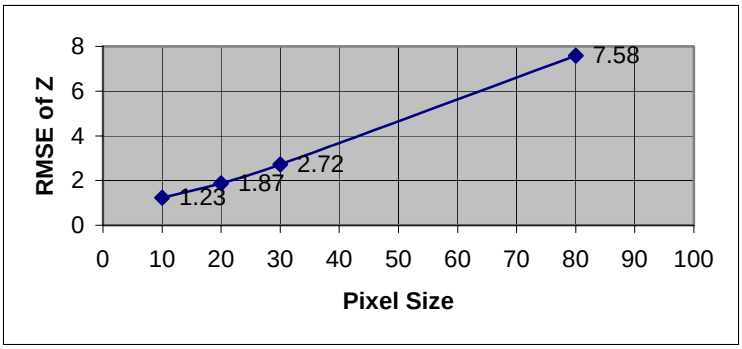

Fig(8.11) The precision of Z-coordinates.

On the other hand, the planmetric precision, which is important for mapping purposes, was found to be 0.71, 1.19, 2.44 and 3.48m facing the pixel size of 10, 20, 30 and 80µm respectively (Fig(8.12)).

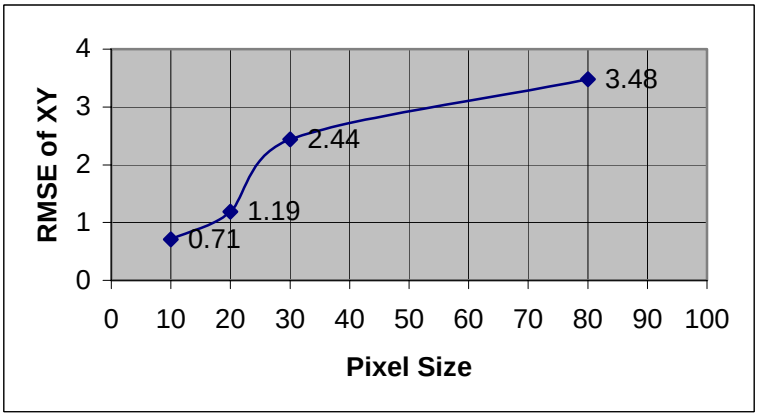

Fig(8.12) The planimetric precision.

From the above discussion it can be seen that the 20µm pixel size is a compromise between precision and economy.

8.9 SCALE OF MAPPING

By assuming that the measurement on the map conventionally can be taken up to 0.5mm using direct measuring tools, the suitable maximum

horizontal and vertical mapping scales can be computed for each scanning resolution depending on the accuracy obtained above.

8.9.1 PLANIMETRIC SCALE

From the assumption discussed in section(8.9) above, and the precision obtained in table(8.7), the maximum planimetric scale for each pixel size is computed to be as shown in table(8.8) below.

RESOLUTION (μm)	COMPUTED SCALE	SUITABLE PLANIMETRIC SCALE
10	1:1420	1:1500
20	1: 2380	1:2400
30	1:4880	1:4900
80	1:6970	1:7000

Table(8.8) Maximum planimetric scales.

A graph in Fig(8.13) is a plot of the suitable planimetric scale against scanning resolution, from which equation(8.3) can be derived to estimate the maximum planimetric scale to the pixel resolution as follows:

$$y = -1.6364x^2 + 230x - 909.09 \text{ ------(8.3)}$$

Where,

y is the maximum estimated planmetric scale number,

x is the pixel size in μm.

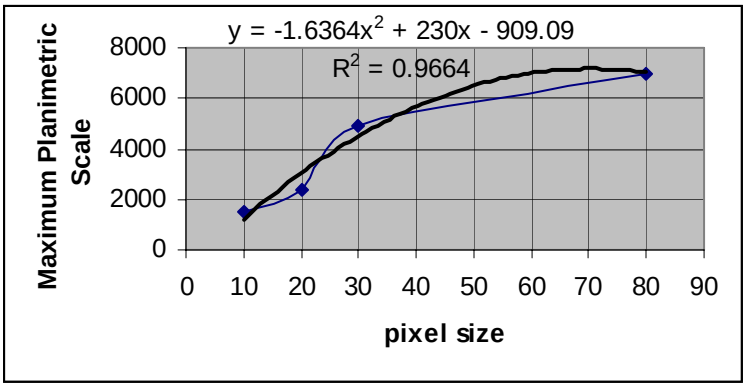

Figure(8.13) Maximum estimated planimetric scale number.

8.9.2 VERTICAL SCALE OF MAPPING

By referring to the *Z*-coordinate precision obtained from the results above (table (8.7)), the maximum vertical scale is computed to be as shown in table(8.9).

RESOLUTION	COMPUTED VERTICAL SCALE	SUITABLE VERTICAL SCALE
10	1:2460	1:2500
20	1:3740	1:3800
30	1:5440	1:5500
80	1:15160	1:15200

Table(8.9) Maximum vertical scale.

A graph in Fig(8.14) is plotted to represent the pixel size against the maximum vertical scale then a polynomial is derived – using Microsoft Excel program- to fit the graph by the following polynomial equation:

$$y = 0.6554x^2 + 123.02x + 1166.2 \text{ -------- (8.4)}$$

where,

y is maximum vertical scale number, and

x is the pixel resolution in µm.

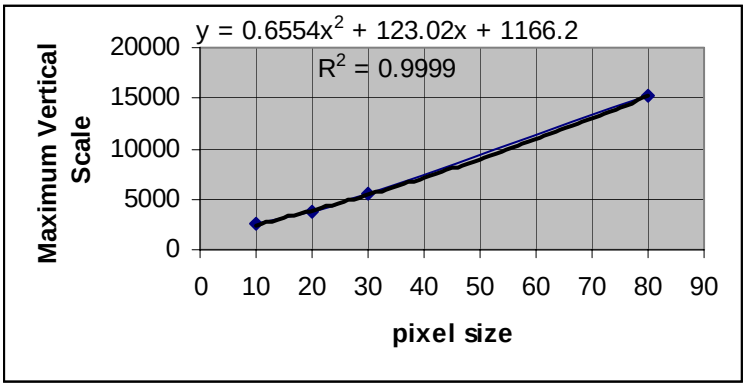

Figure(8.14) Pixel size against maximum vertical scale number.

8.10 DIGITAL IMAGE RECTIFICATION

ERDAS IMAGINE 8.5 software package Fig(8.15) was used for producing a rectified digital image of the study area. The accuracy of the measured *X* and *Y*- horizontal coordinates was tested using this software against the pixel resolution for the resolution of 20, 30 and 80 only (10µm resolution was not included here because it takes a large memory size and slows down roaming process).

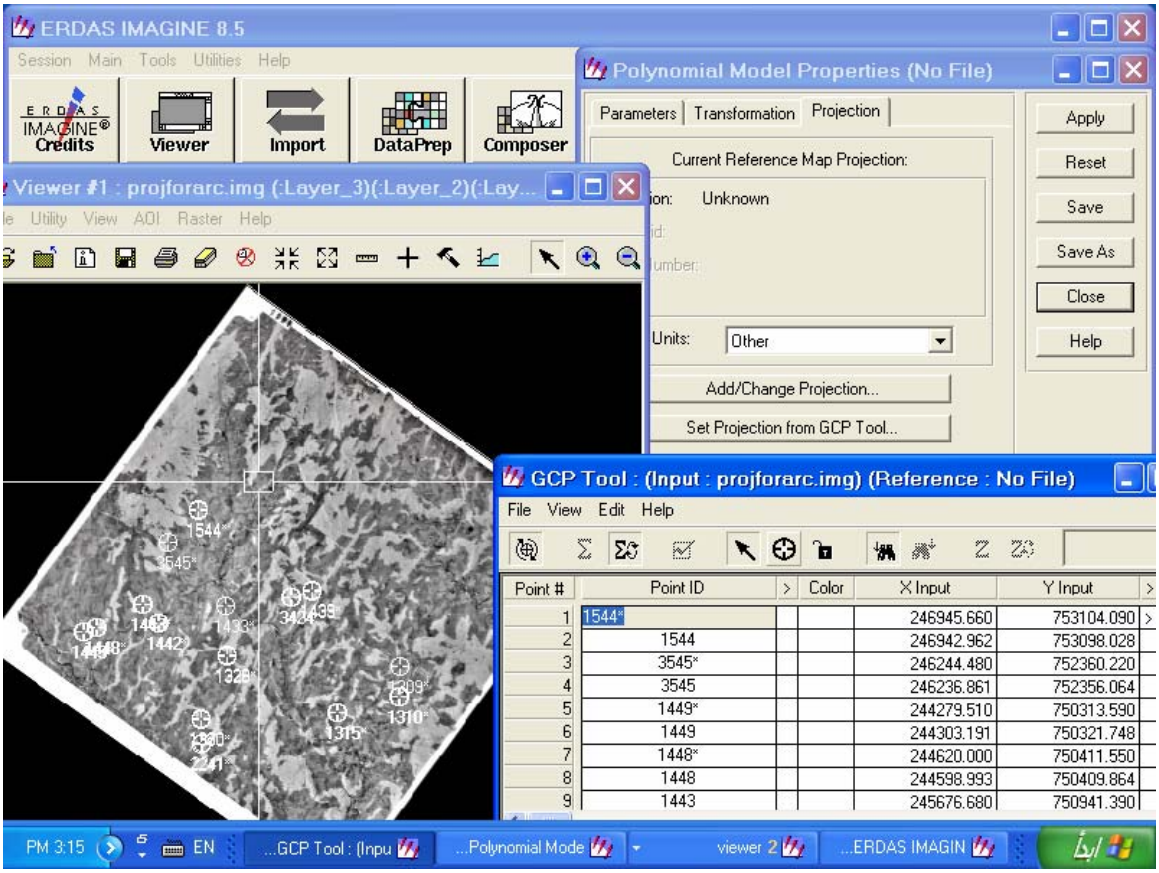

Figure(8.15) ERDAS 8.5 sample page.

Four control points were used to rectify the image of the study area using first order polynomial. This is done by adjusting the four control points on the image then, resampling the original image to get a new rectified image. Table(8.10) below demonstrates the first result obtained for the image of 20µm pixel size.

POINT	DERIVED COORDINATES(m)	
	X	Y
1	752360.52	246244.48
2	750411.52	244620.38
3	750940.43	245672.38
4	751254.12	246550.26
5	750893.62	247558.51
6	749751.49	247587.48
7	751083.56	249069.57
8	748301.99	247018.01
9	747734.43	247032.38
10	748455.93	250128.01
11	749510.49	251573.54
12	748813.49	251537.63
13	749251.94	247800.8

Table(8.10) Results obtained for the rectified image of 20µm pixel size.

The image that was scanned with 30µm pixel size is re-sampled after rectification and the coordinates of the check points were measured as listed in table(8.11) below.

POINT	DERIVED COORDINATES(m)	
	X	Y
1	752360.57	246244.45
2	750410.45	244620.21
3	750940.36	245672.12
4	751253.84	246550.91
5	750894.62	247559.01
6	749751.45	247587.17
7	751083.53	249069.86
8	748301.87	247018.12
9	747734.64	247033.61
10	748455.79	250129.02
11	749510.60	251573.34
12	748814.20	251538.22
13	749251.94	247800.8

Table (8.11) Results obtained for the rectified image of 30µm pixel size.

Finally, the image that was scanned with 80µm pixel size is re-sampled after rectification and the coordinates of the check points were finally derived and the results were listed in table(8.12) below.

POINT	DERIVED COORDINATES(m)	
	X	Y
1	752359.92	246245.77
2	750414.44	244621.19
3	750940.07	245671.02
4	751252.51	246553.57
5	750894.86	247560.99
6	749749.99	247586.06
7	751084.97	249071.03
8	748302.56	247018.54
9	747734.85	247036.04
10	748455.25	250130.55
11	749509.90	251575.87
12	748817.05	251538.62
13	749251.94	247800.8

Table(8.12) Results obtained for the rectified image of 80µm pixel size.

By the inspection, of the above three results obtained from digital rectified images it can be seen that the precision is very low even in the image of 20µm pixel resolution. This is due to the relief displacement. Remember that relief displacement is proportional to the height of the

measured point, and that the study area is of mountainous nature. Table(8.13) represents the precision of the rectified images estimated by the root mean square error.

RESOLUTION (μm)	RMSE(m)		
	X	Y	XY
20	13.34	11.52	17.63
30	13.38	11.99	17.97
80	13.79	13.33	19.18

Table(8.13) The precisions of rectified image.

Analyzing the results in table(8.13) it can be seen that increasing the pixel resolution slightly improve the precision of the measured rectified image coordinates. This is due to the fact that the measurements were taken from a single image. Figure(8.16) represents the planimetric precision of the rectified image and its pixel resolution. From this graph it can be said that the planimetric precision of a rectified digital image is proportional linearly to the pixel size.

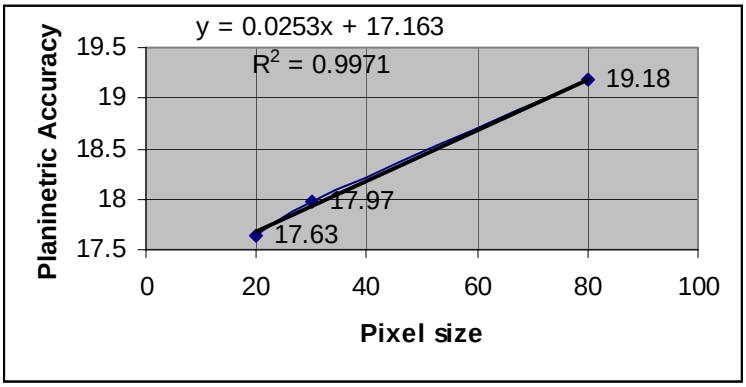

Figure(8.16) Precision of rectified image against pixel resolution.

The justification of relief displacement is supported with an additional test in flat terrain. Fig(8.17) below represents an aerial photo of Khartoum center at scale 1:20,000 and 152mm camera focal length.

Figure(8.17) Area of flat terrain.

A number of check points were selected in the image and their ground coordinates were observed with Lieca 5000 differential GPS system. The reference instrument was situated at Sudan university of science and technology and the rover instrument was moved over the required points to observe the coordinates on Universal Transverse Mercator system (UTM) as listed in table(8.14) below.

Point	Ground Coordinates(m)	
	X	**Y**
1	5181291.55	3304571.81
2	5181620.37	3303901.57
3	5181139.66	3304579.08
4	5181019.26	3304320.80
5	5180962.63	3304203.89
6	5180947.30	3304011.10
7	5181481.84	3303256.65
8	5182282.70	3301990.17
9	5182459.31	3301544.73

Table(8.14) Measured ground coordinates.

The image was then scanned with Ultrascan by resolution of 20μm and subjected to digital rectification as discussed later. The results of the measured points of the rectified image is listed in Table(8.15).

Point	Derived Coordinates(m)	
	X	**Y**
1	5181292.47	3304570.26
2	5181623.02	3303899.39
3	5181139.88	3304578.75
4	5181024.12	3304326.61
5	5180962.95	3304203.65
6	5180949.80	3304013.63
7	5181479.58	3303257.17
8	5182282.53	3301990.32
9	5182456.48	3301546.02

Table(8.15) Derived coordinates.

The precision of the result was evaluated by computing the root mean square error of the derived coordinates which was found to be 2.38m in *x*-coordinates and 2.35m in y-coordinates that means the planimetric precision is 3.34m compared with 17.63m in mountainous terrain using the same resolution. This can produce maps of 1:6700.

8.11 IDENTIFICATION OF POINTS

Resolution in digital photogrammetry is important not only for plotting of details but also important for identification of control points used for adjusting the models, aerial triangulation, or rectification of a single photographs.

Control points used in this research were easily identified when using scanning resolution of 10 and 20μm and with some difficulty and few efforts when using 30μ. This can simply be shown in figure(8.18) and figure(8.19).

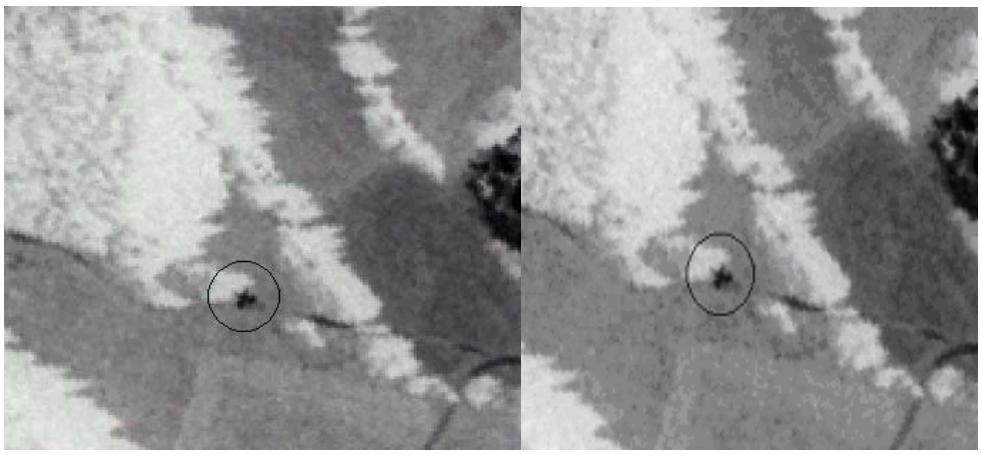

(a) (b)

Figure(8.18) A typical control point (a) with 10μm and (b) with 20μm pixel size.

Figure (8.19) A typical control point

with 30µm pixel size.

Figure (8.20) below demonstrates the shape of control point when using 80µ-scanning resolution. It can be noted that the shape is distorted and it is difficult to identify and measure, which may introduce confusion and mistakes.

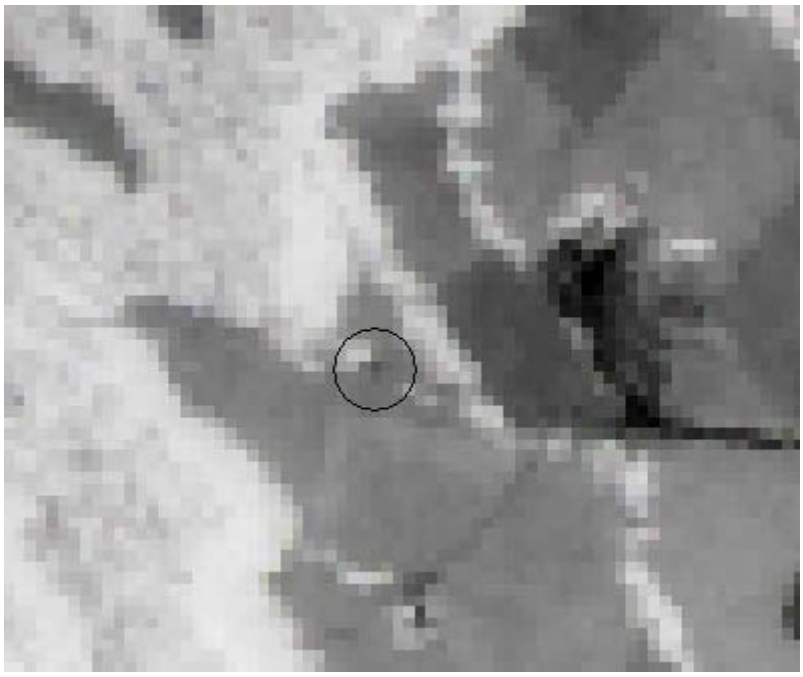

Figure(8.20) A typical control point

with 80μm pixel size.

8.12 CONTOURING

After determining the object space coordinates of points. Contour maps for the study area have been generated from the results obtained by the different resolutions.

The actual object space coordinates of points are used to derive a contour map of the study area as shown in appendix (A). On the other hand appendix (B) represents a three dimensional representation of the study area.

Appendices (C), (D), (E) and (F) demonstrate contour maps derived from the result of 10, 20, 30, and, 80μm resolution of study area (stereomodel of Switzerland) with contour interval of 10m using SURFER package. Note that some contour lines were changed with the change in pixel resolution.

Chapter 9

CONCLUSIONS

Chapter 9

CONCLUSIONS AND RECOMMENDATIONS

9.1 CONCLUTIONS

The recent rapid development in computer technology demonstrates that computer is the language of the day. Surveying applications utilize this technology in data acquisition, adjustment, analysis, and mapping.

These developments cause the theory of digital photogrammetry to escape from papers and seminars to real world. And no doubt that digital photogrammetric workstation is one yield of these developments in photogrammetry.

Digital photogrammetric workstations are interactive workstations. Their role in digital photogrammetry is even more prominent than that of analytical plotters in classical photogrammetry.

Soft copy workstations have begun to spread as a very expensive system built with many propriety components to affordable or reasonably priced system comprising mostly off-the-self components. It is creeping now to replace all other types of conventional plotters.

Then it can be concluded that digital photogrammetric workstation provides important advantages. These include:

- The ability of image processing at the operator's fingertips. These may include enlargements, reductions, contrast enhancements, and

do not require a photographic laboratory. Digital Photogrammetric Workstations (DPW) now may replace a conventional photographic laboratory.

- Traditional photogrammetric equipments, such as point transfer devices and comparators, are no longer required. Digital photogrammetric workstation is more universal than any other type of plotter.
- The absence of any moving mechanical-optical parts make digital photogrammetric workstation more reliable and potentially more accurate since no calibration procedures are necessary.
- Digital photogrammetric workstation offers more flexibility in viewing and measuring several images simultaneously. This is a great advantage in identifying and measuring control points and tie points.
- Several persons can view images or a model simultaneously. This is useful in case where design data are superimposed on a model.
- Digital photogrammetric workstation is more user friendly than the analytical plotter. As more photogrammetric procedures will be

automated, the operation of digital photogrammetric workstation requires less specialist's operator. Conventional photogrammetric analogue plotters or even an analytical plotter requires a high skill level operator. On the other hand digital photogrammetric workstation operating system does not requires a high skill level operator but an operator who knows how to use the computer.

- Moreover, some photogrammetric applications become easier, such as aerial triangulation and ortho-photo production.

- The disadvantages in DPWs are including technical problems such as storage, roaming, and so on, most of these problems are no longer existing.

Also this research work has focused on the theory and results of a part of digital photogrammetry that is concerned with analyzing geometrical precision of the derived models from stereo-pairs scanned with different pixel sizes and test the suitability of each result for the suitable mapping scale. Moreover, this research work examines the precision of the rectified or resampled images with different pixel resolution using ERDAS software.

Taking into a count the fact that, the scanner resolution does not improve the photographic resolution (always decrease it), and that, the photographic resolution depends largely on photographic emulsion, lens resolution, and scale of photography. Also assuming that aerial photography is of a good resolution, one can think of the effect of scanning resolution on the derived accuracy.

By referring to all results of measurements taken from the models created from different scanning resolutions using DPW and by referring to the results of the ERDAS investigation measurements carried out in this research work, one can conclude the following:

1. Increasing the image resolution directly increases digital image size; therefore, digital photogrammetric projects need large data storage such as USB of 80GB memory size or more, which is now available besides the easy-travelers that assist to use an external hard disk. And from the results in chapter 8 it can be said that memory size can be estimated for the Utrascan 5000 scanner by the equation:

$$y = 170548x^{-2.0017} \text{ ----------(9.1)}$$

Where,

y is the estimated memory size in Mb,

x is the required pixel size in µm.

2. Due to the large amount of data to be processed, sufficient RAM should be available. Therefore, it was found to be that slow roaming is obtained with the increase of image resolution.

3. Resampling of a rectified image delays with the increase of memory size i.e. take a long time. An efficient processor is needed in digital photogrammetry.

4. The relation between the pixel size and the accuracy is nonlinear.

5. Scanning the photographic images with resolution of 10μm pixel size is suitable for all photogrammetric works including aerial triangulation and digital elevation modeling since the triangulation points can easily be identified. Also it can be used to develop planimetric maps of 1:1500 scale or smaller. This resolution can be used in contouring large-scale topographic maps to produce maps of 1:2500 scales or smaller.
6. Images can be scanned with pixel size of 20μm if planmetric maps of scale 1:2400 and smaller, or contour maps and profiles of vertical scale of 1:3800 or smaller are to be derived. This pixel size is also suitable for aerial triangulation purposes. Since control points can be

distinguished on the digital image, and it can be said that 20µm is a compromise between accuracy and economy.

7. If it's necessary for a particular project to drive planimetric maps of scale 1:4900 and contour maps of 1:5500 or smaller. It is recommended to scan the hard copy images with photogrammetric scanner applying pixel resolution of 30µm.

8. Up to 80µm pixel size, the planimetric scale can be estimated from the pixel size by applying the following polynomial equation

$$y = -1.6364x^2 + 230x - 909.09 \text{------} (9.2)$$

Where,

y is the maximum planimetric scale factor,

x is pixel size in µm.

9. Vertical scale required for topographic mapping, and contouring can be estimated from the scanning resolution by the equation

$$y = 0.6554x^2 + 123.02x + 1166.2 \text{--------} (9.3)$$

Where,

y is maximum vertical scale factor, and

x is the pixel resolution in µm.

10. Planimetric accuracy of a rectified digital image is proportional linearly to the pixel size.

11. It is not suitable to take measurement from a rectified single image of a mountainous nature.

12. Increasing the pixel resolution slightly improves the accuracy of the taken measurement from a single rectified image (about 2.5%).

13. In flat terrain such as Khartoum, digital rectified image of 1:20,000 scale and 20µm resolution can be used to produce maps of 1:6600 scales or smaller.

14. The 80µm pixel size used for scanning the photographic images distort small features. Therefore, it is difficult to identify the control points used for orienting digital images. In spite of this problem the resolution can produce planmetric accuracy of 3.48m, which can be used to derive planmetric map of 1:7000. The same resolution can produce vertical accuracy of 7.58m, that can produce maps of 1:15200 vertical scales or smaller.

9.2 RECOMENDATIONS

This work did not cover all aspects of digital photogrammetry and the application of a digital photogrammetric workstation. The model tested in this work was only of a mountainous terrain beside a flat area was also tested for comparison. In addition to that digital rectification was only a test applied in the ERDAS package. Based on this research work and the previous work of other investigations, further work can be carried out along the following lines:

1. Taking digital aerial photographic stereopairs with different scales, and compare the results of the measured ground coordinates of models created with digital photogrammetric workstation and the ERDAS software.

2. Investigate the results that can be obtained using images directly acquired with digital camera.

3. Examine the accuracy of automated digital terrain model generation in digital photogrammetric workstation.

4. Try to use satellite imageries in digital photogrammetric workstation and examine the results that can be obtained.

5. Intensification of control points through the area assists to create a digital terrain model of the test area using ERDAS package. Then

this model can be compared with that created using digital photogrammetric workstation.

6. Examine the capability precision of creating digital orthophotographs in digital photogrammetric workstation.

7. Since the root mean square error was taken here as a measure of accuracy of the derived results neglecting other source of errors. It is possible to use other different statistical models such as ω- test and τ-test to detect gross error of the measured coordinates.

BIBLIOGRAPHY
AND
REFERENCES

BIBLIOGRAPHY AND REFERENCES

1. Akiyoshi, S. H. (1985), Bundle Adjustment in No Need Of Approximations of Parameters, Fokuyama University, Fokuyama, 729-02, Japan, ISPRS Commission- III.
2. Ali, A. E. (1992), Finite Element Technique Versus Polynomial Solution in Parallax Heighting From Space Photogrammetry, Math. Comput. Modelling Vol.16, Nom4.
3. Bernhardsen, T. (2000), Geographical Information Systems, An Introduction, 2End Ed., John Wiley, and Sons, Inc. Canada.
4. Cross, P. A (1982), Advanced Least Square Applied To Position Fixing, Working Paper Number 6, North East London Polytechnic, 205pp.
5. Elassal, A. A. (1985), Design of general Data Reduction System For Analytical Photogrammetry, Paper Presented to ASP Semi-Annual Convention- San Fransisco.
6. El-Beik, A. H. and Masaad, E. M. (1993), An Automted Image Metrology System, INT. J. P. Remote Sensing, Vol.14,No.6 .
7. Floyd, F. S. (1997), Remote Sensing, principles and interpretation, W. H. Freeman and company, New York, USA.
8. Gamal, H. S. (2004), On the suitability of conic section in a single –photo resection, camera calibration, and photogrammetric triangulation. Ph. D. thesis, the Ohio State University.

9. Gonzalez, R. C., and Wood, R. E. (1993), Digital Image Processing, Adison-Wasley Pub. Co., New York, USA.
10. Gorani, M. A, and Zomrawi, N. M. (2004), The effect of 80μm resolution on the DPW, Sudanese Engineering Society Juornal.
11. Gorani. M. A, and Zomrawi, N. M. (2005), Collinearity condition equation with 6-terms via 10-terms. Sudanese Engineering Society Juornal.
12. Harris, R. (1987), Sattelite Remote Sensing, An Introduction, Routledge & Kegan Paul, Lodon.
13. Institute. E. S. R. (1997), Understanding GIS, Environmental System Research Institute, Inc., New York Street, California, USA.
14. Institute. E. S. R. (2004), What is Arc GIS, Environmental System Research Institute, Inc., New York Street, Redlands,CA 92373-5100, USA.
15. Janssen, L. L. (2000), Principles of Remote Sensing, An Introduction, ITC Educational Series 2, the Netherland.
16. John, R. J. (1996), Introductory Digital Image Processing, a remote sensing perspective, 2ed, Prentice Hall, Inc, New Jersey, USA.
17. Kennie, T. J. & Petrie, G. (1993), Engineering Surveying Technology Paperback ed., Blackie Academic and Professional, Glasgow, G64 2nZ, UK.
18. Kilford. W. K. (1989), Elementary air Surveying, 3rd ed. Pintman Publishing. Murchison,D. E., Surveying And Photogrammetry Newnes-Butterwo Rths, London.
19. Methley, B. D. (1993), Computational Models in Surveying and Photogrammetry.

20. Mikhail, E. M. (1995), Reverse Methods In Phototgrammetyric Data Reduction, Photogrammetric Engineering And Remote Sensing.
21. Miller, D. R. (2005), Landscape Visualization Using DEM Data Derived From Digital Photogrammetry, http://www. Digital Photogrammetry/Landscape.
22. Miller, A. B. (1993), Soft Copy Photogrammetric Workstations, Photogrammetric Engineering And Remote Sensing.
23. Novak, K. (1992), Rectification of Digital imagery, Photogrammetric Engineering And Remote Sensing.
24. Petrie, G. (1997), Developments in Digital Photogrammetric Systems For Topographic Mapping Applications, ITC Journal.
25. Slamma. L. L. (1980), Manual of Photogrammetry, 4-th ed., Falls Church, Virginia.
26. Schenk. T.(1999), Digital Photogrammetry. Terra Science, Laurelville/OH, 428p.
27. Wolf, P. R. (1985), Elements of Photogrammetry with Air Photo-interpretation and Remote Sensing, 2 ed.
28. http://www. Erdas. com. (2005), Geographic Imaging made simple, Online Manual, Versions 8.5.
29. http://www. Esri. Com, 2005.
30. Wong, K. W. (1980), Mathematical Formulation And Digital Analysis in Close Rang Photogrammetry, Photogrammetric Engineering and Remote Sensing.
31. Zheng, Y. J. (1995), Digital Photogrammetric Inversion: Theory and Application to Surface Reconstruction, Photogrammetric Engineering and Remote Sensing Vol 4.

Appendix (A)

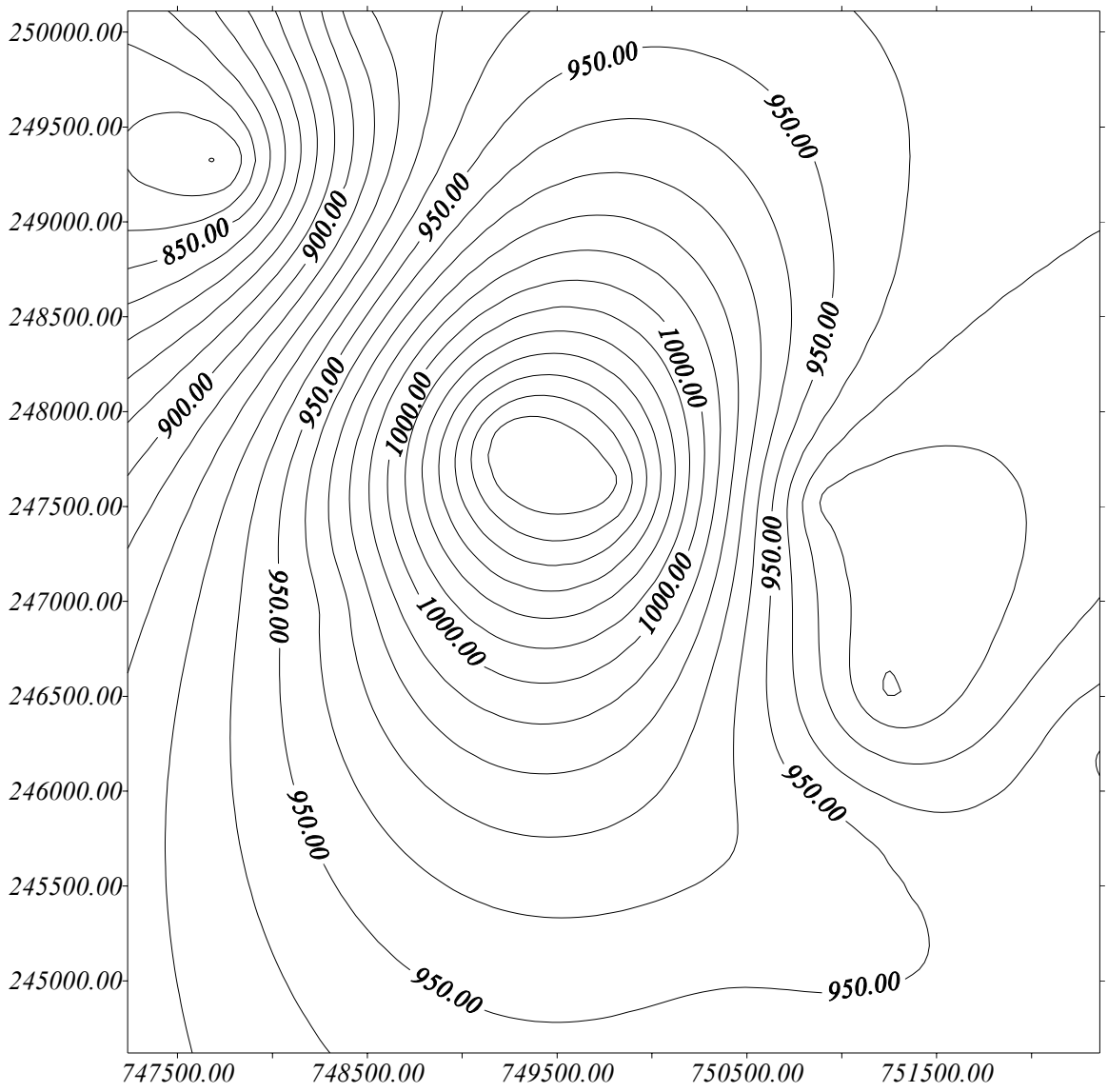

CONTOUR MAP OF THE STUDY AREA (SWITZERLAND).

Appendix (B)

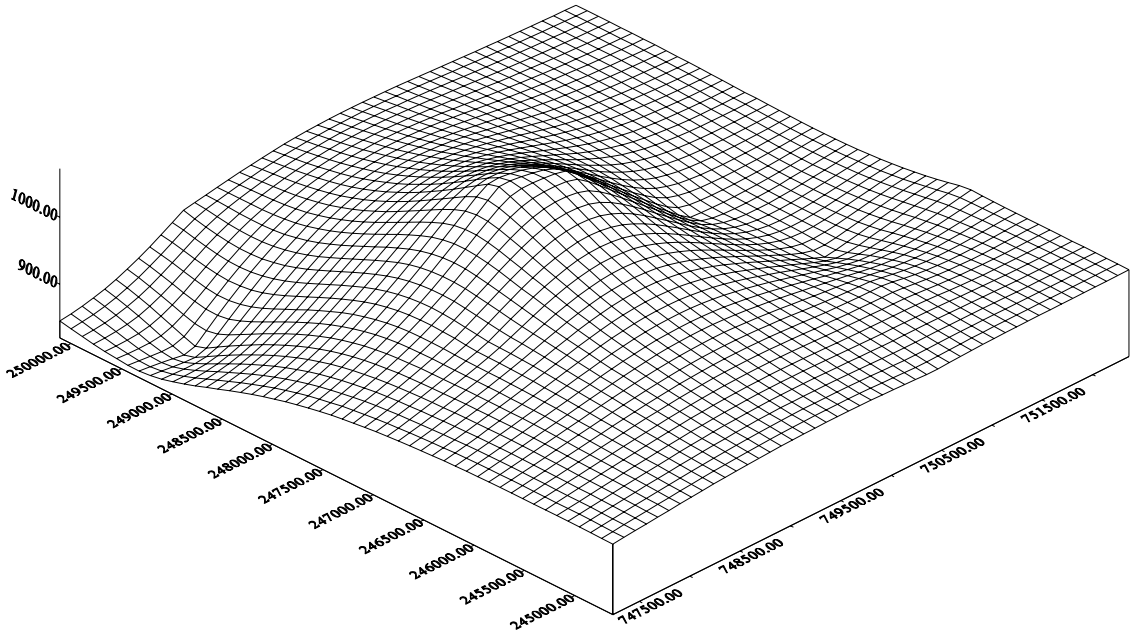

3-D REPRESENTATION OF THE STUDY AREA (SWITZERLAND).

Appendix (C)

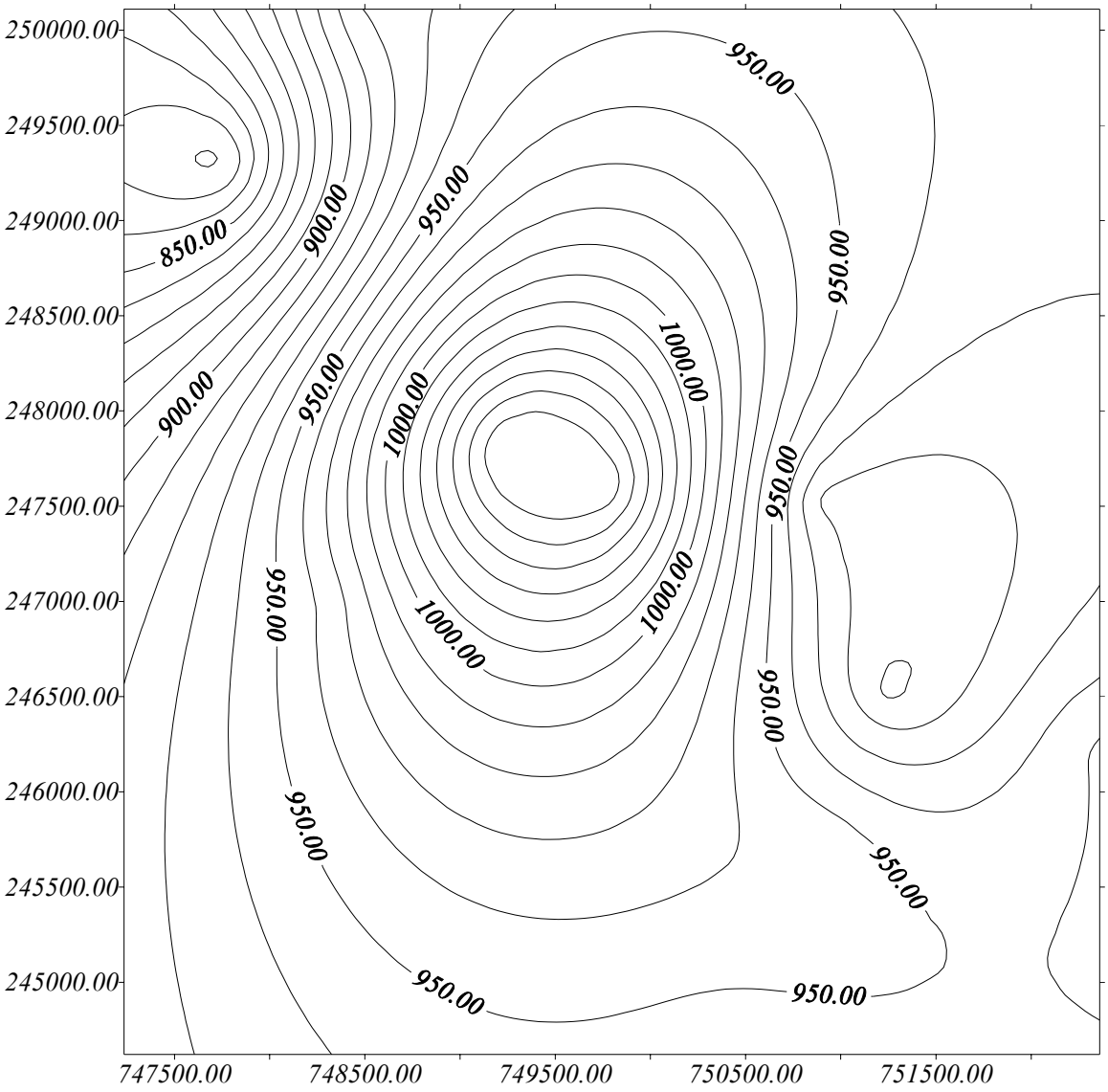

CONTOUR MAP OF THE RESULT OF THE 10μm RESOLUTION OF STUDY AREA (SWITZERLAND).

Appendix (D)

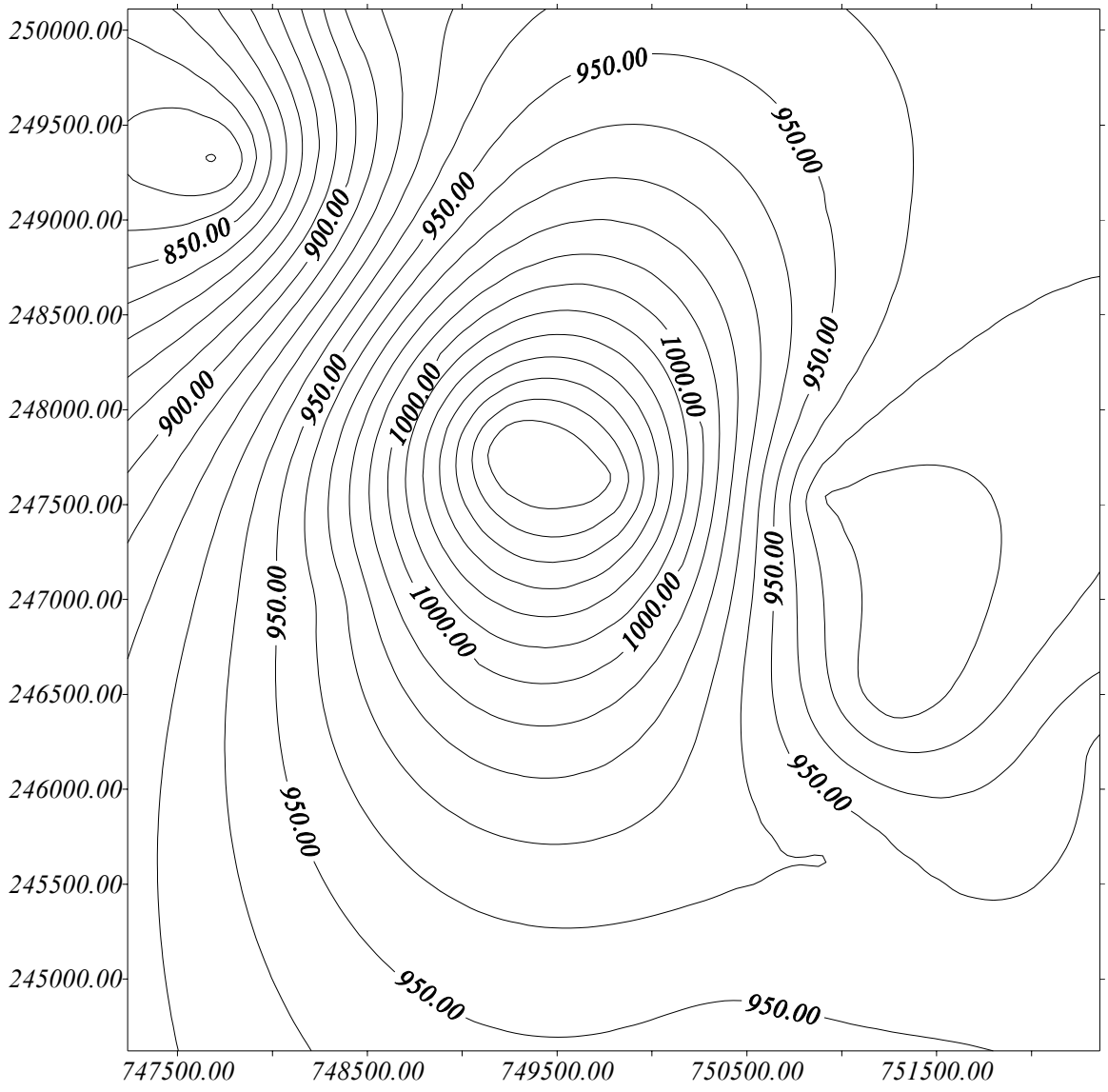

CONTOUR MAP OF THE RESULT OF THE 20μm RESOLUTION OF STUDY AREA (SWITZERLAND).

Appendix (E)

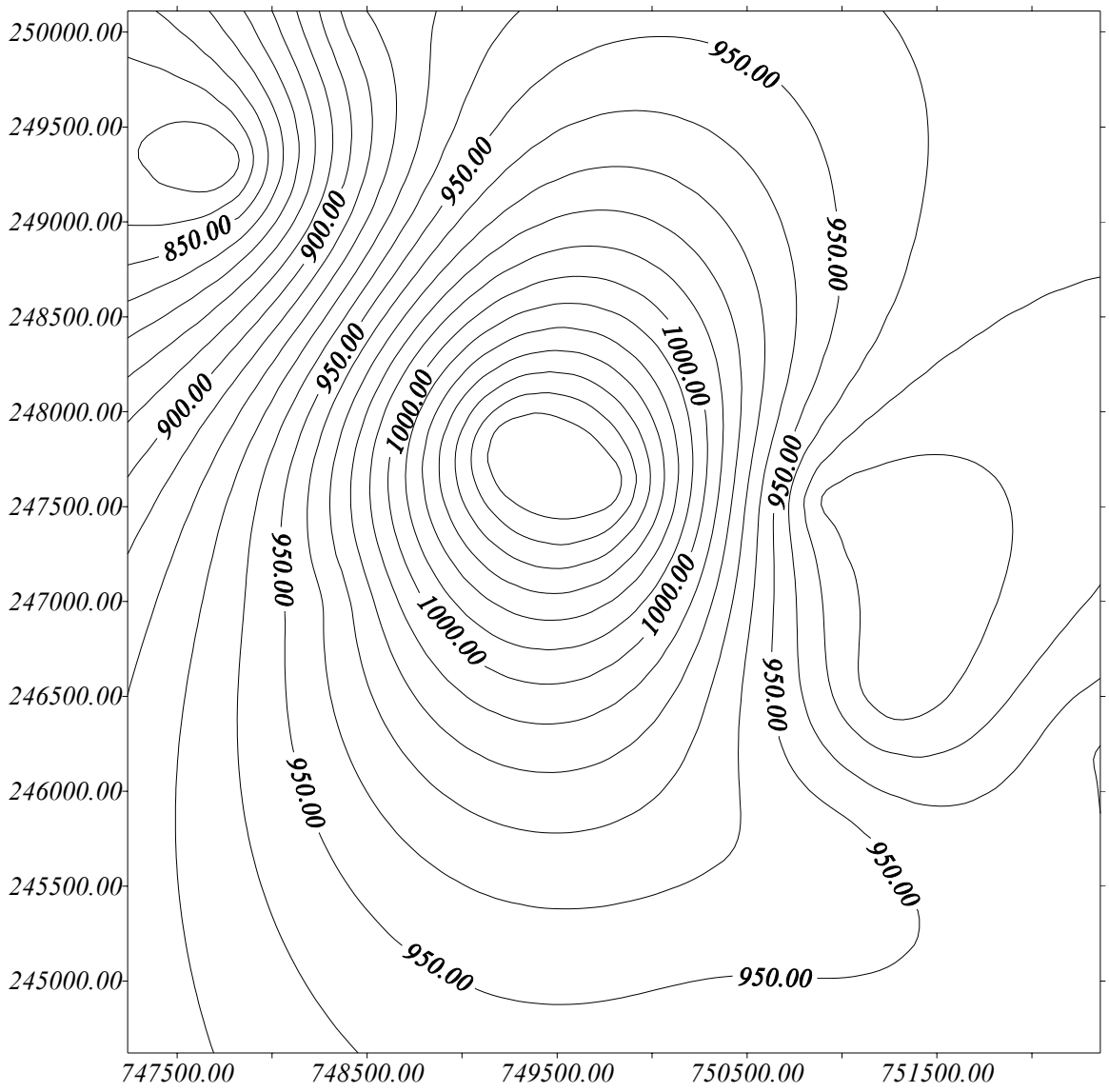

CONTOUR MAP OF THE RESULT OF THE 30μm RESOLUTION OF STUDY AREA (SWITZERLAND).

Appendix (F)

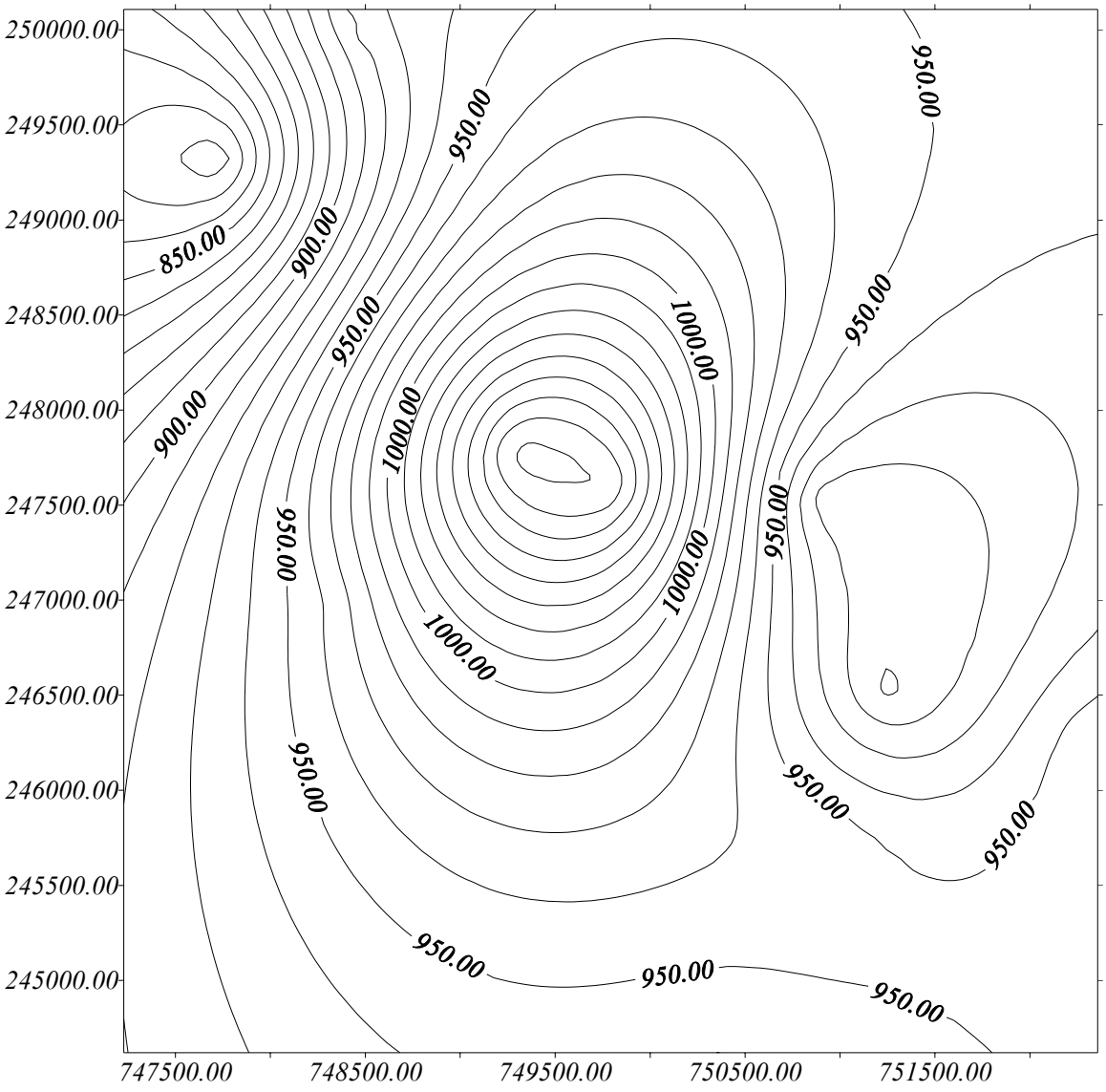

CONTOUR MAP OF THE RESULT OF THE 80μm RESOLUTION OF STUDY AREA (SWITZERLAND).